University of Alberta

Metabolomic Markers of Pneumonia:

in vivo and *in vitro* Study to Determine Diagnostic Markers

by

Andriy Cheypesh ©

A thesis submitted to the Faculty of Graduate Studies and Research

in partial fulfillment of the requirements for the degree of Master of Science

in

Experimental Medicine

Faculty of Medicine

Edmonton, Alberta

Spring 2008

Library and
Archives Canada

Published Heritage
Branch

395 Wellington Street
Ottawa ON K1A 0N4
Canada

Bibliothèque et
Archives Canada

Direction du
Patrimoine de l'édition

395, rue Wellington
Ottawa ON K1A 0N4
Canada

Your file Votre référence
ISBN: 978-0-494-45792-4
Our file Notre référence
ISBN: 978-0-494-45792-4

NOTICE:
The author has granted a non-exclusive license allowing Library and Archives Canada to reproduce, publish, archive, preserve, conserve, communicate to the public by telecommunication or on the Internet, loan, distribute and sell theses worldwide, for commercial or non-commercial purposes, in microform, paper, electronic and/or any other formats.

The author retains copyright ownership and moral rights in this thesis. Neither the thesis nor substantial extracts from it may be printed or otherwise reproduced without the author's permission.

AVIS:
L'auteur a accordé une licence non exclusive permettant à la Bibliothèque et Archives Canada de reproduire, publier, archiver, sauvegarder, conserver, transmettre au public par télécommunication ou par l'Internet, prêter, distribuer et vendre des thèses partout dans le monde, à des fins commerciales ou autres, sur support microforme, papier, électronique et/ou autres formats.

L'auteur conserve la propriété du droit d'auteur et des droits moraux qui protège cette thèse. Ni la thèse ni des extraits substantiels de celle-ci ne doivent être imprimés ou autrement reproduits sans son autorisation.

In compliance with the Canadian Privacy Act some supporting forms may have been removed from this thesis.

While these forms may be included in the document page count, their removal does not represent any loss of content from the thesis.

Conformément à la loi canadienne sur la protection de la vie privée, quelques formulaires secondaires ont été enlevés de cette thèse.

Bien que ces formulaires aient inclus dans la pagination, il n'y aura aucun contenu manquant.

Canada

Abstract

Streptococcus pneumoniae- and *Staphylococcus aureus*-caused pneumonias are accompanied by slightly different profiles of pathological and biochemical processes with undiscovered metabolic consequences. We predicted that these processes result in unique metabolic profiles in urine, serum and broncho-alveolar lavage (BAL) fluid of mice, infected will these bacteria. We also predicted that metabolic changes during epithelial lung cells infections with these bacteria can correlate with damage of host cells and mitochondria. We found unique metabolic profiles during *S. pneumoniae*-infection of infected mice are different than the profiles of uninfected controls. Metabolic profiles during *S. aureus* infection (preliminary data) are different than in uninfected and infected with *S. pneumoniae* mice; this can be potentially used for diagnosis and prognosis of pneumonia. We also found correlations between changes in metabolite concentrations and degree of cell death during *S. pneumoniae*-infection. This can help to describe mechanisms of metabolic changes during mice infection.

Acknowledgements

- Dr. Paige Lacy for supervision and support of the project, designing mouse pneumonia model experiments, very valuable ideas, comments, and suggestions
- Dr. Tom Marrie for supervision and support of the project, very valuable ideas, comments, and suggestions
- Dr. Carolyn Slupsky for supervision of the project, very valuable ideas, comments, and suggestions, for teaching me NMR spectra acquisition and analysis
- Dr. Marek Duszyk for supervision of the project, very valuable ideas, comments, and suggestions
- Dr. Greg Tyrrell and Sandy Shokoples for providing bacterial strains, broth, plates for bacteria culture, high quality bacteria spreaders, and advice on bacterial culture
- Dr. Ryan McKay and Shana Regush for teaching me NMR spectra acquisition
- Dr. Idong Obiefuna, James Dooley, Melanie Abdel, and Rattanjeet Vig for advice on technical aspects of animal studies
- Dr. Florentina Duta, Dr. Valentin Duta, Dr. Tae Chul Moon, Dr. Samira Muñoz, René Déry, Dr. Farzana Shaheen, and Mazyar Ghaffar for teaching me general techniques of cell culture and advising on aspects of cell culture experiments
- Dr. Dorothy Rutkowski, Dr. Francis Davoine, Dr. Wole Odemuyiwa, and Dr. Marcelo Marcet-Palacios for teaching and advising on flow cytometry

- Dr. Ramses Ilarraza and Dr. Narcy Arizmendi-Puga for teaching confocal laser scanning microscopy
- Hao Fu and Dr. Kathryn Rankin for advice on NMR spectra analysis
- Dr. Dalia Abdel Latif and Dr. Wole Odemuyiwa for advising to use 600-700 nm wavelength of spectrophotometer for bacterial count
- Cory Ebeling and Dr. Farnam Ajamian for advising on centrifugation

Table of Contents

Chapter 1. General Introduction 1

1.1. Pneumonia: description and diagnosis......2

1.1.1. Epidemiology and etiology of pneumonia......3

1.1.1.1. Risk groups......5

1.1.1.2. Routes of infection......6

1.1.2. Current methods of determination of etiology and severity of pneumonia......6

1.1.2.1. Clinical manifestation......6

1.1.2.2. X-ray analysis......7

1.1.2.3. Bacteriological methods to determine etiologic diagnosis of pneumonia......8

1.1.2.3.1. Sputum analysis......9

1.1.2.3.2. Other methods......10

1.1.3. Metabolic changes in humans with pneumonia......11

1.2. Pathogenesis of pneumonia and potential changes in metabolism......12

1.2.1. Systemic changes in homeostasis and their influences on metabolism......12

1.2.1.1. Hypoxia......12

1.2.1.2. Local and systemic acidosis......13

1.2.1.3. Decreased food uptake......14

1.2.1.4. Toxic syndrome......14

1.2.1.5. Oxidative stress……………………………………..15

1.2.1.6. Metabolic changes due to cytokine action…..15

1.2.1.7. Changes in osmolality of biofluids
and osmolytes…………………………………………..16

1.2.1.8. Bacteremia……………………………………..17

1.2.2. Local changes in lung during pneumonia………………18

1.2.2.1. Virulence factors of *Streptococcus pneumoniae*…………………………………………...18

1.2.2.2. Virulence factors of *S. aureus*………………..21

1.2.2.3. Damage of extracellular matrix………………22

1.2.2.4. Local release and action of cytokines ……..….23

1.2.2.5. Reactive Oxygen Species (ROS) and
proteases………………………………………………....23

1.2.2.6. Cell damage and death………………………..24

1.2.2.7. Time course of local changes during
pneumonia ……………………………………………....25

1.2.3. Metabolism of *S. pneumoniae* and *S. aureus*……………29

1.2.3.1. Energy metabolism…………………………........30

1.2.3.2. Metabolism of amino acids……………………….30

1.2.3.3. Biologically active compounds…………………..34

1.2.3.4. Interconnections between metabolism and
virulence factors of *S. pneumoniae* and *S. aureus*……..….35

1.3. Experimental models of bacterial-cell interaction and the study of

bacterial factors of pathogenicity..36

1.4. Experimental mouse pneumonia model....................................38

1.5. Metabolomics as a part of system biology.................................41

1.6. Central hypothesis and objectives..47

Chapter 2. Cell Culture Model of Bacteria-Cell Interaction.......................50

2.1. Introduction..51

2.2. Materials and methods..65

2.2.1. Cell media...65

2.2.2. Cell line...65

2.2.3. Bacteria..66

2.2.4. Infection experiments...59

2.2.5. NMR analysis..59

2.2.5.1. Filters...59

2.2.5.2. NMR experiments...60

2.2.5.3. Data analysis...60

2.2.6. Microscopic observation of cell morphology................................61

2.2.7. Fluorescence microscopy 61

2.2.8. Bacterial count..62

2.3. Results..62

2.3.1. Metabolomics of lung cells infected with *S. pneumoniae*.....62

2.3.1.1. Concentrations of TCA cycle intermediates.........62

2.3.1.2. Concentrations of amino acids.........................62

2.3.1.3. Energy metabolism.......................................63

2.3.1.4. Bacterial-derived metabolites.........................63

2.3.1.5. Other metabolites (nicotinamide, niacinamide, and pantothenate).........................69

2.3.2. Changes in cell viability during infection.........................69

2.3.2.1. Changes in mitochondrial potential and evaluation of preferential cell death.........................69

2.3.2.2. Microscopic observation of A549 cells.........................69

2.3.3. Dynamics of *S. pneumoniae*.........................69

2.3.3.1. Bacterial count.........................69

2.4. Metabolites in supernatants of A549 cell line infected with *S. aureus*.........................74

2.4.1. TCA cycle intermediates.........................74

2.4.2. Metabolism of amino acids.........................75

2.4.3. Energy metabolism.........................75

2.4.4. Bacterial-derived metabolites.........................75

2.5. Conclusions.........................75

Chapter 3. Mouse pneumonia model.........................81

3.1. Introduction.........................82

3.2. Materials and methods.........................85

3.3. Results.........................92

3.3.1. Severity of pneumonia of infected mice.........................92

3.3.1.1. Cross-sectional study with *S. pneumoniae*-infection.........................92

3.3.1.2. Longitudinal study of *S. pneumoniae*-infection.....96
3.3.2. Metabolomics of blood, urine and BAL of *S. pneumoniae*-infected mice.....96
3.3.2.1. Concentrations of TCA cycle intermediates in blood, urine and BAL of *S. pneumoniae*-infected mice.....98
3.3.2.2. Metabolism of amino acids.....98
3.3.2.3. Energy metabolism.....104
3.3.2.4. Osmolytes, membrane constituents, nucleotides, and derivatives.....112
3.3.2.5. Metabolism of creatine.....112
3.3.2.6. Bacteria- and food-derived compounds.....120
3.3.2.7. Conclusion. Metabolomics data of biofluids of the mouse pneumonia model caused by *S. pneumoniae* (cross-sectional and longitudinal studies).....120
3.3.2.8. PCA analysis of urine of *S. pneumonia*-infected Mice.....123
3.3.3. Cross-sectional study with *S. aureus* infection.....123
3.3.4. Metabolomics of urine *S. aureus*–infected mice.....127
3.4. Conclusions.....134
Chapter 4. Summary of Data and Discussion.....136
4.1. Infection of lung cells.....137
4.1.1. Microbiological processes in cell cultures.....137

4.1.2. TCA cycle intermediates..140

4.1.4. Amino acids..142

4.1.5. Bacterial-derived metabolites....................................143

4.1.6. Other metabolites..143

4.2. Mouse pneumonia model..144

4.2.1. TCA cycle intermediates..144

4.2.2. Energy metabolism...152

4.2.3. Metabolism of amino acids.......................................152

4.2.4. Osmolytes with metabolic function and their derivatives....155

4.2.5. Creatine metabolism..155

4.2.6. Food-derived and bacterial-derived compounds..............156

4.2.7. Carbohydrates..158

4.2.8. Components of the cell membrane.................................159

4.2.9. Distribution of metabolites in biofluids...........................160

4.3. Summary...161

4.4. References...160

List of Tables

Number	Name	Page
Table 1.1	Frequencies of infectious agents of community acquired pneumonias (CAP)	4
Table 2.1	Viability of A549 cells after 24 h post infection	57
Table 2.2	Bacterial multiplication during co-culturing with A549 cells after 24 h of incubation	73
Table 4.1	Concentrations of metabolites in the biofluids of mice, infected with *S. pneumoniae*	147-149
Table 4.2	Concentrations of metabolites in urine of mice, infected with *S. pneumoniae* in longitudinal study	150-151

List of Figures

Number	Name	Page
Figure 1.1.	Local changes in metabolites in the lung during pneumonia	19
Figure 1.2.	*S. pneumoniae*-induced apoptosis	20
Figure 1.3.	Glycolysis and the TCA cycle	30
Figure 1.4.	Glucose catabolism in *S. aureus*	32
Figure 1.5.	Bacterial count in bronchoalveolar lavage fluid and lung tissue after intratracheal instillation of *S. pneumoniae*	39
Figure 1.6.	Leukocyte count in bronchoalveolar lavage (BAL) fluid of BALB/c and C57Bl/6 mice after intratracheal instillation of *S. pneumoniae*	40
Figure 1.7.	Amino acid degradation in humans	43
Figure 1.8	Amino acid metabolism in muscles during fasting	45
Figure 1.9.	Metabolism of betaine and transmethylation processes	46
Figure 1.10	Metabolism of creatine and creatinine.	48
Figure 2.1.	Design of experiments of bacteria-cell interactions	54
Figure 2.2.	Concentrations of TCA cycle intermediates in the supernatants of infected with different doses of *S. pneumoniae* 24 h post-infection	64
Figure 2.3	Amino acids in the supernatant of A549 cells, infected with different doses of *S. pneumoniae* 24 h post-infection	65
Figure 2.4.	Glucose and products of glycolysis lactate and pyruvate in the supernatant of A549 cells, infected with different doses of *S. pneumoniae* 24 h post-infection	66
Figure 2.5.	Bacterial-derived metabolites in the supernatant of A549 cells, infected with different doses of *S. pneumoniae* 24 h post-infection	67
Figure 2.6.	Biologically active compounds in the supernatant of A549 cells, infected with different doses of *S. pneumoniae* 24 h post-infection	68
Figure 2.7.	Effect of bacterial infection on mitochondrial potential and cell viability	71

Figure 2.8. Morphology of A549 cells, infected with different doses of *S. pneumoniae* 24 h post-infection 72
Figure 2.9. TCA cycle intermediates in the supernatant of A549 cells infected with different doses of *S. aureus* 76
Figure 2.10. Metabolism of amino acids isoleucine, threonine, and derivative tartrate in supernatant of A549 cells infected with different doses of *S. aureus*. Consumption of isoleucine, threonine, and production of tartrate in DMEM by *S. aureus* 77
Figure 2.11. Glycolysis intermediate concentrations in supernatants of *S. aureus*-infected A549 cells 78
Figure 2.12. Ketones and small organic acid concentrations in supernatants of *S. aureus*-infected A549 cells 79
Figure 3.1. Design of cross-sectional study of mouse pneumonia model 83
Figure 3.2. Design of longitudinal study 84
Figure 3.3. Total cell counts (macrophages and neutrophils) in BAL 24 h post-infection with *S. pneumoniae* 93
Figure 3.4. Bacterial counts in lung tissue and blood 24 h post-infection with *S. pneumoniae* 94
Figure 3.5. Lungs of sham and infected mice 95
Figure 3.6. Production of urine by infected and sham mice in longitudinal study. Average volumes of collected mouse urine 97
Figure 3.7. Concentrations of TCA cycle intermediates in biofluids of mice from cross-sectional study 24 h post-infection with *S. pneumoniae* or sham-treatment 99
Figure 3.8. Concentrations of TCA cycle intermediates in biofluids of mice from cross-sectional study 24 h post-infection with *S. pneumoniae* or sham-treatment 101
Figure 3.9. Concentrations of TCA cycle intermediates *S. pneumoniae* – infected mouse urine. 102
Figure 3.10. Concentrations of TCA cycle intermediates *S. pneumoniae* – infected mouse urine 103
Figure 3.11. Concentrations of essential amino acids in biofluids of mice from cross-sectional study 24 h post-infection with *S. pneumoniae* or sham-treatment 105
Figure 3.12. Concentrations of nonessential amino acids in biofluids of mice from cross-sectional study 24 h post-infection with *S. pneumoniae* or sham-treatment 107
Figure 3.13. Levels of glycine and tryptophan in mouse urine in a longitudinal study of *S. pneumoniae* – infected mice 108
Figure 3.14. Concentrations of energy metabolism intermediates in biofluids of mice from cross-sectional study 24 h post-infection with *S. pneumoniae* or sham-treatment 109

Figure 3.15. Concentrations of glucose and lactate in urine in longitudinal study 111
Figure 3.16. Concentrations of osmolytes, constituents of host cell membranes, and their derivatives in biofluids of mice 113
Figure 3.17. Concentrations of carnitine and O-acetylcarnitine in mouse urine in longitudinal study 114
Figure 3.18. Concentrations of osmolytes, membrane constituents, nucleotides, and derivatives in biofluids of mice from cross-sectional study 24 h post-infection with *S. pneumoniae* or sham-treatment 115
Figure 3.19. Concentrations of choline and ethanolamine in urine in longitudinal study 116
Figure 3.20. Concentrations of creatine and derivatives in biofluids of mice from the cross-sectional study 24 h post-infection with *S. pneumoniae* or sham-treatment 117
Figure 3.21. Concentrations of creatine and guanidoacetate in urine samples from longitudinal study 118
Figure 3.22. Concentrations of creatinine in urine samples from longitudinal study 119
Figure 3.23. Concentrations of bacteria- and food-derived metabolites in biofluids of mice from cross-sectional study 24 h post-infection with *S. pneumoniae* or sham 121
Figure 3.24. Concentrations of acetate and trigonelline in urine in longitudinal study 122
Figure 3.25 PCA plot of urine metabolites of sham and *S. pneumoniae*-infected mice 124
Figure 3.26. PCA plot of urine metabolites of sham and *S. pneumoniae*-infected mice in the longitudinal study. 125-126
Figure 3.27 Cell counts in BAL 24 h post-infection with *S. aureus* 128
Figure 3.28. Bacterial counts in lung tissue and BAL 24 h post-infection with *S. aureus* 129
Figure 3.29. Histology of mouse lungs 24 h post-infection with *S. aureus* 130
Figure 3.30. Concentrations of TCA cycle intermediates and intermediates of energy metabolism in urine of mice treated with *S. aureus* or Sham 131
Figure 3.31 Concentrations of osmolytes, membrane constituents, nucleotides, amino acids and derivatives 24 h post-infection with *S. aureus* or sham-treatment 132
Figure 3.32. Concentrations of bacteria- and food-derived metabolites in urine of mice from cross-sectional study 24 h post-infection with *S. aureus* or sham-treatment 133

List of Abbreviations

A549 cells — human alveolar basal epithelial cells

ADP — adenosine diphosphate

AIF — apoptosis-inducing factor

ATP — adenosine triphosphate

BAL — broncho-alveolar lavage

BAP — blood agar plates

BCAAs — branched chain amino acids

CAP — community-acquired pneumonia

cfu — colony-forming unit

EIA —enzyme immunoassays

EDTA — ethylenediaminetetraacetate

ESR —erythrocyte sedimentation rate

DNA —deoxyribonucleic acid

DMEM — Dulbecco's Modified Eagle's Medium

FBS — fetal bovine serum

HAP — hospital-acquired pneumonia

HBSS — Hanks' balanced salt solution

H/E — hematoxylin eosin stain

IAP — immunocompromised-associated pneumonia

IFN-γ — interferon-γ

IL — interleukin

LDH —lactate dehydrogenase

MIPs — macrophage inhibitory proteins

MRSA — methicillin-resistant *Staphylococcus aureus*

NEAA — non-essential amino acids

NMR — nuclear magnetic resonance

NO — nitric oxide

PC — principal component

PCA — principal components analysis (a multivariate analysis tool)

PCD — programmed cell death

PCR — polymerase chain reaction

PGE_2 — prostaglandin E_2

PVL — Panton-Valentine leukocidin

ROS — reactive oxygen species

SGLT — sodium-glucose co-transporter

SpA — surfactant protein A

SpD — surfactant protein D

SpxB — pyruvate oxidase

TCA — tricarboxylic acid cycle

THB — Todd-Hewitt broth

TLR — Toll-like receptor

TMA — trimethylamine

TMAO — trimethylamine-N-oxide

TNF — tumor necrosis factor

Chapter 1

General Introduction

1.1. Pneumonia: description and diagnosis

Pneumonia is a disease of the lung, characterised by inflammation and consolidation of lung tissue due to respiratory infections (Marrie, 1997). It is caused by more than 100 pathogenic infectious agents, each with slightly different epidemiology, history of disease, symptoms, complications, and pathogenesis (Mandell, 2000; Levison, 1998). The etiologic diagnosis of pneumonia is beneficial for proper treatment and prognosis, but in many cases is difficult or impossible with current methods (Mandell, 2007). Current methods comprise consideration of the history of the disease, a clinical picture of the disease, physical and radiological investigations, laboratory studies of patient samples (to examine pathological processes in the lung) for educated guesses about diagnosis, and bacteriological analysis for definite and suggestive diagnosis (Marrie, 1997; Levison, 1998). New methods of etiologic diagnosis of pneumonia that can give either definite or suggested diagnoses are also beneficial, especially with the recent increase in a risk population, the appearance of new causative agents of pneumonia, and an increase in antibiotic-resistant strains (Marrie, 1997). One of the more novel methods is metabolomics (metabolic profiling) which has been used to determine metabolic changes during diabetes mellitus (Salek, 2007), and damage of kidney (Nicholson, 1985) and liver (Waters, 2006). Metabolomics is the study of small molecular weight compounds with the help of high-throughput methods and multivariate data analysis (such as principal component analysis [PCA] and partial least squares) to describe a holistic picture of metabolic changes in an organism, biofluids, cell, or tissues as a result of environmental influences (German, 2005; van der Werf, 2005; Weckwerth, 2003), including pneumonia. Information obtained by diagnostic methods often has prognostic and monitoring value (Marshall, 1995).

1.1.1. Epidemiology and etiology of pneumonia

Pneumonia and influenza are two of the most common infectious diseases and are leading causes of death in the United States (Anderson, 2005). Pneumonia alone has an incidence of approximately 4 million cases annually and is the sixth leading cause of death in the USA (Mandell, 2000). Worldwide, mortality due to pneumonia is approximately 4 million children and 2 million neonates per year (Ferreira, 2003). In the United States pneumonia causes 600,000 hospital admissions, 64 million patient-days of restricted activity, resulting in $12 out of $23 billion of the yearly cost of treating community-acquired pneumonia (Colice, 2004; Mandell, 2000; Marrie, 1997).

Pneumonia can be classified as community-acquired (CAP), hospital-acquired (HAP), or immunocompromised-associated (IAP) according to the following criteria: the type of causative organism, predisposing factors, its route into the host body, its clinical manifestation, co-morbidities, and complications (Mandell, 2000; Levison, 1998). Some authors also distinguish non-severe and severe CAP and HAP, pneumonia in elderly population of nursery homes, geographically associated pneumonia and recurrent pneumonia (Mandell, 2007; Macfarlane, 2000).

The most common infectious agents causing CAP, are *Streptococcus pneumoniae, Haemophilus influenzae, Staphylococcus aureus, Mycoplasma pneumoniae, Moraxella catarrhalis* (Table 1). Community-acquired pneumonia caused by *Streptococcus pneumoniae* and by *Staphylococcus aureus* are the main subject of the present study.

Causative agent	Contribution (%) (range)
Streptococcus pneumoniae	36% (20-60 %)
Influenza virus	8% (2-8 %)
Mycoplasma pneumoniae	7 % (1-6 %)
Legionella species	6 % (2-8 %)
Haemophilus influenzae	9 % (3-10 %)
Chlamydia pneumoniae	4-6 %
Other viruses	5 % (2-15 %)
Psittacosis/ Q fever	3 % (0-6 %)
Gram-negative enteric bacilli	3 % (3-10 %)
Staphylococcus aureus	2 % (2-5 %)
No identified causative agent	36 % (30-50 %)

Table 1.1 Frequencies of infectious agents of community acquired pneumonias (CAP) with *Streptococcus pneumoniae* being the leading agent in the world. Only a small number of CAP cases have mixed infections (caused by two or more species of bacteria, not shown). The large number of unidentified causes and some discrepancies in different studies suggest imperfections in current diagnostic methods. Modified from Macfarlane, 2000; Schmitt, 2002; Mandell, 2000.

This review will include a summary of risk groups, preferential routes of bacterial invasion into lung alveoli, clinical and laboratory methods of diagnosis of pneumonia, evaluation of severity of disease for prognosis and monitoring, and known data of changes in homeostasis and metabolism.

1.1.1.1. Risk groups

The risk groups for *S. pneumoniae* and *S. aureus*-caused pneumonia are children under 2 years, the elderly over 65, and individuals with predisposing factors who acquire new strains of bacteria, have other respiratory and extrapulmonary diseases (which increase colonisation of bronchi and oropharynx by these bacteria and decrease local immune response), and compromise immune systems (Marrie, 1997; Reynolds, 1994). An increased incidence of pneumococcal pneumonia is observed in people who have changed living or working environments (such as admission to school, army, prison, or starting new job), individuals with chronic obstructive pulmonary disease (COPD), cystic fibrosis, genetic immunoglobulin G_2 or G_4 deficiency, recent viral infection, congestive heart failure (Farr, 1994; Harford, 1950). *S. aureus*-caused pneumonia is relatively rare in healthy adults and happens either in neonates or in patients after viral pneumonia, however *S. pneumoniae*-caused pneumonia still prevail (Reynolds, 1994). Patients with diabetic ketoacidosis, cystic fibrosis, and alcohol abuse (without aspiration of stomach contents) have increased incidence of both *S. pneumoniae* and *S. aureus*- pneumonia (Reynolds, 1994; Marrie, 1997; Kahl, 1998; Levison, 1998; Macfarlane, 2000). In other words, risk groups of pneumococcal and staphylococcal pneumonia overlap significantly, decreasing their usefulness for diagnosis.

1.1.1.2. Routes of infection

Pneumonia starts with lung alveolar infection by pathogens through several routes: aspiration of nasopharyngeal secretion with bacteria during sleep, inhalation of infectious aerosol, hematogenous infection from other sites in the body, direct transportation of bacteria in the trachea and lung during intubation, or spread of bacteria from adjacent infected organs and wounds (Schmitt, 2002). The first mechanism, aspiration of nasopharyngeal secretion, is the most common cause for *S. pneumoniae*- and *S. aureus*-induced CAP (Woods, 1994). The nasopharynx is colonised by *S. pneumoniae* in 5-10% of healthy adults (and 20-40% of healthy children) and by *S. aureus* in 20-40% of healthy adults. The colonisation of one species counteracts with colonisation of the other which possibly decreases the probability of mixed bacterial pneumonia (McNally, 2006; Mandell, 2000; Kluytmans, 1997; and Musher, 1998). Aspiration of nasopharyngeal secretion during sleep occurs in 50% of normal individuals (and in 70% of individuals with severe disease or impaired consciousness), which can lead to pneumonia (Woods, 1994). Person to person spread of strains of *S. pneumonia* and *S. aureus* is probably done by large droplets of aerosol and unwashed hands (Farr, 1994). Small droplets of aerosol (diameter 3–5 μm) can reach alveoli and cause disease, as have been observed with a number of pathogens (for instance *Mycobacterium tuberculosis,* influenza virus, *Legionella* spp., *Histoplasma* spp., *Chlamydia psittaci,* and *Coxiella burnetii,* but rarely by *S. pneumoniae* and *S. aureus*) (Levison, 1998).

1.1.2. Current methods to determine etiology and severity of pneumonia

1.1.2.1. Clinical manifestations

Clinical manifestations of CAP caused by different bacteria are not specific and cannot be used for etiologic diagnosis; however, they are helpful in determination of the other important characteristics of disease: current stage, severity, complications, prognosis, necessary additional diagnostic methods and treatment (Levison, 1998). The most common signs include tactile fremitus, dullness, decreased breath sounds, wheezes, crackles, bronchial breath sounds, and tachypnea, as well as symptoms of fever, cough with or without sputum, decreased appetite, and night sweats (Mandell, 2000). Less frequent symptoms are pleuritic chest pain, rigors, dyspnea, headache, myalgias, and diarrhea (Isselbacher, 1994). Severe pneumonia can manifest itself with dramatically abnormal temperature (lower than 35° C or higher than 40° C), decreased blood pressure, tachycardia, significantly increased respiratory rate, hypoxia (with cyanosis of skin, fingers, and lips), or altered mental status (Mandell, 2007). These symptoms often appear some time after the beginning of lung inflammation, peak at the climax of disease, and disappear after inflammation decreases. Thus, symptoms are important in diagnosis of pneumonia and in monitoring of health status with relatively low sensitivity and specificity of syndromes (Mandell, 2000).

1.1.2.2. X-ray analysis

Chest radiographs are the gold standard for diagnosis of pneumonia (although certainly not perfect) and the findings on the radiograph usually are not indicative of the causative agent of the pneumonia.

1.1.2.3. Bacteriological methods to determine etiologic diagnosis of pneumonia

Bacteriological analysis of sputum samples, blood, and pleural effluent detect presence of bacteria in normally sterile body compartments and are used to make definite, probable or possible diagnosis of pneumonia (Mandell, 2007).

1.1.2.3.1. Sputum analysis

Bacteriological analysis of sputum samples includes visual observation and examination of cultured specimens and sputum. "Dirty" and bloody sputum with an unpleasant odour suggests anaerobic flora, "rusty" sputum suggests *S. pneumoniae* infection (usually some time after the beginning of pneumonia) (Marrie, 1997).

Gram-stained sputum samples (containing > 25 leukocytes and < 10 epithelial cells to be distinguished from saliva), can confirm the presence of *Streptococci, Staphylococci, Haemophilus, Nocardia, Actinomyces, and Aspergillus* (Marrie, 1997; Levison, 1998; Farr, 1994). A large amount of lancet-like Gram-positive encapsulated diplococci suggest *S. pneumoniae* infection (*S. pneumoniae* serotype 3 produce chains more often than other serotypes *in vivo*, but the lancetoid shape of each bacterium is preserved [Forbes, 2002]). Accumulation of grape-like clusters of Gram-positive cocci suggests *S. aureus* infection. Gram-negative bacillus on the slide may be a sign of mixed infection (which can complicate Gram-positive pneumonias) or anaerobic infection; however, Gram-negative bacillus can derive from saliva of mouth or from mucus of the upper airway and thus diagnosis is doubtful (Levison, 1998). Bacteriologic and mouse model experiments show that 10 gram-positive lancet-like diplococci under a low-power field are specific for *S. pneumonia*-caused pneumonia in 85% of cases and sensitive in

62% (Schmitt, 2002). However, this method becomes less efficient with small amount of sputum and is subject to variability between investigators (Mandell, 2007).

Sputum culture is informative for diagnosis of tuberculosis and fungal infections of the lungs, but it has less value for diagnosis of many Gram-positive and Gram-negative bacteria due to contamination with oral microflora, patients who have received antibacterial treatment, or intubated patients (Pentington, 1994). In winter, colonies of *S. pneumonia* and *S. aureus* can be found on the airway mucosa in 50% of relatively healthy people and can contaminate sputum samples (Macfarlane, 2000). Sputum culture is positive for pneumococci in one-half of patients with pneumonia diagnosed by transtracheal aspiration and positive blood culture (Farr, 1994). Pneumonia patients are diagnosed by levels exceeding 10^6 colony-forming units/mL in sputum, 10^4 colony-forming units/mL in lavage fluid, or 10^3 colony-forming units/mL in transtracheal aspirate for proper interpretation of sputum culture (Farr, 1994). *S. aureus* is cultured on 5% sheep blood agar and produce smooth, translucent colonies that are slightly raised above the surface, These colonies appear white-yellow at first and became yellow later, surrounded by transparent halo of β-hemolysis (most pathogenic strains), coagulase-positive or produce extracellular coagulase (most cases), and that can be lysed with lysostaphin (Forbes, 2002). *S. pneumoniae* grows on 5% sheep blood agar and produces small, grey, and glistening colonies with sharp edges and excavation in the centre of each colony, surrounded by α-hemolytic halos, and which are bile-soluble and Optochin-sensitive (Forbes, 2002).

If data interpretation is complicated by colonization of throat bacteria and the patient does not respond to the applied treatment, secretions should be taken by fiberoptic bronchoscopy with a protected brush or device for bronchoalveolar lavage, transtracheal, transbronchial aspiration, or transcutaneous aspiration (Schmitt, 2002). However, due to invasiveness and possible complications, usage of these methods is not very common (Mandell, 2000).

Other bacteriological methods include culture of blood, pleural effluent and serological tests for pneumococcal antigen. A positive blood culture provides a definite etiologic diagnosis with high specificity and low sensitivity, since the culture is positive in approximately 10–20% of cases of bacterial pneumonia (Marrie, 1997; Farr, 1994). Up to 60% of cases of pneumococcal pneumonia have pleural effusion and pneumococci can be recovered in 1-2% of effluents (Taryle, 1978; Storch, 1998), while effluent from other bacterial pneumonias may be infected in approximately 10-30% of cases (Levison, 1998; Joseph, 2003).

1.1.2.3.2. Other methods

Antigen detection tests. Counterimmunoelectrophoresis detects pneumococcal antigens in the urine of 50%, in the serum of 10%, and in the sputum of 75% of patients in 2–3 h of analysis (Navarro, 2004; Farr, 1994). This method (as well as latex agglutination, enzyme immunoassays [EIA] of different pneumococcal antigens [Murdoch, 2001]) is not often used in clinic, but can be potentially useful for patients who have received antibiotic treatment and who produce little sputum (Farr, 1994).

Molecular techniques. The polymerase chain reaction (PCR) analysis of samples is a very sensitive method which may be used to identify many types of pathogens (Renz, 1991; Petit, 1991). However, it is rarely used in clinics for diagnosis of bacterial pneumonias (Mandell, 2000) because of its novelty and some reported false-positive results of detection of bacteria that colonize the nasopharynx or bronchi, but do not cause pneumonia (Pennington, 1994; Ieven, 2004).

Hematological tests. Changes in peripheral blood are used to evaluate severity and immune response during pneumonia; however, they are not specific for different bacterial infections (Schmitt, 2002; Levison, 1998).

Biochemical analysis of blood. Biochemical characteristics of pneumonia are usually not specific and used to evaluate severity of disease in lung, reactivity of organism (acute-phase response), and damage of host cells and organs (slightly increased liver tests [Lewison, 1998]).

1.1.3. Metabolic changes in human with pneumonia

Metabolic changes in the biofluids of patients with pneumonia (as assessed by the measurement of a few metabolites) are nonspecific and reflect mainly disease severity and complications. Increased bilirubin (up to 68 μmol/L in serum) indicates lysis of erythrocytes, hypoxia, and damage of hepatocytes (Musher, 1998). Severe complicated pneumonia is associated with increased urea, creatine, and creatinine, as result of severe catabolic processes and therefore, have prognostic and monitoring value (Brandenburg, 2000). Electrolyte balance may also be compromised: some pneumonia patients develop mild hyponatremia (Lee-Levandrowski, 2002; Marshall, 1995), hyponatremia together with hypophosphatemia indicate Legionnaires' disease (Cunha, 1997).

To summarize, diagnostic methods of bacterial pneumonia show definite, probable or possible etiological diagnosis in approximately 20–30% of cases (Mandell, 2000; Bates, 1992). Combinations of the previously discussed diagnostic methods which test blood, sputum, pleural effluent, and intratracheal aspirates can increase diagnostic efficiency up to 85% of all hospitalised patients with pneumonia (Ruiz-Gonzalez, 1998). However, due to invasiveness of some of these methods, and increased time of etiologic diagnosis, they are unsuitable for current clinical practice. The biochemical and hematological methods also evaluate the severity of the inflammatory syndrome and have prognostic and monitoring value.

1.2. Pathogenesis of pneumonia and potential changes in metabolism

1.2.1. Systemic changes in homeostasis and their influences on metabolism

Systemic changes during pneumonia include hypoxia, acidosis, decreased food intake (due to decreased appetite), weight loss, toxic syndrome (due to inflammation), and increased temperature. These changes influence physiological processes which in turn modify the concentrations of metabolites in biofluids and tissues of patients. Some mechanisms of metabolic changes are known due to either *in vivo* or *in vitro* studies; the rest remain to be described.

1.2.1.1. Hypoxia

Gas exchange, the main function of the lungs, is impaired during pneumonia with subsequent relative respiratory insufficiency (Taylor, 1985). Pneumonia leads to exudation into alveoli with progressive decrease in diffusion of gases (alveolar-capillary block) until alveoli become respiratory dead space. Edema leads to decreased oxygen levels locally in alveoli (hypoxia) and increased carbon dioxide levels (hypercapnia). Shunting of venous blood through poorly ventilated alveoli can further facilitate disturbance in blood gas levels and systemic hypoxia. Hypoxia can lead to numerous changes in lung and systemic metabolism. Local hypoxia can lead to increased anaerobic and decreased aerobic respiration with increased production of lactate in the infected alveoli. Lactate diffuses from tissue into blood due to a concentration gradient with subsequent uptake in liver and utilization for gluconeogenesis (Frayn, 2003). Severe pneumonia and sepsis can lead to significant hypoxia, hypercapnia, and increased lactate concentration in blood (Gernardin, 1996). Hypoxia also leads to increased production of angiotensin II due to activated angiotensin-converting enzyme into the lung (Gillis, 1977) with subsequent changes in distribution of electrolytes and metabolites which I will discuss further.

1.2.1.2. Local and systemic acidosis

Uncompensated hypoxia during severe pneumonia is accompanied by respiratory acidosis (Marshall, 1995). Additional contributing factors are increased production of lactate in the lung and (during severe pneumonia) in tissue, decrease in food intake due to loss of appetite and subsequent lipolysis and gluconeogenesis with production of ketone bodies (relative importance of the later metabolic pathway for mice is not completely known). Increase in hydrogen ion concentration in blood is balanced by augmented secretion of it in the urine (with its subsequent acidification of the urine) and increased ventilation (Marshall, 1995). This process is partially compensated in kidney by catabolism of amino acids and release of ammonia into kidney to increase urine pH and reabsorb sodium ions (Marshall, 1995). Increased catabolism of amino acids for production of ammonia leads to decreased concentrations of amino acids in biofluids and shunting of nitrogen into ammonia rather than into production of urea. Acidification of urine leads to increased reabsorption of some metabolites such as citrate (Brennan, 1988).

1.2.1.3. Decreased food uptake

Decreased appetite leads to decreased food intake as a part of physiologic response to infection. Decreased food intake results in decreased concentrations of food-derived metabolites, such as glucose, amino acids, fatty acids, and other. Decreasing concentrations of glucose in biofluids tend to be rapidly corrected (because of the high importance of glucose for the organism) by increased gluconeogenesis from amino acids, fatty acids, lactate, acetate, and other metabolites (Coffee, 1998). Increased catabolism of amino acids for gluconeogenesis leads to catabolism of proteins (especially in skeletal muscles) to restore the amino acid balance, leading to a net decrease of concentrations of amino acids and increased concentrations of urea in biofluids (Salway, 1994). Wasting of organs and tissues are significant and well described in chronic infectious diseases such as tuberculosis, but less significant *S. aureus* and *S. pneumoniae* infections (Langen, 2006). The general outcome of these processes is increased catabolism and decreased anabolism.

1.2.1.4. Toxic syndrome

During inflammation caused by bacteria, many substances are released locally and systemically: bacterial enzymes, metabolites, components of cell wall and toxins, host cell metabolites, enzymes from damaged and dead cells, and fractions of peptides, lipids and nucleic acids as a result of inflammation and cytokine action. The concentrations of these substances increase in more severe pneumonia, during bacteremia and especially sepsis. The host counteracts these deleterious influences by phagocytosis of larger particles by macrophages in spleen, liver, and other organs, by excretion of smaller peptides in kidney, and uptake of unregulated metabolites by hepatocytes (Amersfoort, 2003). A large proportion of the released metabolites are re-utilised, and some peptides (especially from extracellular spaces) are metabolised by the host's phagocytes and kidney epithelium, but the overall picture is not completely understood and may result in loss of peptides in urine (Marshall, 1995) as part of catabolic processes. Damaged cells may either repair themselves or die, and are replaced by new ones.

1.2.1.5. Oxidative stress

Pneumonia is associated with oxidative stress due to increased production of reactive oxygen species (ROS) by bacteria, and by host immune cells as part of the immune response (Rahman, 2000; Pullar, 1999). The resulting products, such as chlorinated fatty acids, modified proteins, as well as some released enzymes and metabolites, can produce changes and damage in adjacent and distant organs and tissues (Dorman, 2005; Fliss 1988). Increased oxidant production leads to the depletion of many enzymatic and non-enzymatic antioxidants in pneumonia patients (Cemek, 2006). For instance, allantoin may be found in increased concentrations due to oxidation of uric acid (Becker, 1993).

1.2.1.6. Metabolic changes due to cytokine action

During pneumonia with Gram-positive bacteria, the proinflammatory cytokines interleukin 1β (IL-1β), IL-6, and tumor necrosis factor (TNF) are found in the serum of patients and mice, as well as locally in the broncho-alveolar lavage (BAL) and lung (Puren, 1995; Bergeron, 1998). Other cytokines produced during inflammation can be found in lung and BAL, and do not influence the host organism systemically (Gallard, 1994). During bacteremia, and especially sepsis, more cytokines are released into the blood and cause dramatic changes in homeostasis and metabolism (Dinarello, 2001;

Puren, 1995). Changes in homeostasis include greater symptoms of toxicity, edema, disseminated blood clotting and multiple organ failure (Puren, 1995, Li, 1995). Some of the metabolic consequences of systemic cytokine increases have been described, while metabolic changes at lower levels of cytokines, characteristic for mild and moderate pneumonia, remain to be described.

TNF causes initial hyperglycemia and late hypoglycaemia due to acute, significantly increased glucose production by the liver and a less significant but more sustained peripheral glucose uptake, especially by peripheral macrophages (Lang, 1992). The increase in systemic glucose production is due to elevated catecholamines, which also decrease tissue sensitivity to insulin. Low doses of IL-1β cause little to no change in blood glucose concentration; while high levels of IL-1β lead to transient hyper- and hypoglycaemia (Kelley, 2000). IL-1β causes significant hyperinsulinemia, blocked by somatostatin (Lang, 1995). The influence of IL-6 on glucose metabolism is not completely understood; this cytokine increases secretion of growth hormone and adrenocorticotropin, which can potentially change metabolism of glucose, amino acids, and fatty acids (Lyson, 1991).

1.2.1.7. Changes in osmolality of biofluids and osmolytes

Changes in osmolality of biofluids and tissues during pneumonia are rarely significant to be treated separately, but can potentially alter metabolite distribution (Hatson, 2002). Decreased concentrations of phosphates and sodium in blood are sometimes observed during *Legionella* pneumonia, but not *S. pneumoniae* or *S. aureus* pneumonias. Some studies show that some pneumonia patients develop a syndrome of inappropriate antidiuretic hormone secretion (SIADH) with hyponatremia, resulting in decreased osmolality in plasma and increased osmolality in urine, and with normal renal and adrenal function (Marshal, 1995). Host tissues compensate changes in osmolality of biofluids by uptake or excretion of blood osmolytes.

1.2.1.8. Bacteremia

During pneumonia, bacteremia usually develops due to invasion of bacteria into bloodstream after damage and death of pneumocytes and endotheliocytes. Additionally, pneumococci can enter the bloodstream through lymphatic nodes near lung roots or through the nasopharyngeal epithelium into the blood in pneumococcal carriers before development of pneumonia (LeMessurier, 2006). Large doses of invading pneumococci during severe pneumonia, or absence of a spleen, increase the probability of sepsis (DeVelasko, 1995). Pneumococcal pneumolysin facilitates the spread of bacteria into the blood and other host tissues by disrupting epithelial and endothelial layers directly with the help of activated complement (Rubins, 1993). *S. aureus* can enter the blood during pneumonia or from other organs before entering the lung tissue, resulting in different kinetics of the clinical and radiological findings. The ability of *S. aureus* to invade the bloodstream and other host organs and tissues depends on many virulence factors, and its mechanism is not completely known (Krut, 2003) In other words, bacteremia has prognostic (Mandell, 2000) rather than diagnostic value. Some aspects of bacterial kinetics and timing of bacteremia in the context of disease as well as their metabolic consequences remains to be discovered.

1.2.2. Local changes in lung during pneumonia

Changes in concentrations of metabolites during pneumonia can also be the result of local changes in the lung (Figure 1.1).

1.2.2.1. Virulence factors of *S. pneumoniae*

S. pneumoniae directly damages the host cells by releasing the toxin pneumolysin and secreting hydrogen peroxide (Braun, 2002). Pneumolysin is a proteinaceous toxin that enters cells membranes, oligomerizes, and forms pores in the cell membrane (Rubins, 1994). These pores are 30 nm in diameter and are permeable to water, potassium, sodium, and calcium ions, as well as organic molecules with a size equal or less than maltose. This increase in permeability can potentially change the concentrations of metabolites in cells and biofluids. Hydrogen peroxide causes apoptosis of neuronal cells, although it does not cause epithelial or endothelial cell death (Pericone, 2003; Braun, 2002; Rubins, 1992). Both pneumolysin and hydrogen peroxide cause an influx of calcium into host cells, which then can lead to increased mitochondrial permeability transition, increased intramitochondrial pH, release of mitochondrial apoptosis-inducing factor (AIF) and finally apoptosis (Tilley 2005; Braun, 2007). Pneumolysin activates phospholipase A of the host cell membrane (Rubins, 1994), which increases membrane permeability directly and indirectly due to detergent properties of released free fatty acids and lysophosphatides (Figure 1.2). Pneumolysin and hydrogen peroxide inhibit synthesis of phosphocholine by host cells as an additional mechanism of apoptosis (Zweigner, 2004). Activation of the complement by pneumolysin causes additional cell damage if the toxin is oligomerized in the cell membrane (Mitchel, 2000).

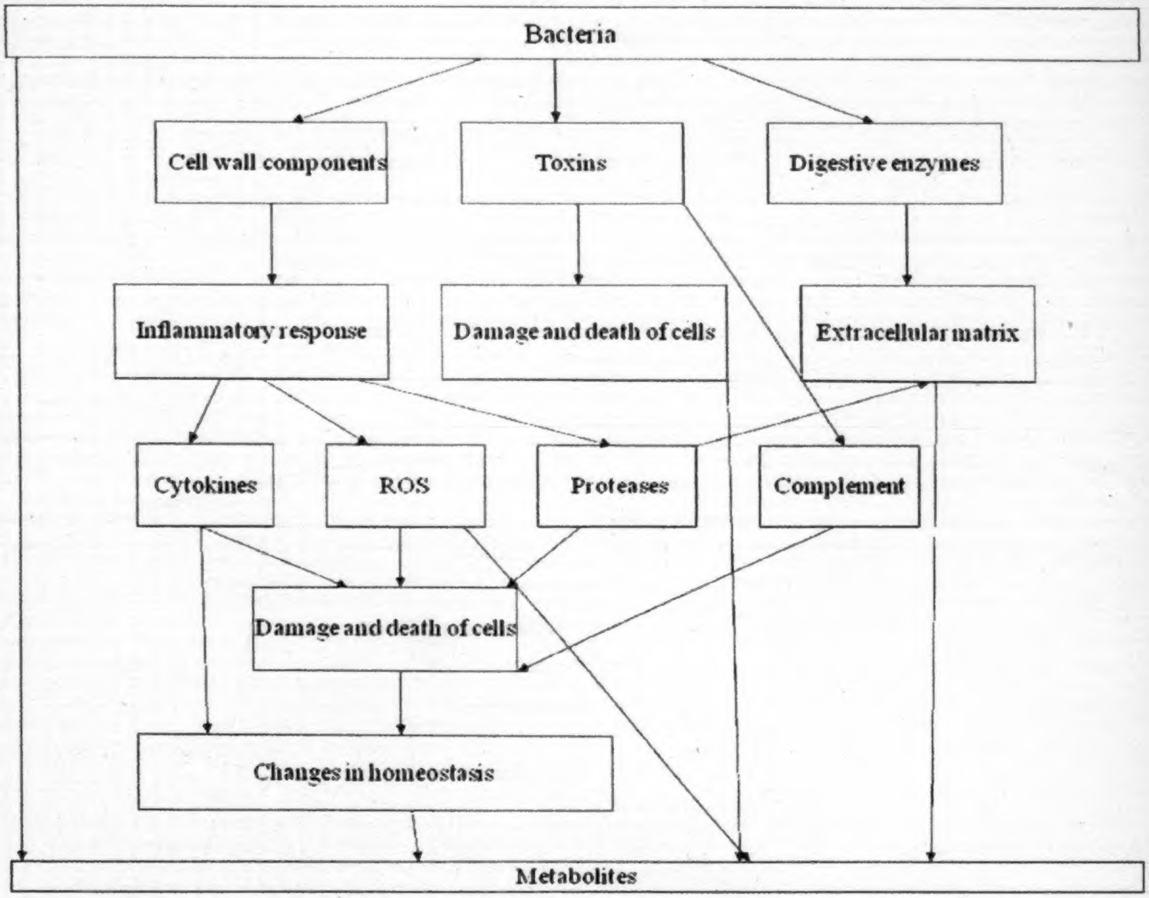

Figure 1.1. Local changes in metabolites in the lung during pneumonia

This figure shows that bacteria may consume some metabolites and produce others, depending on the metabolic pathways utilized by bacteria. Upon destruction by immune factors, bacteria release further metabolites. Bacterial virulence factors damage host cells and extracellular matrix which results in release of metabolites. The subsequent inflammatory response and its associated release of cytokines, ROS, and proteases changes homeostasis of cells directly, and damages host cells which leads to release of additional metabolites.

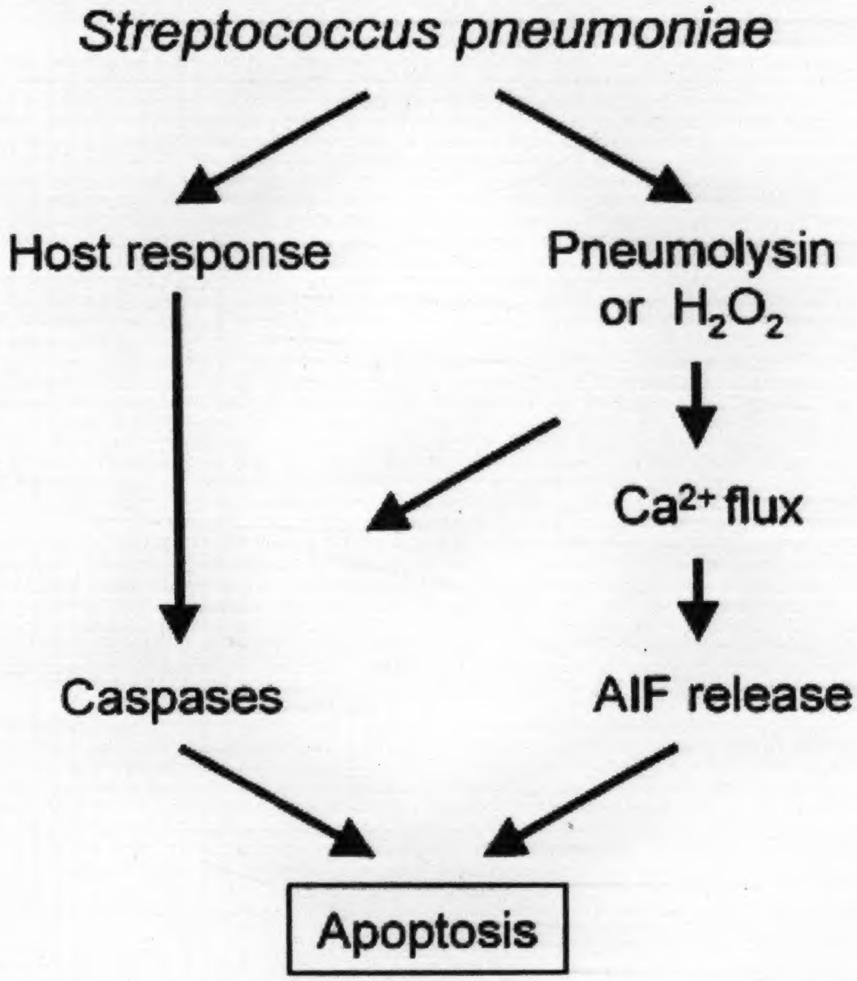

Figure 1.2. *S. pneumoniae*-induced apoptosis. Pneumolysin, hydrogen peroxide, and inflammatory responses in the host induce apoptosis of host cells. Modified from Braun, 2002.

1.2.2.2. Virulence factors of *S. aureus*

S. aureus produces several toxins which includes 4 types of cytotoxins: α-, β-, γ-, and δ-toxin with α-toxin being the most widely expressed among pathogenic strains, and causing the largest necrotic changes when injected into rabbit tissues and lethal for mice (Clancy, 1989). The group of γ-toxins include Panton-Valentine leukocidin (PVL), which attacks and destroys monocytes and neutrophils (Alouf, 2006). PVL-positive strains of *S. aureus* cause necrotising diseases of the skin and lung, resulting in necrotising pneumonia (Labandeira-Rey, 2007; Etienne, 2005). This leukocidin has less defined mechanisms of action and cell damage than α-toxin and usually affects macrophages and neutrophils (Alouf; 2006). The most widely expressed α-toxin creates a channel in the cell membrane with an internal diameter of 20 nm, the channel is freely permeable for sodium and potassium ions, which leads to cell damage and death (Prevost, 2001). There are some discrepancies in the literature about the precise type of cell death due to this hemolysin. *S. aureus* α-toxin causes activation of caspase 8, releases mitochondrial protein cytochrome c, and causes early cleavage of DNA into fragments, which are typical to apoptosis (Bantel, 2001). However, later in the course of apoptosis, ATP becomes depleted, membrane permeability increases, and cells die due to secondary necrosis (Essman, 2003; Haslinger-Loffler, 2006). In other words, the most important host cell-damaging factor of *S. pneumoniae* is pneumolysin; while for *S. aureus* it is α-toxin (Alouf, 2006). Both proteins are membrane- and mitochondria-damaging pore-forming toxins and causes osmotic perturbations (Ratner, 2006), but their influence on host cell and mitochondria metabolism has not been thoroughly studied.

1.2.2.3. Damage of extracellular matrix

Both *S. pneumoniae* and *S. aureus* spread in tissue by producing the enzyme hyaluronidase, which digests hyaluronic acid in extracellular spaces. *S. pneumoniae* spreads by secreting the fibrinolytic enzyme streptokinase, while *S. aureus* clots fibrin around itself (and becomes less susceptible to phagocytes) with coagulase (Brock, 1984). Secreted bacterial lytic enzymes digest complex macromolecules to metabolites outside of bacterial cells, releasing proteins, peptides, lipids, and carbohydrates on the surface of host cells, fibrinogen in the alveolar exudates, hyaluronic acid in the interstitial spaces, and glycocalyx, mucin, and DNA fibres on the surface of bronchi (Blazevich, 1975; Berger, 1938). The level of cell damage and death due to these enzymes is difficult to measure, but is generally considered to be less significant than death due to bacterial toxins (Rubins, 1992). Hyaluronidases and proteases digest cell parts and release sialic acids, peptides, probably hydrocarbons and amino acids; however, pathways of these processes and their relative intensity have not been fully elucidated (Deresiewicz, 1998; Mergner, 1990).

The glycocalyx of cells, proteins in mucin, and proteoglycans in extracellular spaces of interstitium contain large amounts of the carbohydrates glucose, galactose, iduronate, mannose, fucose, N-acetyl-D-glucosamine, and may be damaged by bacterial enzymes and by host immune cells. Proteins inside apoptotic and autophagic cells, and proteins released during necrosis are catabolised to amino acids and peptides, with the peptides being either metabolised by phagocytes and kidney epithelium or filtered into urine with largely unknown details and proportions (Marshal, 1995).

1.2.2.4. Local release and action of cytokines

Gram-positive bacteria (S. *pneumoniae* and *S. aureus*) contain peptidoglycan and lipoteichoic acid which are highly immunogenic (Fischer, 2000; Severin, 2000). Additional immunogenic factors are pneumolysin and α-toxin (Ezepchuk, 1996; Rietschel, 2000). Cell wall components causes local increases in IL-6, IL-8, IL-1, TNF, macrophage inhibitory proteins (MIPs), nitric oxide (NO), and prostaglandin E_2 (PGE_2) (Tuomanen, 2000). TNF is crucial for host response, but at high doses it causes apoptosis of cells (Kerr, 2002). Deficient complement activation by cell wall components of both bacteria and pneumolysin leads to depletion of complement and damage of endothelial cells with increased permeability (Tuomanen, 2000; Hostetter, 2000).

1.2.2.5. ROS and proteases

Activated leucocytes produce ROS accompanied by local decreases in glucose and release of numerous proteases from their granules (Kettle, 1997). Defence factors of neutrophils and macrophages cause different tissue damage (Thukkani, 2005). Superoxide, hydrogen peroxide and hypochlorous acid differentially cause death of phagocytosed bacteria with potential release of bacterial metabolites (Rosen, 2002; Hampton, 1998). ROS also denature enzymes and subsequently cause sublethal damage and cell death due to necrosis or apoptosis depending on tissue type, and concentrations of ROS and antioxidants (Englert, 2002; Jenner, 2002; Pullar, 1999; Hampton, 1998; Vaux, 1996). Mouse pneumonia model studies suggest that cell and tissue damage during the immune response, which happens preferentially at 24-48 h post-infection, is more significant than damage and death due to bacterial virulence factors at earlier periods of inflammation (Bergeron, 1998).

1.2.2.6. Cell damage and death

Apoptosis is a type of programmed cell death, which serves in survival and homeostasis of an organism (Michaelson, 1991). Morphologically, it is accompanied by nuclear chromatin condensation, karyopyknosis, shrinkage of cells, cleavage of cell proteins and DNA by caspases, well-preserved membrane integrity, phagocytosis of entire cells by macrophages without release of macromolecules into biofluids, and an absence of subsequent inflammation (Kerr, 1991). Apoptosis is generally considered not to be harmful for host (Haslett, 1999), but massive apoptosis of cells can promote subsequent apoptosis of other cells in the lung (Rydell-Törmänen, 2006, Wang, 2006). Massive apoptosis of cells in the lung during lobar pneumococcal pneumonia is believed to be the main reason for increased permeability of the lung epithelium and subsequent significant edema. Apoptosis is suspected to be very important in the pathogenesis of complications due to pneumonia, such as acute lung injury and acute respiratory distress syndrome. Metabolically, apoptosis induced by TNF and interferon-γ (IFN-γ) is characterized by preserved or increased levels of ATP in cells and decreased lactate production (Lutz, 2005). Some cell lines exhibit a transient increase in fructose-1,6-phosphate and glyceraldehyde 3-phosphate (Woods, 1998). Apoptosis is often associated with increased intracellular concentrations of lipids, phosphocholine, and phosphoethanolamine (Viola, 2000).

Necrosis is characterised by cell membrane damage, release of intracellular compounds, and subsequent inflammation (Michaelson, 1991). Metabolically, necrosis is often associated with decreased ATP concentrations and no changes in choline concentration (Valonen, 2004, Lutz; 2005).

Autophagic cell death is characterised by sequestration of part of the cytoplasm, organelles, and ingested bacteria into double membrane vesicles, formation of autolysosomes, and digestion of enclosed parts of the cell (Deretic, 2006; Amano, 2006). Some authors divide cell death with active processes of autophagy into two groups: type II and type III programmed cell death (PCD). Type II PCD is morphologically similar to apoptosis and contains a number of lysosomes in the cytoplasm. Type III PCD is characterised by early loss of membrane integrity and morphologically similar to necrosis. Metabolically, autophagy has not been fully characterised, but increased processes of protein catabolism and release of amino acids together with observations that autophagy is active during starvation can suggest increased release of small molecular weight components.

In other words, during inflammation in the lungs, host cells undergo damage from bacterial virulence factors, ROS, proteases from immune cells, and local changes in homeostasis as well as other factors (Berger, 1938; Blazevich, 1975). These sublethal changes can ultimately lead to cell death due to apoptosis or necrosis (Behnia, 2006; Chen, 1994) with the release of intracellular metabolites and enzymes. Changes in metabolite concentrations may be superseded by systemic changes due to hypoxia, decreased pH, or decreased food uptake.

1.2.2.7. Time course of local changes during pneumonia

The discussion in this section is based on mouse pneumonia model studies of Mohler, 2003; Dallaire, 2001; Gingles, 2001

Normal lungs

At the onset of infection, inhaled bacteria in drops of nasopharyngeal secretion may be destroyed by surfactant, secreted phospholipases, antibacterial peptides, surfactant protein A and D (SpA and SpD), lysozyme, activated complement, alveolar macrophages, and type II pneumocytes, among others (LeVine, 2000). Activated complement and phagocytosis by macrophages usually grant protection from specific bacteria, especially if the host has previously encountered the pathogen and has specific antibodies (Pennington, 1994). The antibodies may be absent, not present in sufficient quantities, or neutralised by specific bacterial proteases, therefore increasing the probability of pneumonia. Occurring at this moment, a small release of substances from dead bacteria such as endotoxins, metabolites, bacterial enzymes, and nasopharyngeal secretions are phagocytosed by alveolar macrophages. Alveolar macrophages may phagocytose and clear inhaled foreign particles and bacteria in the alveoli, usually without extracellular secretion of ROS, proteolytic enzymes, and subsequent lung damage.

Initiation of inflammation

Surviving bacteria adhere to specific targets in the lung (such as receptors on cell surfaces) and start multiplying, spreading to tissues, interstitial spaces, and potentially blood. If left unchecked, bacteria multiply in the alveoli, invade cells, spread to other alveoli through pores of Kohn, spread to the interstitial tissue and to the blood, and cause tissue damage with bacterial toxins and secreted enzymes, leading to activation of the immune system. Different bacteria employ slightly different profiles of bacterial virulence factors, which lead to different intensities of pathologic processes in the lung and potentially different metabolic consequences at this stage of inflammation. At early stages of infection, *S. pneumoniae* uses its polysaccharide capsule (with relatively low immunogenity and antiphagocytic function), the factor H-binding component, and pneumococcal surface protein S (PspA) to reduce cytokine production and recognition of bacteria by complement and macrophages. At these stages *S. pneumoniae* multiplies significantly in the alveoli without large inflammation. At later stages, a fraction of the pneumococcal population undergo lysis by immune factors, with release of highly immunogenic cytoplasmic toxin, pneumolysin, cell wall components (peptidoglycan and lipoteichoic acid) to deplete complement, induce host cell damage, reduce phagocytosis, increase spread, and thus promote bacterial survival (Tuomanen, 2000; De Velasko, 1995). *S. aureus* does not have capsule and cell wall components that are highly immunogenic, which together with numerous secreted toxins and enzymes causes increased immune response from the very beginning of infection (Dinges, 2000). Some bacteria cause localised inflammation (which can lead to focal necrosis and abscesses in the lung), while the others tend to cause more significant edema and more rapidly spread to the blood and lung interstitium. In other words, at early stages of pneumonia, alveoli undergo damage by apoptosis or necrosis of type I and II pneumocytes, endotheliocytes, exudation of plasma into the lung airspaces, and release of intracellular metabolites and enzymes. The specifics of these processes and their relative intensity and timing depend on the bacterial factors of pathogenicity and the local immune response.

Prolongation of inflammation

If the bacterial inoculum fails to be destroyed, then bacterial products, cell damage, and cytokines from infected alveoli further stimulate the immune response

(Chong, 1987). Specifically, monocytes and macrophages migrate to the lung from the blood, become activated, phagocytose bacteria, and produce a plethora of ROS and proteases (Chapman, 2002). The extent and pathways of microbial digestion and resultant products have not been fully elucidated, but probably include digestion of proteins to peptides through cellular machinery common to antigen-presenting cells. If bacteria levels are still high, immune reactions involve migration of neutrophils to the lung and activation to continue bacterial killing (Dallaire, 2001). Neutrophil activation involves release of many types of ROS (such as superoxide ion and hydroxyl radicals, hydrogen peroxide, hypochlorous and hypobromous acids), proteases (lysozyme, acid hydrolases), and other factors (lactoferrin, arginase). The chemical reactivity and the efficiency in killing bacteria of these antimicrobial factors cause significant collateral damage to the host tissue. Failure to maintain a strong neutrophil-driven immune response in the mouse pneumonia model leads to sepsis and host death (Wang, 2001). Excessive exudation of serum into alveoli and activation of neutrophils can lead to a severe complication of pneumonia: acute respiratory distress syndrome.

Histological features of inflammation in the lung include exudation of serum into lung interstitium and alveoli (edema), damage and changes to alveolar architecture, increased permeability in lung vessels, increased sputum production, and decreased respiratory function. On the cellular level, types I and II alveolocytes die due to neutrophil-derived inflammatory factors and shed from basement membrane, alveolar walls become disrupted, and interstitial cells and endotheliocytes undergo cell death.

Resolution phase

During reparation, cell debris from necrotic and apoptotic cells, neutrophils, exudated erythrocytes, and fibrin are cleared by macrophages without activation or a pro-inflammatory response. Severe inflammation in the lung can lead to secondary necrosis of a fraction of neutrophils and subsequent lung damage (Rydell-Törmänen, 2006). Type II pneumocytes multiply, partially differentiate to type I pneumocytes, and repair damaged alveoli without local fibrosis. Alveolar structure and functions are restored and systemic changes of the inflammation vanish. Biochemical processes are shifted towards anabolic processes of synthesis of macromolecules from metabolites, as a part of cell proliferation. Clinically, the host restores its healthy characteristics: activity, mobility, food uptake, and so on.

1.2.3. Metabolism of *S. pneumoniae* and *S. aureus*

S. pneumoniae and *S. aureus* are pathogenic microorganisms, which are adapted to live in the host organism and therefore receive nutrients from the host. For many species of bacteria, or even strains of the same species, it can be evolutionarily advantageous to simplify their own metabolism and obtain more metabolites from the host (Somerville, 2003). Additionally, many pathogenic bacteria have a complex life cycle which includes spreading and living in metabolically different environments, such as mucus droplets, mucous membranes, alveoli, interstitial spaces, blood, and intracellular spaces. Some studies have shown that the bacterial growth phase, metabolic pathways, and factors of pathogenicity depend on the growth environment (LeMessurier, 2006; Rice, 2005; Miller, 1973). Therefore, the known *in vitro* metabolic requirements of pathogenic bacteria potentially may be different from metabolites that are consumed *in*

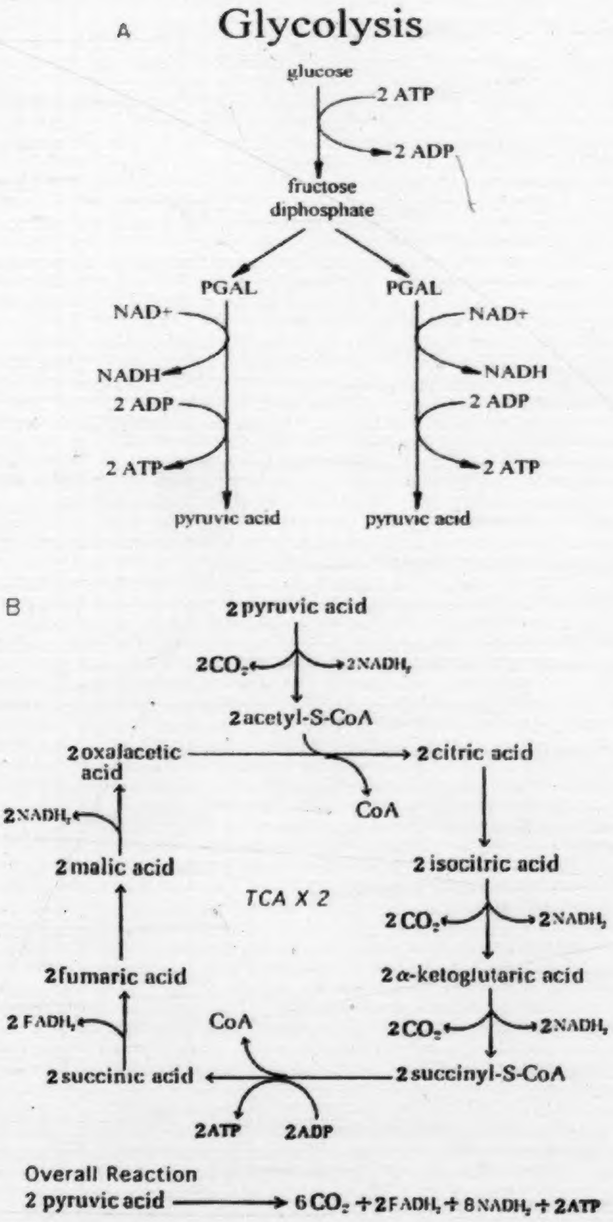

Figure 1.3. Glycolysis and the TCA cycle. (A) Glycolysis is a source of energy, pyruvate, and reduced nicotinamide adenine dinucleotide. (B) The TCA cycle, also known as the Krebs cycle, is a source of energy pyruvate, reduced nicotinamide adenine dinucleotide phosphate, and intermediates of amino acid synthesis. Modified from Todar, 2006.

vivo (Becker, 2005; Smith, 2007, White, 2007). Generally, while some bacterial species possess the complete tricarboxylic acid (TCA) cycle (Figure 1.3) and can produce most of their essential amino acids from TCA cycle intermediates (for instance, *S. aureus*); others have lost part of the cycle and depend on the host to obtain amino acids or amino acid predecessors (for example, *H. influenza*); while a third group of bacteria have no TCA cycle and consume amino acids or their intermediates from the host (for instance, *S. pneumoniae*). Additionally, many lactic acid bacteria can use citrate as energy source (Drider, 2004), but evolutionary-related pneumococci were not reported to have this ability.

1.2.3.1. Energy metabolism

S. pneumoniae employ glycolysis with the production of lactate as a primary source of energy. Pyruvate oxidase of *S. pneumoniae* produces the by-product hydrogen peroxide, which is one of the virulence factors of pneumococci that damage host cells and other bacteria (Pericone, 2000).

In anaerobic conditions, both *S. pneumoniae* and *S. aureus* consume glucose, catabolise it to pyruvate, which is reduced to lactate (*S. pneumoniae*) that is secreted, or decarboxylated to acetate with production of adenosine triphosphate (ATP) (especially *S. aureus*) and acetate is secreted into the medium. If the glucose level in the environment becomes low and oxygen concentration is high, *S. aureus* consumes acetate and catabolises it in the TCA cycle (Somerville, 2003) to carbon dioxide and water (Figure 1.4). This switch in energy metabolism is often accompanied by a switch from exponential to post-exponential phases.

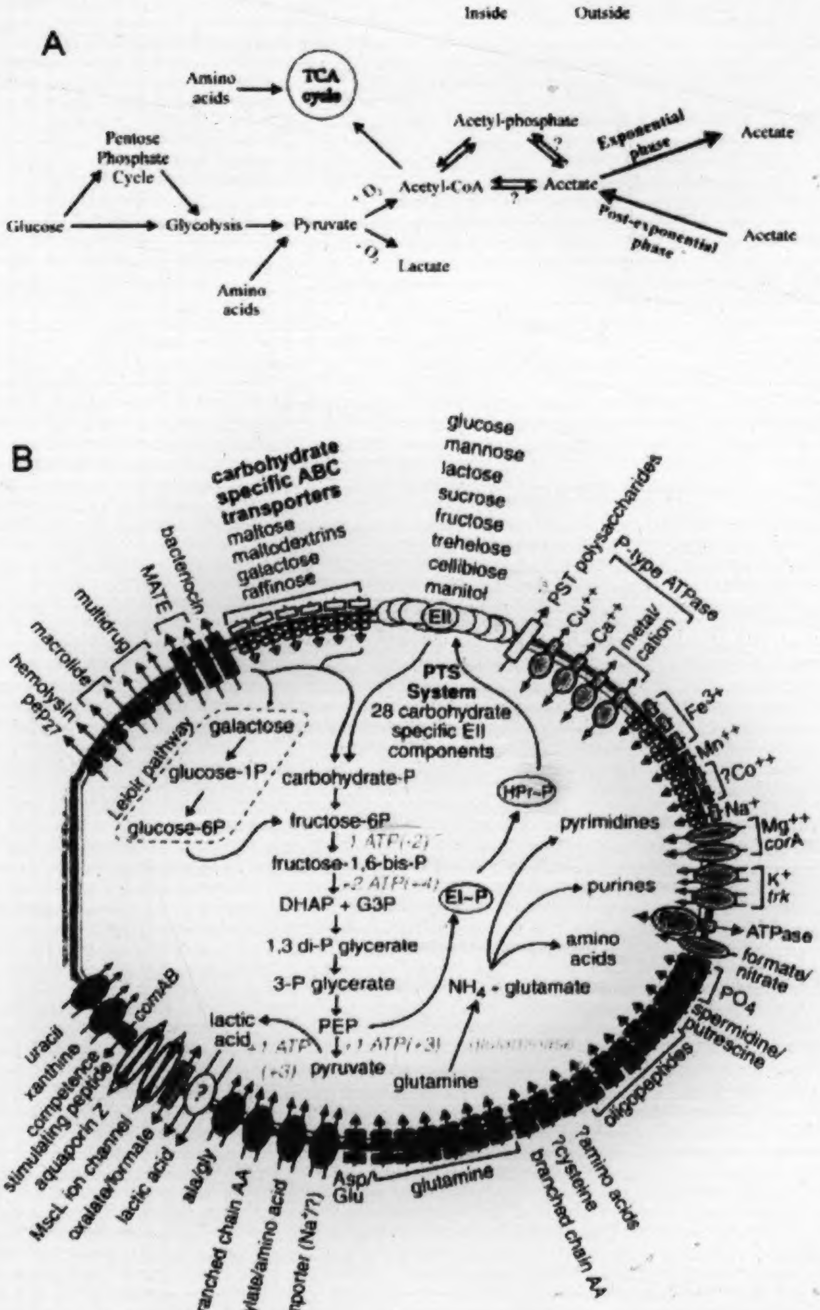

Figure 1.4. (A) Glucose catabolism in *S. aureus.* Green arrows indicate pathways preferentially active in the exponential growth phase; red arrows show pathways

Figure 1.4. (A) (continued) preferentially active in post-exponential phase; black arrows show hypothetical reactions. Modified from Somerville, 2003.

(B) Uptake and secretion of metabolites by *S. pneumoniae*. The glycolytic pathway shows catabolism of glucose (and other carbohydrates) into pyruvate and lactate. Amino acids and oligopeptides are absorbed or synthesised following consumption of glutamine. Oxalate, formate, nitrate, metal-ions, and hydrogen ions are cations contributing to the pneumococcal electrolyte balance. F_0F_1-ATPase serves as a hydrogen ion pump rather than for oxidative phosphorylation. Question marks indicate lack of data. Modified from Hoskins, 2001.

1.2.3.2. Metabolism of amino acids

Genomic analysis of *S. pneumoniae* serotype 6 has shown that essential amino acids required for its growth are aspartate (as well as its derivatives lysine, methionine, threonine, and isoleucine) and glutamate (as well as arginine); glycine, histidine, and leucine (Hoskins, 2001). On the other hand, valine was also shown to be required for growth (Sicard, 1964), which may be due to differences between strains. Apparently, glutamine is an important source of nitrogen for the synthesis of amino acids, purines and pyrimidines (Kloosterman, 2006; Hoskins, 2001).

Amino acids essential for *S. aureus* include: arginine, cystine, phenylalanine, proline and valine (Miller, 1973) with glucose as a main source of energy and carbon. Many strains also require glycine and leucine to be present in the environment (Lincoln, 1995). Instead of glucose, glutamic acid may be used as a source of energy, carbon, and nitrogen, and can decrease the need for exogenous proline and valine (Miller, 1973). Many strains of *S. aureus* have additional requirements of histidine, isoleucine, lysine, methionine, tryptophan and tyrosine, probably due to the loss of the bacterium's abilities to synthesise these amino acids (Lincoln, 1995).

S. aureus actively absorbs proline, glycine, and betaine from the medium as well as synthesizes these metabolites and mannitol to protect itself from osmotic stress (Graham, 1992; Edwards, 1981).

1.2.3.3. Biologically active compounds

S. pneumoniae has the genes for biosynthesis of pyridoxal, but lacks abilities to produce biotin, choline, and pantothenate (Hoskins, 2001). Choline, a very important nutritional metabolite, is present in pneumococci in relatively high concentrations unlike *S. aureus* (Garcia, 2000).

S. aureus requires nicotinic acid, pantothenate, thiamine, and biotin for its growth (Miller, 1973). It can consume choline and catabolise it to betaine at high osmolality in the medium in case of low betaine concentration (Graham, 1992).

1.2.3.4. Interconnections between metabolism and virulence factors of *S. pneumoniae* and *S. aureus*

Similarities in bacterial metabolism and expression of virulence factors likely derive from evolutionarily established phases of bacterial-host interaction.

For instance, colonisation of the host's body by bacteria require proper adherence to host tissue, the ability to live in a relatively poor nutritional environment, an ability to avoid a specific immune response (secreted immunoglobulin A and antimicrobial peptides), and an ability to suppress the growth of other bacteria. Infection of the lung alveoli, blood, interstitial tissue, and adjacent organs, requires different profiles of adhesins, invasins, and virulence factors that alow counteracting macrophage- and neutrophil-driven immune responses. Depletion of local nutrients, high local concentrations of bacteria, or death of part of bacterial population are accompanied by release of cytotoxic and immunogenic virulence factors (as described above) which help to damage adjacent cells, to protect bacteria, and to facilitate the spread of bacteria. Host cell damage and death result in release of nutrients and facilitate further bacterial growth. Some host metabolites, such as lactate, modulate virulence of bacteria (Smith, 2007)

Pyruvate oxidase (SpxB) of *S. pneumoniae* produce H_2O_2 and it is regulated differently *in vivo* and *in vitro,* for instance, it is down-regulated when pneumococci enter the blood (Belanger, 2004; LeMessurier, 2006). Many other factors of pathogenicity of *S. pneumoniae* including pneumolysin are regulated differently depending on the growth phase and environment (Bae, 2006; Rice, 2005). Pneumolysin is a cytoplasmic toxin that is released after death of the bacteria (Tweten, 2001). Mechanisms of influences of nutrients on bacterial factors of pathogenicity have not been described. 6-Phosphogluconate dehydrogenase also serves for adhesion of pneumococci to lung epithelium (Daniely, 2006).

In *S. aureus*, α-toxin and many other secreted virulence factors are produced in post-exponential growth phase (Ziebandt, 2004; Dunkan, 1972), which is thought to kill host cells and thus release intracellular metabolites after depletion of extracellular nutrients. These secreted cytolysins and proteases are produced under positive control of accessory gene regulator (agr), staphylococcal accessory regulator and negative control of the alternative sigma factor B; precise roles of all these compounds have not been described (Alouf, 2006). Production of some staphylococcal virulence factors, such as δ-toxin, and growth yield directly depend on bacterial TCA cycle (Vuong, 2005; Somerville, 2003; Somerville, 2002). Overall, many aspects of significance of host metabolism for bacterial pathogenesis are unknown.

1.3. Experimental models of bacterial-cell interaction and the study of bacterial factors of pathogenicity

Studies of interactions between bacteria and cultured cells and the role of particular factors of pathogenicity include measurements of bacterial adhesion, internalisation, and replication of internalised bacteria inside host cells; study of the survival of bacteria inside host cells despite the processes of autophagy; study of the stimulation of cytokine production and cytotoxicity; and study of bacterial factors of pathogenicity and preferential cell death pathways (necrosis, apoptosis, or autophagy). Different bacteria and even different strains of the same bacteria use different profiles of pathogenicity to promote their survival in the host (DeAzavero, 1988).

Adhesion of bacteria to host cells is an important first step for colonisation and infection (Daniely, 2006). Non-adherent bacteria on the mucosa are washed away with mucus and have decreased or abolished pathogenicity *in vivo* (An, 2000). Changes in host cells metabolism due to adhesion of *S. aureus* and *S. pneumoniae* have not been described; however, absence of bacterial type III secretion system in their genomes suggests insignificant alterations in cell homeostasis during adhesion (Henderson, 1999, Braun, 2002). Binding to Toll-like receptors stimulate apoptosis, which is compensated by concomitant activation of nuclear factor κB (NF- κB) (Wajant, 2005).

The invasiveness of bacteria has been shown to increase bacterial pathogenicity and facilitate spread by transcytosis, and may be studied by counting invading intracellular bacteria. It is also important to study internalisation of bacteria—an active process of hijacking the intracellular cytoskeleton or a passive process of receptor cross-linking by bacteria and internalisation (Henderson, 1999). Intracellular bacteria avoid autophagy (Schmid, 2006) by escaping autophagosomes and either actively multiply and kill host cells (Dinges, 2000; Bayles, 1998) or establish intracellular persistence with episodes of cell-killing and tissue damage. Cytokines are released by cells upon contact with bacteria, bacterial cell wall components, and bacterial toxins and by-products; they coordinate the immune response (Fournier, 2005). Cytotoxicity of bacteria and bacterial toxins are very important aspects of bacteria-cell interactions and often correlate with pathogenicity of bacteria *in vivo.* Bacterial toxins can induce cell death (Bantel, 2001) in the form of necrosis (by damaging cellular structures or disrupting cellular metabolism) or by apoptosis (by stimulating specific pathways of programmed cell death) (Chen, 1994).

1.4. Experimental mouse pneumonia model

Mouse models of pneumonia have been used to determine the pathogenesis of different stages of pneumonia, to study the immune response during pneumonia, to reveal the importance of different factors of bacterial pathogenicity, and to measure the efficiency of antibiotics in treatment. Different mouse strains are specifically susceptible to pneumococcal pneumonia. (Gingles, 2001) We have chosen C57Bl/6 for their moderate susceptibility and increased survival times over other mouse strains. Infection of mice may be done by intratracheal injection, bronchoscope-assisted intratracheal instillation, or intranasal inoculation of virulent bacteria (Su, 2004). After infection, the mouse health status may be evaluated in terms of gravity of the disease by direct observation, cell counts in bronchoalveolar lavage fluid, and histology of the lung (Preston, 2004) (Figures 1.5, 1.6). Other methods include hematology (white blood cell count and leukocytic formula), measurement of mean survival time, lung weight changes, myeloperoxidase concentration in blood and lung, and increase in lung vessel permeability. Studies of virulence factor-deficient mutants and the relative contribution of each factor have revealed potential therapeutic targets. Drug efficacy and monitoring of drug concentrations in different tissues are important tests to be made before new drugs can be used for clinical treatment.

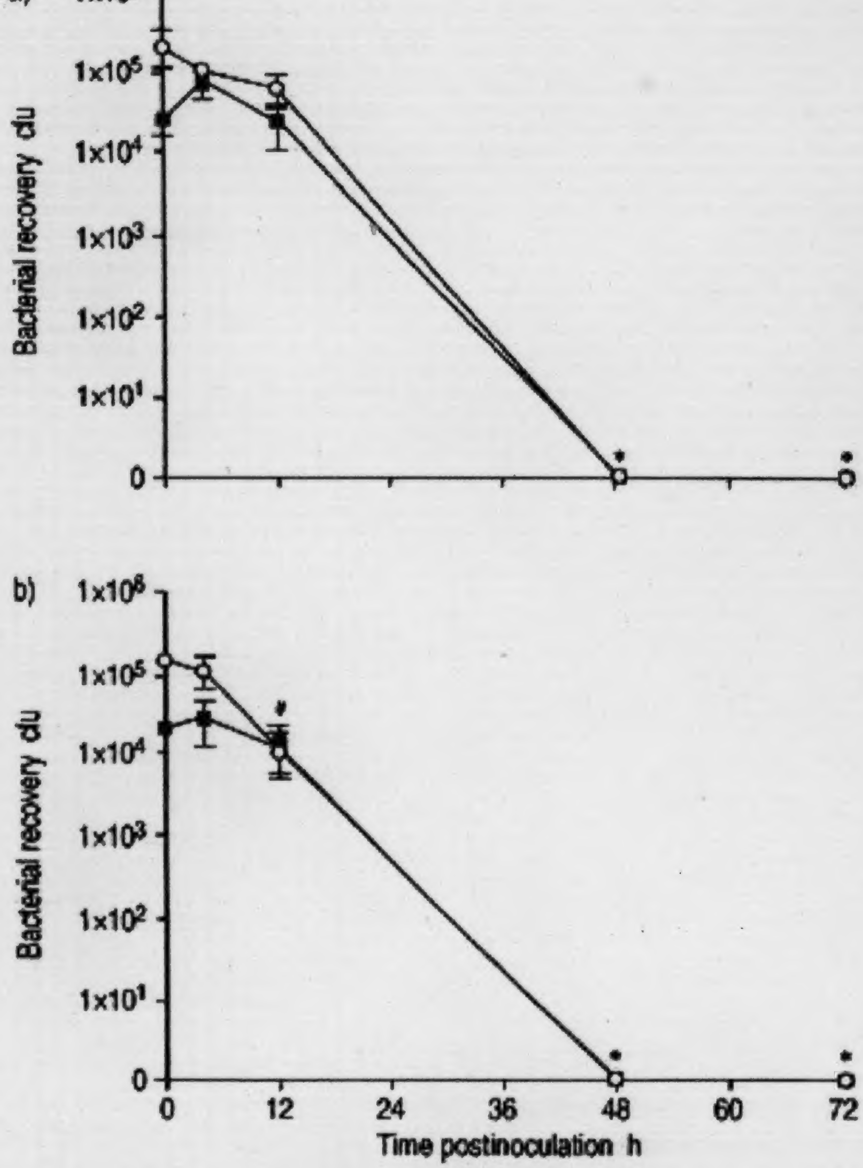

Figure 1.5. Bacterial counts in bronchoalveolar lavage fluid (open circles) and lung tissue (filled squares) after intratracheal instillation of 2 x 10^5 cfu *S. pneumoniae* in: a) BALB/c and b) C57Bl/6 mice at different time points. Modified from Preston, 2004.

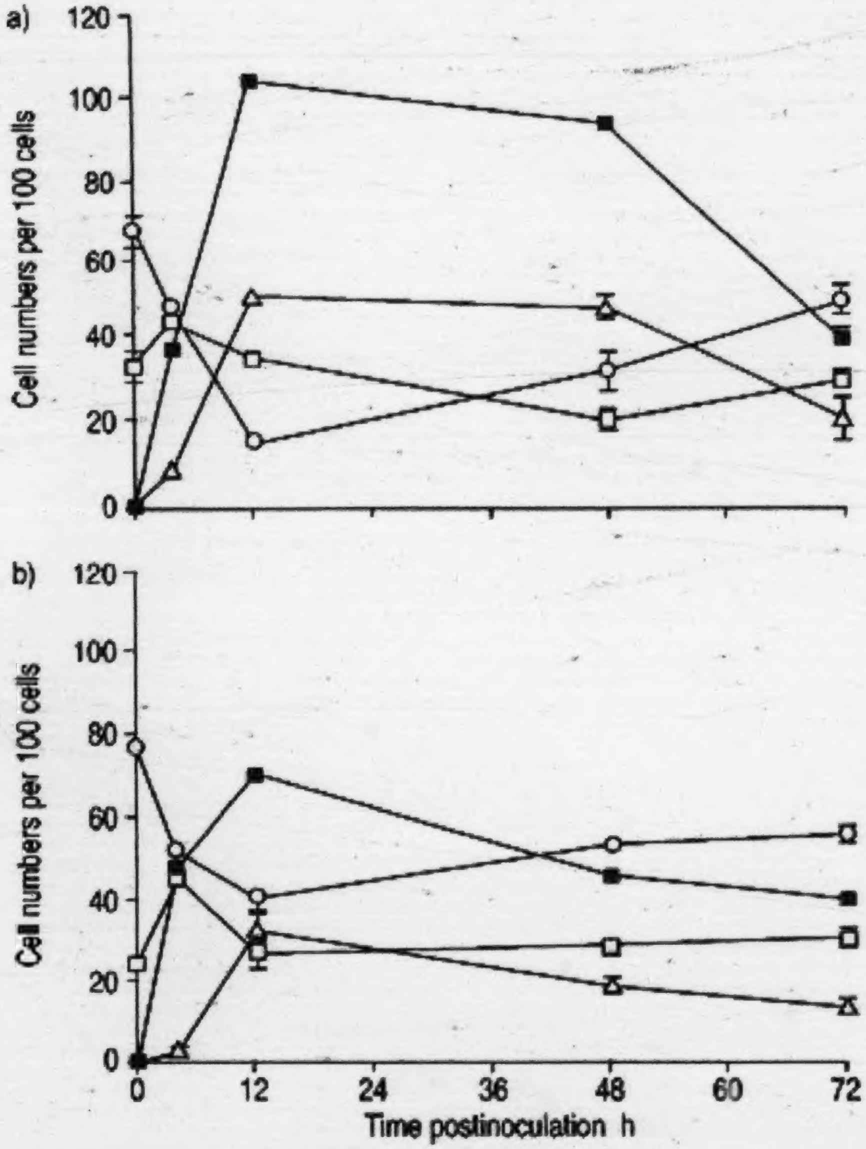

Figure 1.6. Leukocyte counts in bronchoalveolar lavage (BAL) fluid of a) BALB/c and b) C57Bl/6 mice after intratracheal instillation of 2 x 10^5 cfu *S. pneumoniae.* Macrophages (open circles), lymphocytes (open squares) and neutrophils (open triangles) are shown. Modified from Preston, 2004.

1.5. Metabolomics as a part of system biology

A growing interest in creating a holistic picture of processes within biological systems in health and disease has generated a need for a systems biology approach. (Kell, 2004). Current high-yield and high-throughput technical and data processing methods allow the study of activation of genes (transcriptomics), and synthesis or degradation of proteins (proteomics) during disease (Rochfort, 2005).

Metabolic changes are augmented compared with the dynamics of genes and proteins, and are easier to detect (Reo, 2002). This happens because changes in gene activity results in the transcription of a few a molecules of mRNA, which is increased by synthesis of many molecules of enzymes, and then is further amplified by the production or degradation of large quantities of metabolites (Reo, 2002). Experiments in genomics, transcriptomics, and proteomics are more laborious, time consuming and expensive than in metabolomics (Rochfort, 2005). Unlike genomics, current metabolomics methods cannot detect all metabolites due to variety of chemical properties and technical limitations (Watson, 2006). A useful metabolomic technique is nuclear magnetic resonance (NMR)-based metabolomics which offers high-resolution between different metabolites, relatively high sensitivity, ease of sample preparation, and the possibility of analyzing spectra on multiple occasions.

NMR-based metabolomics uses magnetic resonance measurements of atomic nuclei (usually hydrogen) with acquisition of spectra of samples. Subsequent analysis of NMR spectra includes identification simultaneously with measurement of concentrations of metabolites. Measurement of many metabolites in samples provides us with the opportunity to identify patterns of metabolic markers in a particular disease.

Metabolomics derives from measurements of individual compounds and describes patterns of metabolites (Kussmann, 2006). The metabolic profile of each sample is subjected to statistical, clustering analyses, and data mining methods to find patterns of changes that are specific to different diseases. Statistical methods and data mining attempt to find correlations between changes in metabolites (Camacho, 2005). These findings are used for thegeneration of hypotheses, which are tested by classical methods. The principal components analysis (PCA) is one of the methods of pattern recognition that calculates two or three principle components (PC) from the array of concentrations. PCs are a measure of variance of the metabolites with corresponding weighting coefficients. Each PC is unrelated to other PCs and presents differing variance. The first three PCs contains the largest amount of information about the corresponding array of data. Plotting PCs on a 3-dimensional map allows visualisation of the metabolic profile of samples. This helps to transform the array of concentrations (or processed spectra) into their location on the map (Nicholson, 1999; Pears, 2007).

There are approximately 9,000 known metabolites in biofluids of human described by different complementary techniques; many more are yet to be discovered (Wishart, 2006). Most metabolites, measured by NMR metabolomics, belong to a few groups of metabolic pathways, such as energy metabolism (Figure 1.3), tricarboxylic (TCA) cycle, amino acid metabolism (Figure 1.7), metabolism of nucleotides and osmolytes, and derivatives of food and gut microflora (Wishart, 2006). Many metabolites of the same biochemical pathway change synchronously during different physiological and pathological conditions (Lee, 2006). Some metabolites derive from several pathways, and the relative significance of their origin is not completely known, particularly in

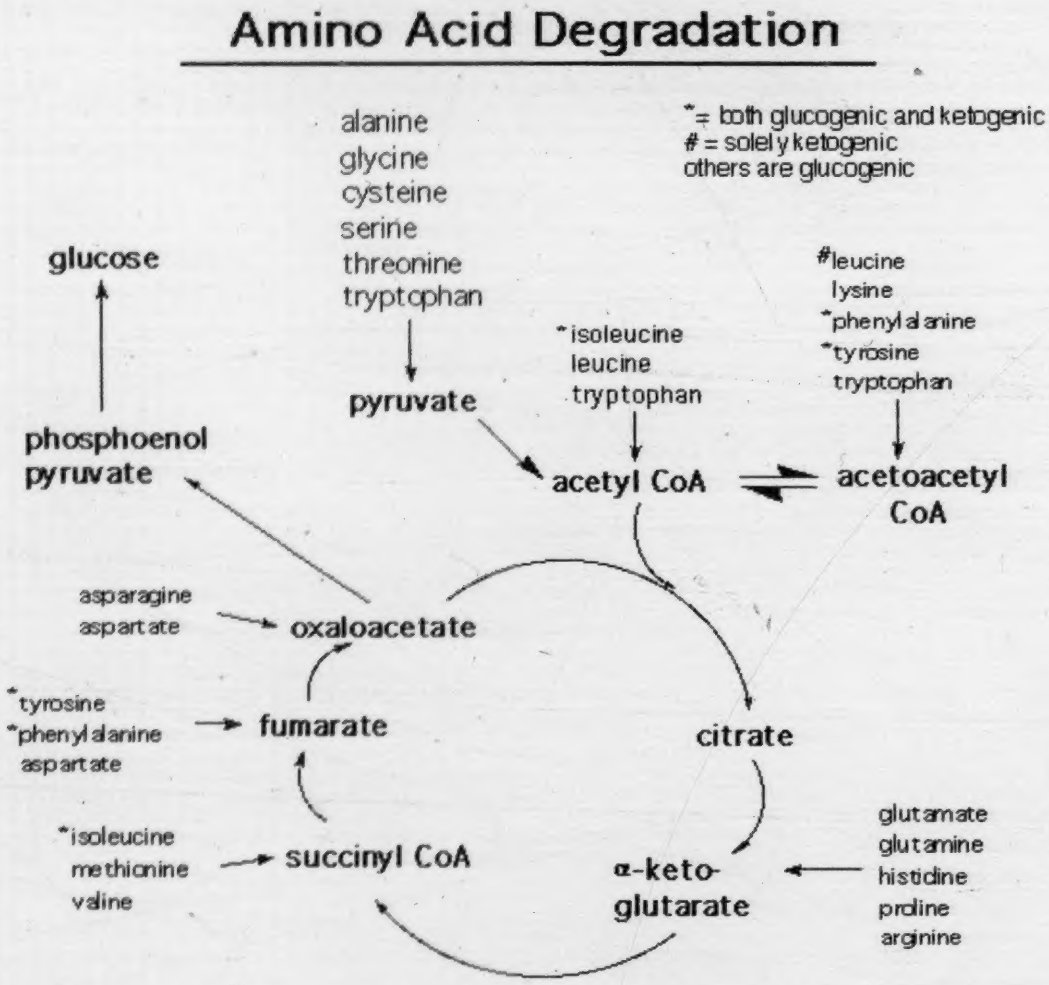

Figure 1.7. Amino acid degradation in humans. Modified from Stryer (1995).

different diseases. For instance, many infectious diseases and starvation lead to release of amino acids from muscles, with some common (Figure 1.8) and specific aspects (Wannemacher, 1977).

Osmolytes are metabolites that help to maintain osmolar pressure inside cells. Known metabolites with osmolytic function are some methylamines, such as carnitine, betaine (N,N,N-trimethylglycine), trimethylamine-N-oxide (TMAO) and the amino acid derivative taurine (Peluso, 2000; Cuisinier, 2002). Other methylamines such as creatine and creatinine do not have osmolytic function according to present knowledge. Changes in the osmolality of biofluids lead to a redistribution of the osmolytes between tissues and biofluids (Peluso, 2000). Additional factors, that influence the levels of osmolytes in biofluids are food intake (since many of them are food-derived products), endogenous synthesis in liver and kidney (small amounts), and catabolism for synthesis of other metabolites or methyl donors (Craig, 2004; Figure 1.9). Trimethylamine can derive from seafood, from food-derived carnitine, betaine, and TMAO (Zhang, 1999); as well as from asymmetric dimethylarginine (Tsikas, 2007). Glycolate is present in plant food (Frederick, 1973; Kisaki, 1969; Tolbert, 1969; Tolbert, 1968) and is synthesized in peroxisomes during peroxidation (Zhen, 2007). Formate is present in plant food (Grodzinski, 1979), synthesized by gut microflora (Dumas, 2006; Macfarlane, 2003; Sawers, 2003) and by host cells during peroxisomal oxidation of branched-chain fatty acids (Mannaerts, 2000).

Phenylacetyglycine is described as a putative marker of phospholipidosis; its urine levels have been shown to decrease during the response of the mammalian host to bacterial colonisation in the gut (Nicholls, 2003).

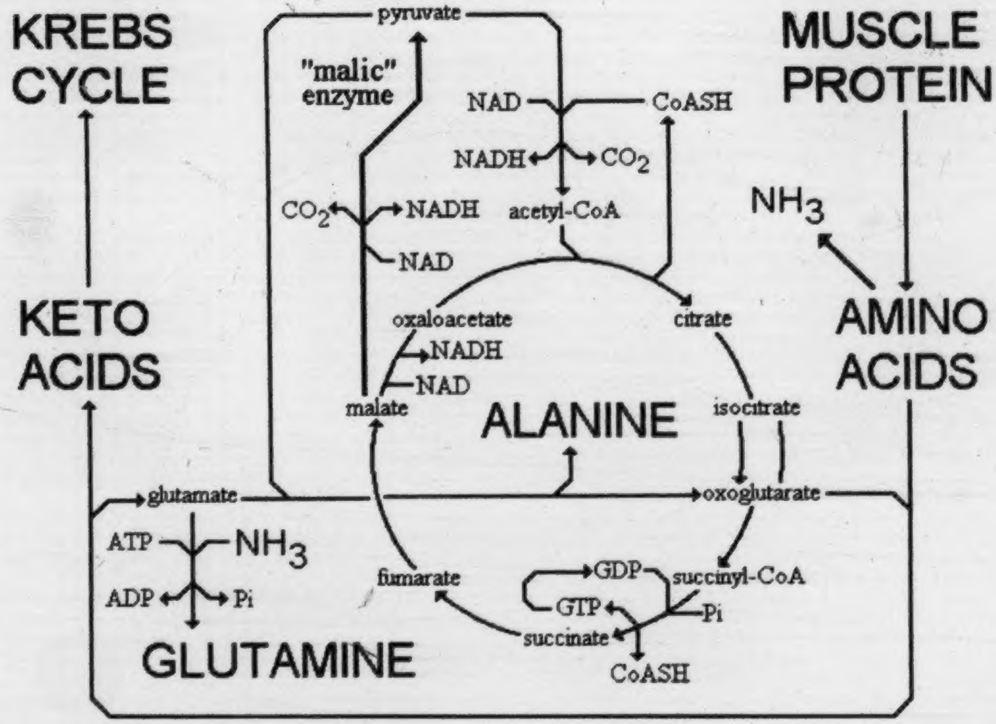

Figure 1.8. Amino acid metabolism in muscles during fasting. Modified from Illingworth, 2007.

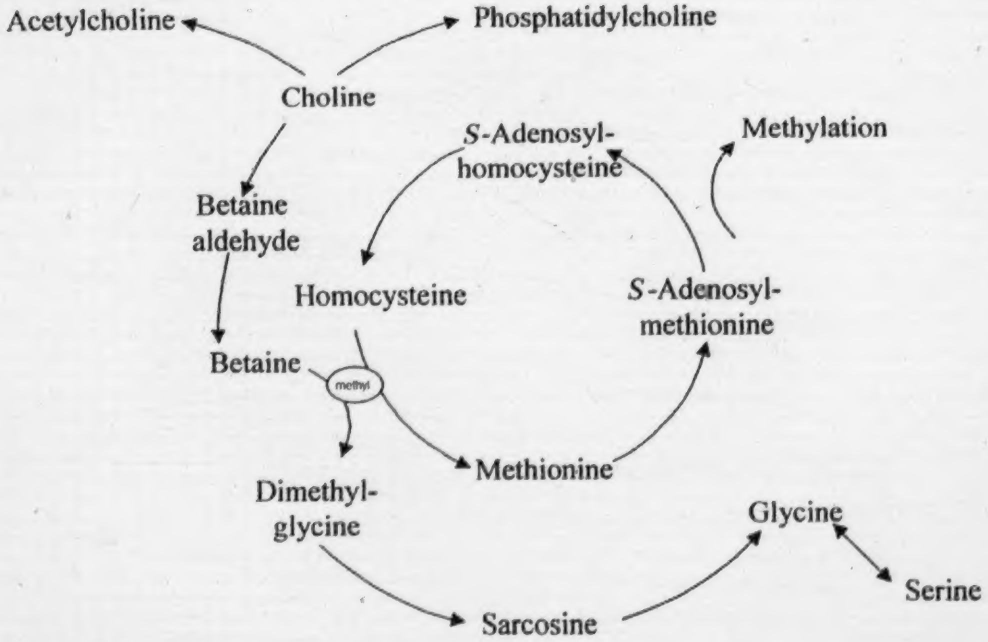

Figure 1.9. Metabolism of betaine and transmethylation processes. Modified from Craig, 2004.

Gut microorganisms produce, among others, acetate, formate, benzoate, and some vitamins, which are absorbed by host and enter sytemic circulation (Egert, 2006; Nicholson, 2004). Hypothetically, acetate can be used by host through conjugation with CoA and subsequent utilization into intermediate and energy metabolism (Nicholson, 2005). Hippurate is not produced directly by bacteria, but is produced in liver during conjugation of benzoate with glycine (Nicholson, 2005; Schachter, 1954), and a significant part of benzoate derives from metabolism of gut microflora (Schwab, 2001; Geng, 1999).

Creatine is synthesized in the liver from arginine and glycine and transported into the skeletal and smooth muscle cells (Wyss, 2000) (Figure 1.10). Muscles contain 98% of total creatine in the body, where this metabolite (along with creatine kinase) serves as an energy shuttle. The concentrations of creatine and creatine kinase in skeletal muscles are five times larger than in smooth muscle and cardiac cells; this reflects differences in the physiology of contraction of muscles (Rodgerson, 1991). Each day, approximately 1.5% of total creatine in humans is degraded into creatinine. Elevated level of creatinine is observed during diseases of skeletal muscles and their damage; reduced levels of creatinine are found during wasting of muscles (Hartmann, 2002; Decombaz, 1979). Serum creatinine concentration may be elevated due to decreased blood flow in kidney (during hypotension and shock, for example) (Hartmann, 2002).

1.6. Central hypothesis and objectives

Based on the knowledge in the literature regarding the mechanisms of *S. pneumoniae* and *S. aureus* infection in pneumonia, we know that each species of

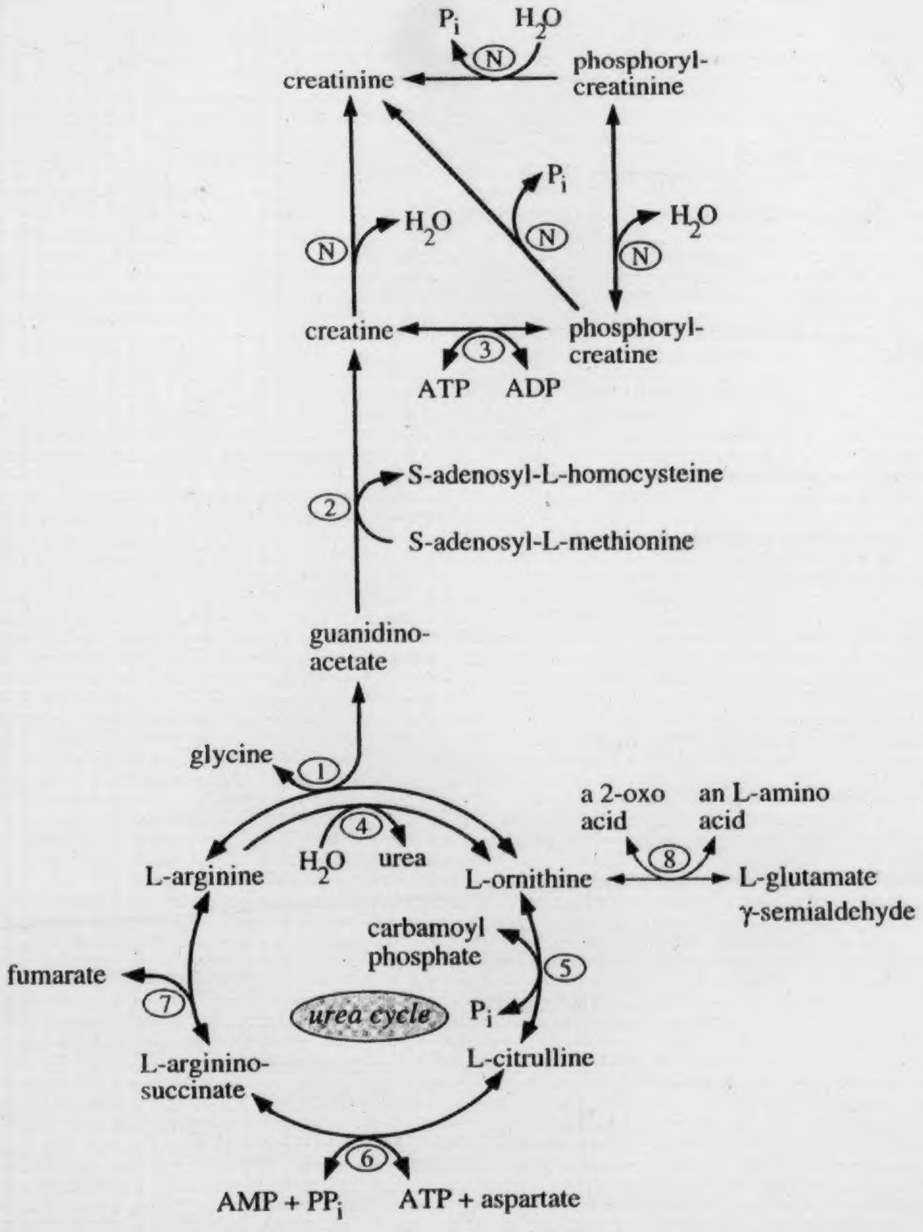

Figure 1.10. Metabolism of creatine and creatinine. Modified from Wyss, 2000.

bacterium causing infection in humans has a different impact on host responses. The host response to bacterial infection involves the release of a wide range of molecules, including acute phase proteins, immune factors, and small molecule metabolites.

Combined with this, each species of bacterium generates its own unique profile of metabolites. The use of NMR to analyze these metabolites provides us with a powerful tool to generate metabolic profiles in controlled animal and cell culture studies. Therefore, I hypothesize that a unique pattern of processes occurring in response to bacterial infection can produce a specific metabolic pattern in the host. It follows that we will be able to detect these unique profiles of metabolites in bronchoalveolar lavage, blood, and urine samples by nuclear magnetic resonance analysis coupled with targeted profiling of metabolites. Using a mouse model of pneumonia, I propose to examine these specific tissue compartments to reveal a unique profile of metabolites. Understanding the metabolomics of bacterial infection in lung epithelial cells will also suggest mechanisms of metabolic patterns at the cellular level.

Chapter 2

Cell Culture Model of Bacterial-Cell Interaction

2.1. Introduction

Infection of lung alveoli by pathogenic bacteria leads to numerous changes in homeostasis and metabolism of lung tissue, cell damage and death as a result of numerous pathological processes in the lung: release of bacterial virulence factors, local immune reactions, and systemic responses. Local and systemic changes in metabolism during pneumonia can potentially overlap, diminish, or augment each other. Different alveoli are at slightly different stages and intensities of the pathologic processes of pneumonia at each period of time (Corrin, 2006). Therefore, precise correlations between stages of disease and metabolic fluctuations or between changes in cell homeostasis and changes in released metabolites are difficult to describe using *in vivo* models. An i*n vitro* study of alveolar cell-bacteria interaction and subsequent cell damage and death will describe metabolic profiles at different stages of bacteria-cell interaction without systemic and immune reactions and correlate with known metabolic profiles of apoptosis and necrosis of cell lines induced by chemicals and cytokines. This research can also be useful for prospective studies of metabolic alterations by specific bacterial virulence factors which could correlate known modes of action of toxins (for example, damage of eukaryotic membranes, mitochondria, lysosomes) and release of cellular metabolites or alterations of metabolic pathways. This study can stimulate ongoing research of the influence of cytokines and other factors of acute phase response on metabolism of different host cell types. Ultimately, prospective *in vivo* studies of metabolic alterations by bacterial toxins, enzymes, metabolites, and host cytokines can strengthen application of metabolic profiles as the diagnostic and monitoring markers for use in clinic.

Studies of cell-bacterial interactions during inflammation include the usage of primary cell lines or derivative secondary cell lines originating from the organ or tissue of interest. These studies aim to mimic processes in the lung during pneumonia using different cell types, often with human bronchial type II pneumocyte-derived A549 cells, which are a type of lung epithelial cell (Daniely, 2006). Type II pneumocytes are located on the luminal surface of alveoli and make up 50% of the total number of lung epithelial cells (17% of the total number of cells in alveoli), and 10% of the total volume of alveoli (Baum, 1998). Among their numerous functions in the lung, type II pneumocytes produce surfactant, move fluid from the luminal side of alveoli to the interstitium by pumping sodium ions, repair injury of epithelial tissue by proliferation and transformation into type I cells, and participate in inflammation (Oei, 2004; Baum, 1998). They also recognize Gram-positive and Gram-negative bacteria through Toll-like receptors (TLRs) and secrete specific cytokines. Specifically, type II pneumocytes produce interferon-γ and TNF in the lung and secrete nitric oxide and antioxidants, including extracellular superoxide dismutase (Baum, 1998). During pneumonia, type II alveolar epithelial cells become damaged and are often destroyed at the culmination of disease; they are repaired by hyperplasia and elevated surfactant secretion in recovery stages (Bergeron, 1998). A549 cell lines have preserved the ability to secrete the main component of the surfactant lecithin (ATCC, 2007), to express TLR-2 and TLR-4 (Armstrong, 2004), and to secrete IL-8 in response to lipopolysaccharide or lipoteichoic acid from bacteria.

We used the A549 cell line to model metabolic changes during lung cell infection with *S. pneumoniae* and *S. aureus*. Our experiments aimed to mimic the nidus of infection in the lung during pneumonia with different concentrations of bacteria in the center and on the edge of the nidus, with a corresponding degree of cell damage. Low initial concentrations of bacteria are expected to cause sublethal damage of the majority of cells, accompanied by slight changes in homeostasis and metabolism, while a high concentration of pathogens is expected to result in cell death with profound changes in metabolism. Metabolic profiles of infected cells were assessed by NMR analysis of cellular supernatants. Increased concentrations of bacterial-derived metabolites (lactate, acetate and possibly formate, products of deamination of amino acids) are expected to correlate with increasing doses of bacteria and bacterial multiplication. Depletion of glucose, amino acids (lysine, methionine, threonine, isoleucine, arginine, valine, and potentially other amino acids), and some biologically active compounds (biotin, choline, and pantothenate) are expected to correlate with bacterial multiplication, as well as with host cell survival and preservation of metabolic functions of lung cells (Becker, 2005; Somerville, 2003; Hoskins, 2001). Changes in other amino acids and TCA cycle intermediates in the lung during bacterial infections have not been described yet.

Morphological changes in cells were determined by bright field visual microscopy of cells, stained by Giemsa stain (Kerr, 1991; Atkinson, 1998). Mitochondrial membrane potential and membrane-phospholipid asymmetry loss were also assessed (LaCasse, 2005). The viability of the cells and the permeability of the cell membrane were measured using Trypan blue. Bacterial dynamics at the beginning and the end of experiments were determined by bacterial count.

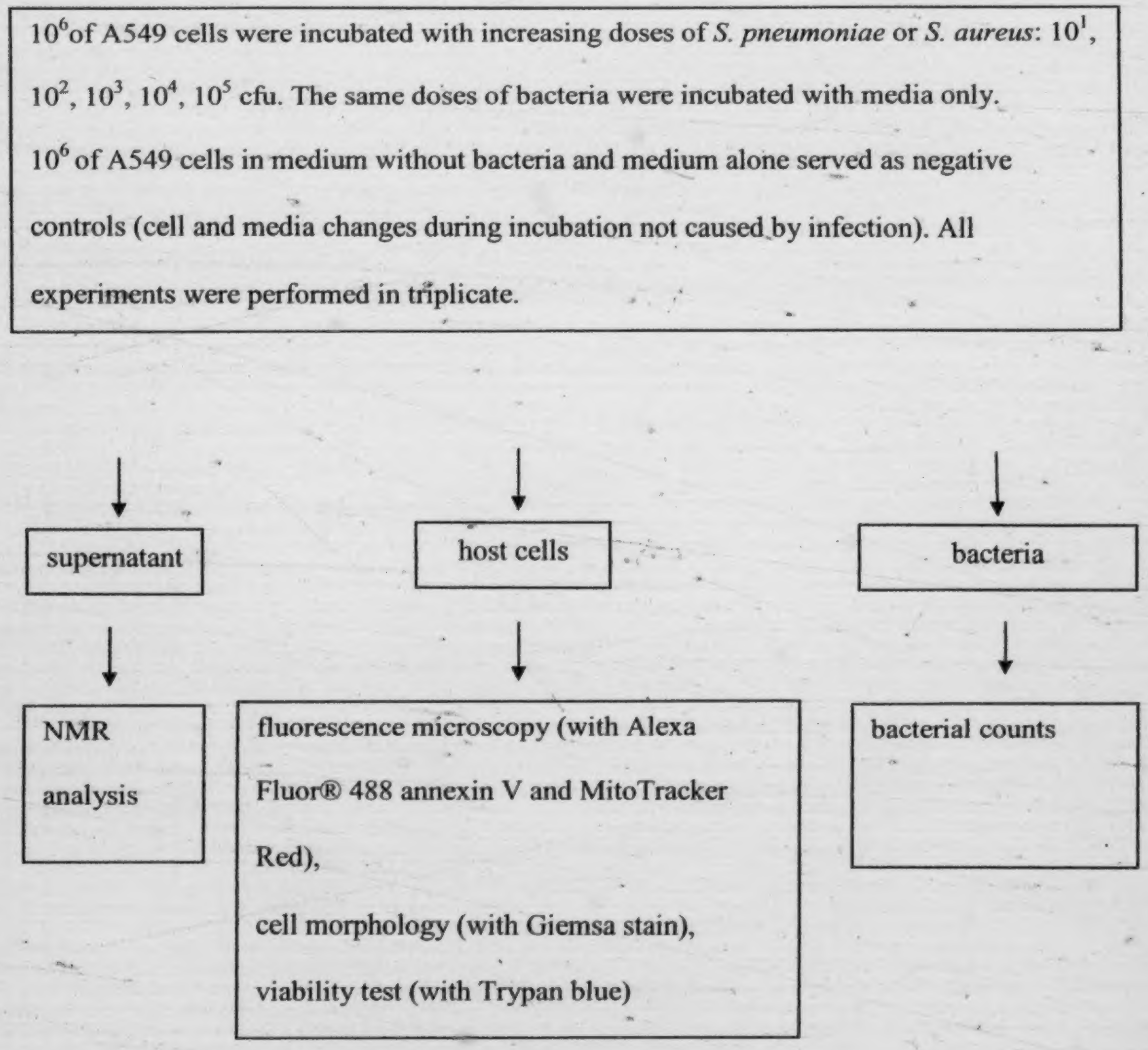

10^6 of A549 cells were incubated with increasing doses of *S. pneumoniae* or *S. aureus*: 10^1, 10^2, 10^3, 10^4, 10^5 cfu. The same doses of bacteria were incubated with media only. 10^6 of A549 cells in medium without bacteria and medium alone served as negative controls (cell and media changes during incubation not caused by infection). All experiments were performed in triplicate.

supernatant
host cells
bacteria
NMR analysis
fluorescence microscopy (with Alexa Fluor® 488 annexin V and MitoTracker Red),
cell morphology (with Giemsa stain),
viability test (with Trypan blue)
bacterial counts

Figure 2.1. Design of experiments of bacteria-cell interactions.

Bacterial multiplication and dynamics were determined by bacterial count at the beginning and end of experiments.

2.2. Materials and methods

2.2.1. Cell media

The mitochondrial potential of A549 cells was determined by staining with MitoTracker Red from the Vibrant Apoptosis kit #11 (Invitrogen, Carlsbad, California, USA). Phosphatidylserine externalization on apoptotic cells was measured by staining with Alexa Fluor® 488 annexin V, from Vibrant Apoptosis kit #11 (Invitrogen, Carlsbad, California, USA). Dulbecco's Modified Eagle's Medium (DMEM), 100x (200 mM) L-glutamine, 100x non-essential amino acids (NEAA), 10x Hanks' balanced salt solution (HBSS), 10 % fetal bovine serum (FBS), 0.25% Trypsin solution in 0.02% ethylenediaminetetraacetate (EDTA), and Giemsa stain were purchased from Invitrogen (Carlsbad, California, USA). Tissue culture 6-well plates and 30 mm cell culture plates were purchased from Corning Inc. (Corning, N Y, USA). Slides, coverslips; and Diff-Quick stain were purchased from Fisher Scientific (Mississauga, ON, Canada).

2.2.2. Cell line

The human bronchial epithelial cell line A549 was a gift from Dr. Florentina Duta (Pulmonary Research Group, University of Alberta). The cells were cultured on 6-well plates in complete DMEM growth medium, supplemented with NEAA, 2 mM L-glutamine, and 10% FBS at physiological conditions (37°C, 5% CO_2 and humidified atmosphere). After two doublings of cell numbers at 85% confluence of A549 cells (corresponding to 10^6 cells), the medium was removed and replaced with two ml serum-free DMEM (with L-glutamine and NEAA), followed by two washes with HBSS and two washes with serum-free DMEM. Plates with cells and media only were pre-incubated for 2 h at physiological conditions (37°C, 5% CO_2 and humidified atmosphere) and infected with corresponding bacteria. Cells for staining experiments were cultured on sterile coverslips on the bottom of 30 mm cell culture plates as was done for the 6-well plates.

To determine cell viability, plates with cells were centrifuged at 300 *g* for 10 min to pellet detached cells. Supernatant was removed with a vacuum suction system until 200 μL/well was left. A volume of 200 μL of 0.1% solution of Trypan blue stain was added to each well. Plates were shaken by hand to ensure equal distribution of stain and placed on ice for 5 min. Cells were observed at high-field resolution (63X objective) and cells on 5 fields were counted. The viability of cells was expressed as the percentage of live cells (transparent cells, which exclude stain) out of total cell numbers (Table 2.1).

2.2.3. Bacteria. Todd-Hewitt broth (THB), 5 % sheep blood agar plates (BAP), and strains of *S. pneumoniae* and *S. aureus* were gifts from Dr. Gregory Tyrrell and Sandy Shokoples of the Northern Alberta Provincial Laboratory. Work with bacteria was done according to biohazard safety regulations at the University of Alberta. Using a conventional invasion assay, *S. pneumoniae* (strain 04SR2228) was selected by Sandy Shokoples as the most invasive strain among the collection of clinical isolates available, and was typed as serotype 14. The strain of *S. aureus* used in this study was the clinical isolate, methicillin-resistant, Panton-Valentine leukocidin (PVL) positive and α-toxin positive (as suggested by β-haemolysis of erythrocytes of BAP). Strains of bacteria were stored frozen at – 80 °C (to decrease changes of phenotype after multiple passages in different experiments and decreased probability of mutations).

Treatment	0 cfu	10^1 cfu	10^2 cfu	10^3 cfu	10^4 cfu	10^5 cfu
Cell viability, average	96%	88 %	72 %	66 %	54 %	42 %

Table 2.1. Viability of A549 cells after 24 h post infection with *S. pneumoniae* as determined by Trypan blue exclusion assay *(n* = 2).

When needed, bacterial strain aliquots were thawed, grown on BAP with 2 passages, and cultured in THB for 6 h until the middle log phase of exponential growth, as measured by turbidity of the suspension of not more than 0.5 on the McFarland scale (to decrease probability of confluence-caused death of bacteria [Brock, 1984]). THB was used for culturing *S. aureus* and serum-free DMEM for washing bacteria and cell infection, which did not cause bacterial death (as assessed by colony count). For culturing *S. pneumoniae,* THB was diluted with DMEM (1:2 v/v) to adjust the osmolality of the growth media to normal value and to preserve pneumococci from osmotic stress and death (results not shown). Bacteria were washed three times by centrifugation of suspension, discarding supernatant with bacterial toxins, enzymes and metabolites and resuspension of bacterial pellet with serum-free DMEM pre-warmed to 37° C. Bacterial doses for cell infection were 10^1, 10^2, 10^3, 10^4, 10^5 cfu per 100 μL of serum-free DMEM with error of 10% as assessed by colonies count of 10^2 cfu/100 μL on BAP. Suspensions of *S. pneumoniae* or *S. aureus* at required concentrations were prepared using the turbidimetric method (Watson, 1969): transmittance of the bacterial suspension, measured by a Beckman DU-640 spectrophotometer (Beckman Coulter, Inc., USA), was compared to standard curves of transmittance versus concentrations of bacterial suspensions; serial dilutions were made until the required concentrations were achieved. Precautions were taken in preparing similar bacterial doses in different experiments, and were determined to differ one from another by less than 10% using the following approaches:

- The wavelength of transmitted light at 686 nm was selected experimentally as giving the most reproducible measurements for these bacteria.

- The cuvette for the spectrophotometer was rinsed with bacterial suspension before measurements, and increased concentrations of bacterial suspensions were used until the required concentration was obtained.
- Very diluted or concentrated suspensions were avoided (outside of the range $5 \times 10^7 - 5 \times 10^8$ cfu/ml).
- Dose-response curves of transmittance for different bacterial concentrations were generated and robustness of this method was confirmed by colony count.

2.2.4. Infection experiments

Plates with A549 cells in 2 ml of serum-free DMEM alone were infected with corresponding doses of bacteria in 100μL of serum-free DMEM or the same media without bacteria. After infection, plates with A549 cells and media were incubated at physiologic conditions (37ºC, 5% CO_2 and humidified atmosphere). After 24 h supernatant samples were harvested, processed (according to a developed protocol), and stored frozen until further NMR metabolomics analysis.

2.2.5. NMR analysis

Supernatants of infected cells were processed according to a developed protocol, followed by acquisition of NMR spectra and analysis of known metabolites.

2.2.5.1. Filters. Nanosep Omega 3 kDa molecular weight cut-off filters (Pall Life Sciences, USA) were washed with double distilled water seven times according to a developed protocol. This was a critical step which removed contaminating glycerol that was added to all filtration membranes as a preservative. Glycerol generated significant interference in NMR spectra. After each wash, filters were disassembled and surfaces were rinsed with water, after which filters were reassembled, 300 μL of water was pipetted inside, and filters were centrifuged at 13,000 *g* for 10 min. Filters were used immediately after washing while they were still moist to avoid membrane drying or damage.

Cell supernatants were collected, centrifuged free of detached cells (at 300 *g* for 6 min at 4°C) and bacteria (at 13,000 *g* for 10 min at 4°C), and stored at -80°C before the analysis. One day before analysis, samples were quickly thawed and filtered through pre-washed Omega Nanosep 3000 Da cut-off filters. Samples were stored in ice during processing to decrease metabolite degradation.

2.2.5.2. NMR experiments. A volume of 585 μL of each sample together with 65 μL of internal standard (Chenomx, Edmonton, Canada) was pH adjusted to 6.8 and samples were analyzed with a 600 MHz NMR spectrometer by Dr. Carolyn Slupsky, Shana Regush, Kathryn Rankin and Hao Fu at the Magnetic Resonance Diagnostic Centre, University of Alberta. Targeted profiling was carried out using the Chenomx NMR Suite version 4.6 software by Dr. Slupsky or Mr. Fu to simultaneously determine the identities and concentrations of specific metabolites. Metabolites with very low concentrations, or very complex spectra, which overlapped significantly with other metabolites or noise, were ignored during analysis to decrease the probability of false-positive results.

2.2.5.3. Data analysis. Concentrations of metabolites were processed to find mean and standard error of the mean, and values were plotted with GraphPad Prism v 4.0. Metabolites were grouped according to the most significant known or hypothetical physiological function and biochemical pathways. Some metabolites may be synthesized by overlapping pathways. Statistical difference between uninfected and infected samples (where applicable) was determined by two-way ANOVA using GraphPad Prism v 4.0.

2.2.6. Microscopic observation of cell morphology

Cell cultures of A549 cells in complete DMEM growth media were grown on coverslips, which were cut to fit inside 30 mm Petri dishes. Cell monolayers were prepared and treated as described above. Slides were stained with Giemsa stain or Diff-Quick stain, mounted on slides with mount media and analyzed at high magnification (63X objective) of bright-field microscopy. For Diff-Quick stain coverslips were stained with methanol fixative, buffered eosin and phosphate-buffered azure B for 30 s, 30 s, and 45 s respectively, washed, air-dried and mounted. For Giemsa stain, cells were fixed with methanol : PBS solution (1:1 v/v) and with absolute methanol for 5 min, stained with undiluted Giemsa stain for 5 min with agitation, washed with water, followed by centrifugation at 300 *g* at 4°C for 7 min after addition of each solution.

2.2.7. Fluorescence microscopy

Cells for fluorescent microscopy were processed with Apoptosis Assay Kit #11 according to the manufacturer's recommendations with modifications. Cells in 6-well plates were grown to confluence, infected, centrifuged to pellet detached cells, and supernatant was removed as described above. Cells were detached with EDTA Trypsin solution, washed twice with HBSS (with 100 μL of FBS at first to facilitate pelleting of cells), and stained according to the manufacturer's recommendations. Necrotic cell samples were prepared by incubating A549 cells with 2 mM H_2O_2 for 4 h at 37 °C. Staining of samples of 10^6 cells involved a 30 min incubation at 37 °C with 0.1 μM working solution of MitoTracker Red dye and 15 min incubation at room temperature with 5 µL of Alexa Fluor® 488 annexin V, followed by washing with PBS. Samples were placed on ice, mounted on slides and analyzed immediately by fluorescent microscopy. Additionally, the appearance of cells was monitored by picture acquisition to describe changes over time.

2.2.8. Bacterial count

At 24 h post infection, bacterial concentrations in supernatant, were determined by serial dilutions and plating on blood agar plates (BAP) in separate experiments. A volume of 100 µL of each sample was serially diluted with PBS with osmolality adjusted by addition of 5% (v/v) 10 x HBSS in proportions 1:100, 1:10,000, 1:100,000 and 1:1,000,000. Each dilution was plated in duplicate on BAP, incubated for 24-36 h at physiological conditions (37°C, 5 % CO_2 and humidified atmosphere), and colonies of bacteria were counted.

2.3. Results

2.3.1. Metabolomics of lung cells, infected with *S. pneumoniae*

2.3.1.1 Concentrations of TCA cycle intermediates

Upon infection of A549 cells with increasing doses of *S. pneumoniae*, we found that TCA cycle intermediates 2-oxoglutarate and fumarate were elevated at low concentrations of bacteria, but then decreased upon increasing bacterial concentrations (Figure 2.2). In contrast, succinate increased with elevated bacterial doses. Citrate levels in cellular supernatants were not changed significantly.

2.3.1.2. Concentrations of amino acids

Supernatants from A549 cells infected with *S. pneumoniae* showed increased levels of the amino acids alanine and glutamate at high doses of bacteria (Figure 2.3 A).

Glutamine, lysine, and methionine showed progressive decreases with increasing numbers of bacteria (Figure 2.3 B).Concentrations of asparagine and glycine, as well as the amino acid derivatives 2-oxoisocaproate and 3-methyl-2-oxovalerate, showed similar decreases with increasing dose of pneumococci (results not shown). Other amino acids analysed in this study (arginine, aspartate, histidine, isoleucine, leucine, phenylalanine, proline, serine, tryptophan, tyrosine, valine, and threonine) showed no change (Figure 2.3C).

2.3.1.3. Energy metabolism

Higher concentrations of bacteria were associated with increased consumption of glucose and pyruvate (Figure 2.4). In correlation with this, we found elevated concentrations of lactate in response to increasing concentrations of bacteria. Lactate is the end-product of glycolysis of both host cells and *S. pneumoniae*.

2.3.1.4. Bacterial-derived metabolites

As expected, higher concentrations of bacteria were associated with increased concentrations of acetate and formate, as well as with increased levels of isovalerate and unknown metabolite (Figure 2.5). These metabolites likely derive from bacteria, as supernatants of uninfected A549 cells had negligible levels of these metabolites.

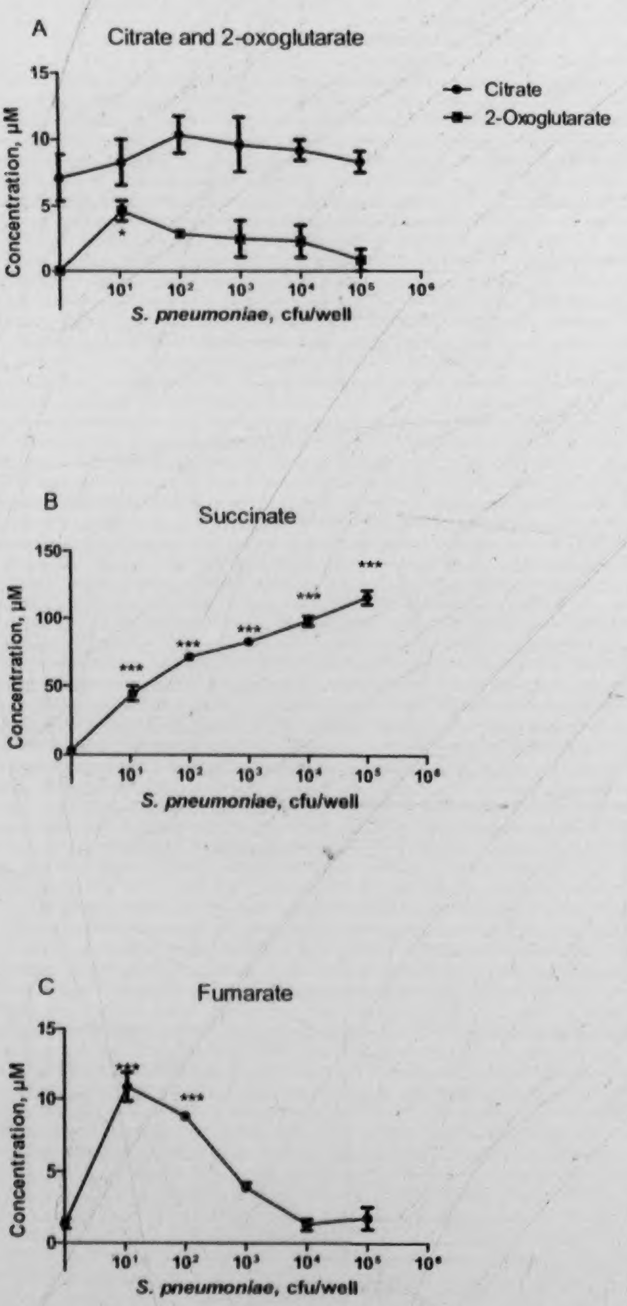

Figure 2.2 Concentrations of TCA cycle intermediates in the supernatants of infected with different doses of *S. pneumoniae* 24 h post-infection. * $p < 0.05$; *** $p < 0.001$ compared with non-infected cells ($n = 3$).

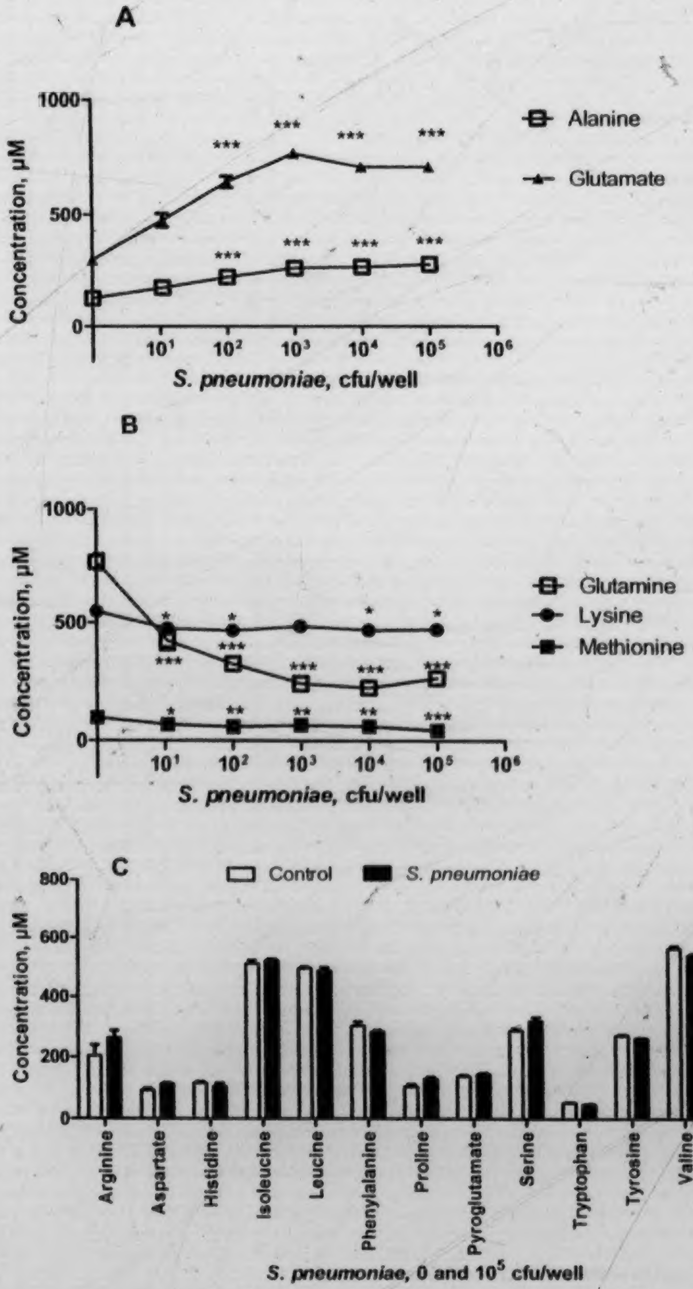

Figure 2.3. Amino acids in the supernatant of A549 cells, infected with different doses of *S. pneumoniae* 24 h post-infection. (A) Significantly increased amino acids: alanine and glutamate. (B) Significantly decreased amino acids. (C) Amino acids with insignificant changes. * $p < 0.05$; ** $p < 0.01$; *** $p < 0.001$ compared with non-infected cells ($n = 3$).

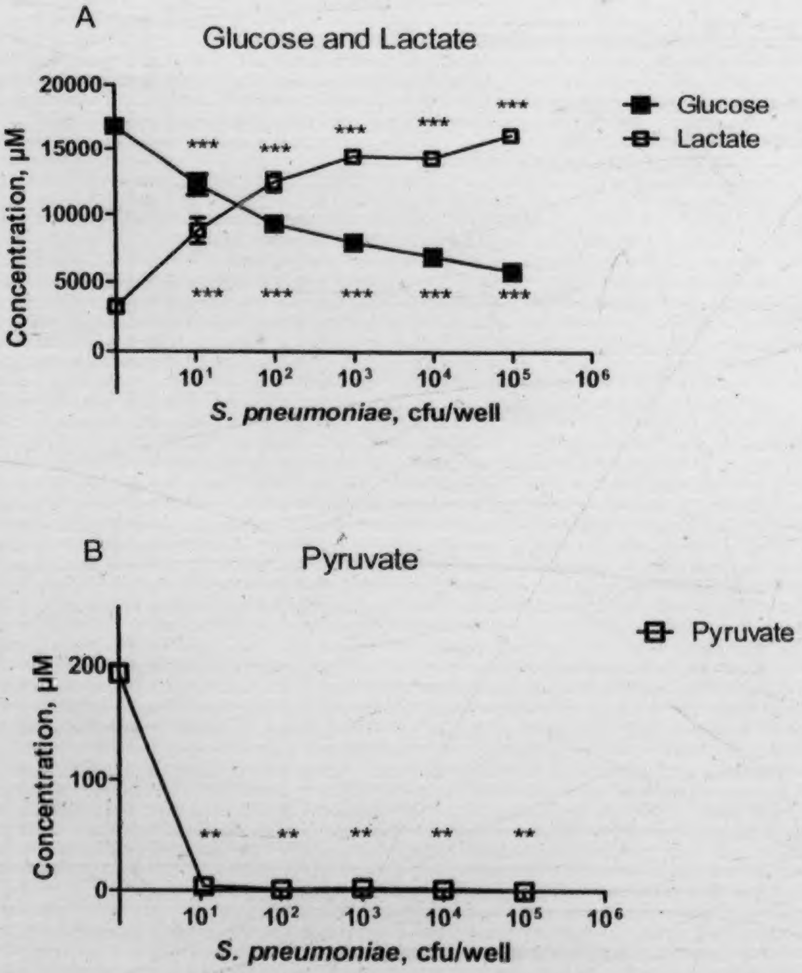

Figure 2.4. Glucose and products of glycolysis lactate and pyruvate in the supernatant of A549 cells, infected with different doses of *S. pneumoniae* 24 h post-infection. ** $p < 0.01$; *** $p < 0.001$ comparing with non-infected cells ($n = 3$).

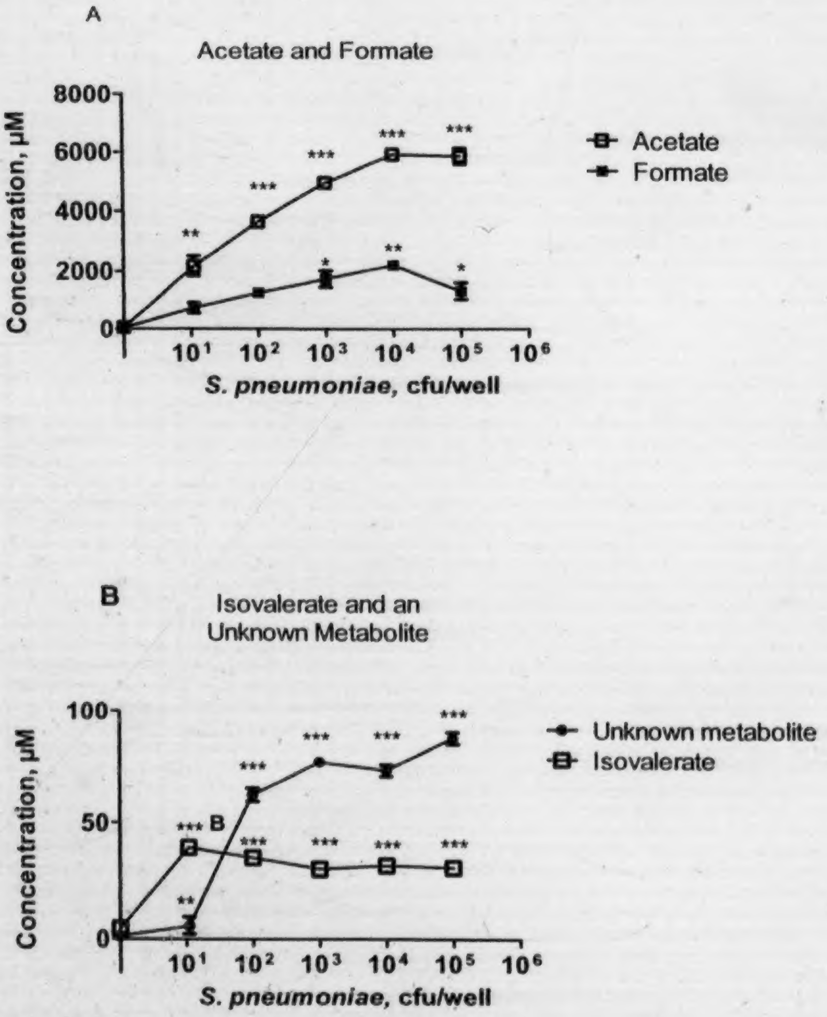

Figure 2.5. Bacterial-derived metabolites in the supernatant of A549 cells, infected with different doses of *S. pneumoniae* 24 h post-infection. (A) Acetate and formate. (B) Isovalerate and an unknown metabolite. * $p < 0.05$; ** $p < 0.01$; *** $p < 0.001$ compared with non-infected cells ($n = 3$).

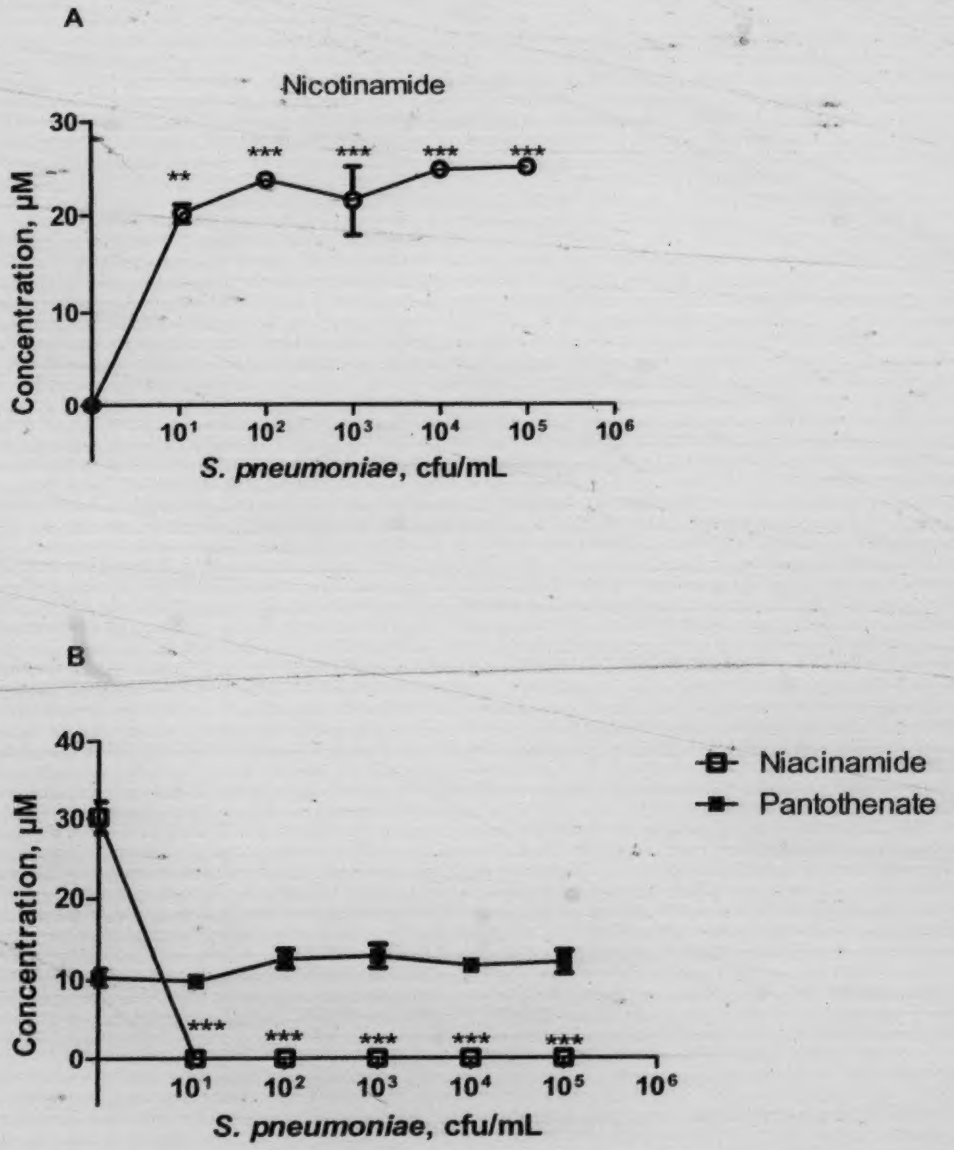

Figure 2.6. Biologically active compounds in the supernatant of A549 cells, infected with different doses of *S. pneumoniae* 24 h post-infection. (A) Nicotinamide. (B) Niacinamide and panthothenate. * $p < 0.05$; ** $p < 0.01$; *** $p < 0.001$ compared with non-infected cells ($n = 3$).

2.3.1.5. Other metabolites (nicotinamide, niacinamide, and pantothenate)

The nicotinamide concentration was negligible in samples of uninfected cells, but increased upon infection with bacteria (Figure 2.6). Niacinamide concentration decreased simultaneously with infection. Surprisingly, pantothenate (a required metabolite for *S. pneumoniae,* Chapter 1) concentrations were almost unchanged after infection.

2.3.2. Changes in cell viability during infection

2.3.2.1. Changes in mitochondrial potential and evaluation of preferential cell death

Analysis of the mitochondrial potential revealed a gradual decrease in potential from normal level in control uninfected cells to very low levels in cells incubated with 10^5 cfu of *S. pneumoniae* and absent in control necrotic cells (Figure 2.7). Externalization of phosphatidylserine of cell membranes of infected A549 (as compared uninfected cells) suggests apoptosis of A549 cells.

2.3.2.2. Microscopic observation of A549 cells

Microscopic observation revealed typical apoptotic changes in morphology of the increasing fraction of cells with increasing bacterial concentrations. These morphologic changes were characteristic for apoptosis: karyopyknosis (decreased diameter of nuclei and appearance of more condensed dark granules of nuclei due to margination of chromatin at first with hyperchromatic appearance of whole apoptotic nuclei later), decreased cell size and volume of cytoplasm, deformation of shape of nuclei and cells depending on stage of apoptosis (Figure 2.8).

2.3.3. Dynamics of *S. pneumoniae*

2.3.3.1. Bacterial count

The bacterial concentration in the media increased many fold over 24 h (from ~ 8 x 10^5 to 1.6 x 10^8 cfu respectively) (Table 2.2).

Following 24 h of co-culture with A549, bacterial concentrations in media increased between 1,600-fold (with 10^5 cfu initial concentration) to 120,000-fold (with 10^2 cfu initial concentration). Thus, bacterial growth over the 24 h period of culture was optimal at a starting concentration of 10^2 cfu and was lowest at 10^5 cfu. This may suggest that at 10^5 cfu/well bacteria have multiplied and entered a stationary phase or possibly died at some time point after infection. Preliminary data suggested that 1-10 % of bacteria in the wells with 10^5 cfu were dead after 24 h post-infection (results not shown).This estimation was done by counting bacteria using a hemocytometer (which approximately estimates both dead and live bacteria together) and subsequent subtraction of number of live bacteria (from colony count, Table 2.2). This method is subject to error due to the presence of cell debris with size of bacteria, and other methods (for instance, flow cytometry with differential staining [Diaper, 1992]) may be used for more accurate count of dead and live bacteria.

Bacterial counts in DMEM without A549 cells showed no changes in bacterial concentrations after 24 h of incubation. In other words, *S. pneumoniae* remained viable, but did not multiply. This suggests that bacterial growth is dependent on the presence of host cells.

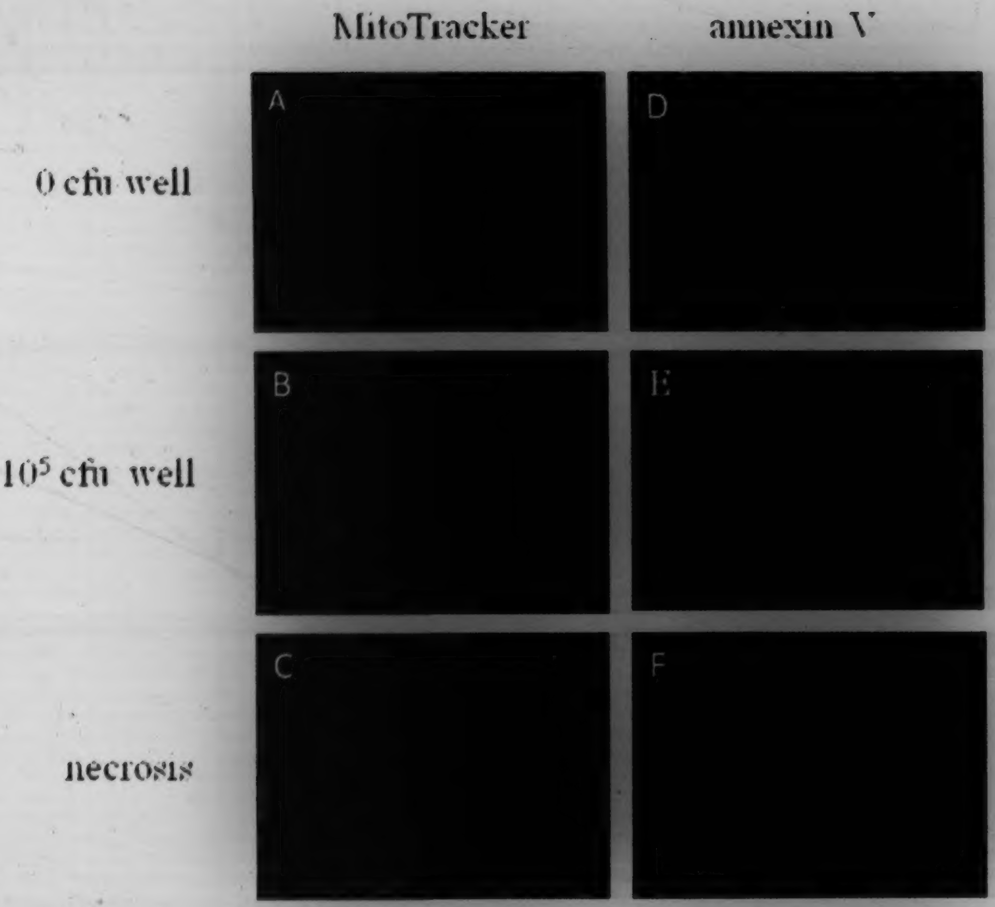

Figure 2.7. Effect of bacterial infection by *S. pneumoniae* on mitochondrial potential and cell viability. (A) Uninfected A549 cells, stained with MitoTracker Red. (B) A549 cells, infected with 10^5 cfu/ well *S. pneumoniae* serotype 14 for 24 h, stained with MitoTracker Red. (C) A549 cells with induced necrosis, stained with MitoTracker Red.(D) Uninfected A549 cells, stained with Alexa Fluor ® 488 annexin V. (E) A549 cells, infected with 10^5 cfu/ well *S. pneumoniae* serotype 14, stained with Alexa Fluor ® 488 annexin V. (F) A549 cells with induced necrosis, stained with Alexa Fluor ® 488 annexin V. Magnification, 40X.

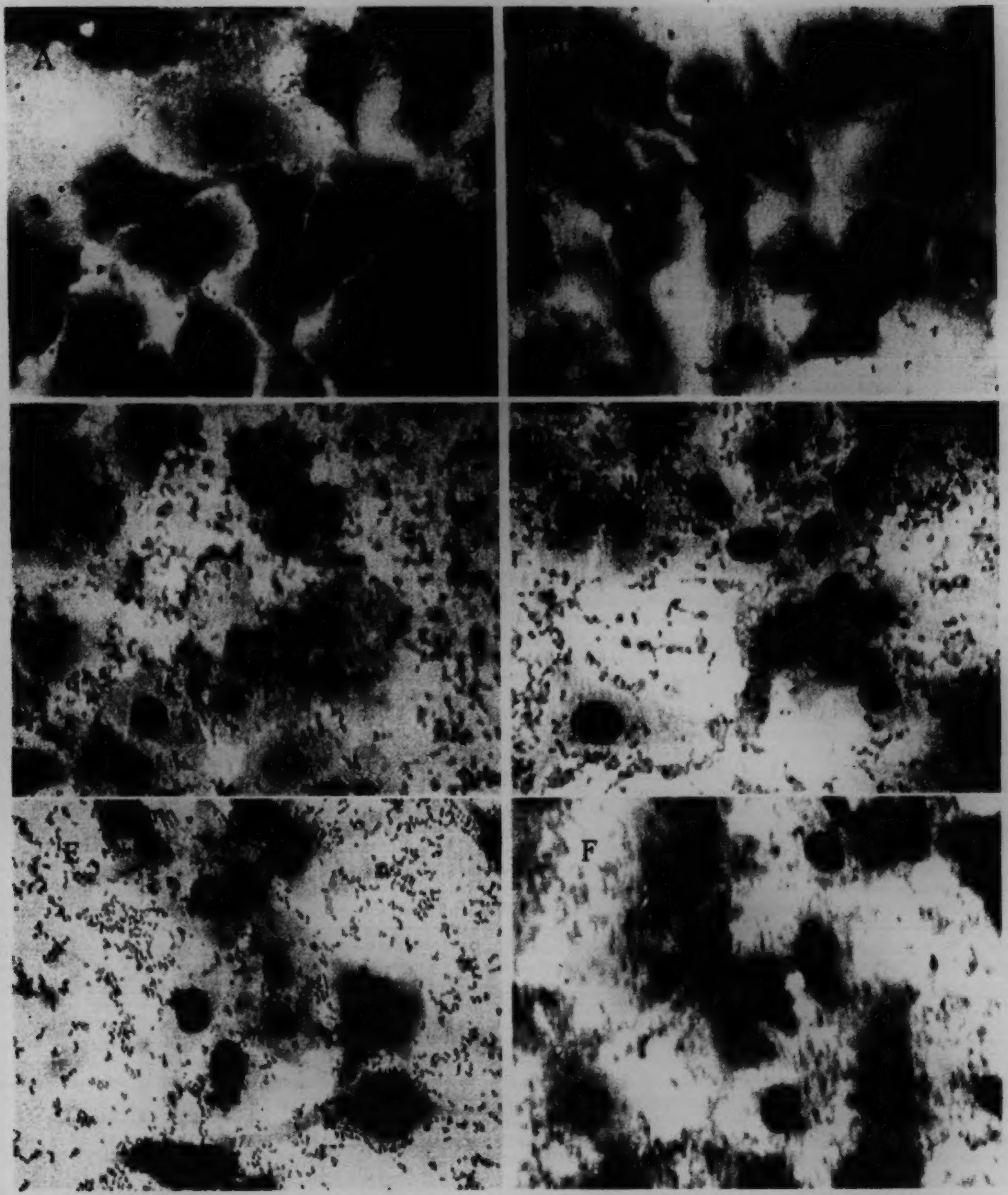

Figure 2.8. Morphology of A549 cells, infected with different doses of *S. pneumoniae* 24 h post-infection. Giemsa stain. (A) Control uninfected A549 cells. A549 cells were infected with (B) 10^1 cfu, (C) 10^2 cfu, (D) 10^3 cfu, (E) 10^4 cfu, or (F) 10^5 cfu of *S. pneumoniae* serotype 14. Magnification, 40X.

Initial concentration, cfu/well	0	10^1	10^2	10^3	10^4	10^5
Concentration after 24 h, cfu/well (average)	0	8 x10^5	1.2 x 10^7	9 x 10^7	1 x 10^8	1.6 x 10^8

Table 2.2. Bacterial multiplication of *S. pneumoniae* during co-culture with A549 cells after 24 h of incubation ($n = 2$).

2.4. Metabolites in supernatants of A549 cell line infected with *S. aureus*

Pilot experiments with *S. aureus* (Panton-Valentine leukocidin-positive methicillin-resistant, clinical isolate) were conducted with A549 cells. NMR analyses of supernatants were similar to those done with *S. pneumoniae* serotype 14, except that serum-free media DMEM with L-glutamine did not contain NEAA. We collected supernatants and analyzed metabolite concentrations as described above. Likely as a result of less nutritionally rich media after 24 h incubation, *S. aureus* did not multiply as significantly as *S. pneumoniae*; as well, the number of dead cells was visibly reduced (results not shown).

The observed damage and death of cells in experiments with *S. aureus* at each concentration were proportionally smaller than for the *S. pneumoniae* experiments. For instance, cell death after infection with 10^5 cfu of *S. aureus* was similar to that after infection with 10^4 cfu of *S. pneumoniae. S. aureus* multiplied better in the presence of A549 than in DMEM alone (observation under an inverted microscope).

2.4.1. TCA cycle intermediates

The concentrations of TCA cycle intermediates increased dose-dependently with bacteria, which corresponded with visually observed progressive cell damage (Figure 2.9). Citrate and 2-oxoglutarate showed increased levels in *S. aureus* experiments. This finding correlated with reduced cell death at high doses of *S. aureus* compared to that seen at high doses of *S. pneumoniae.* Succinate and fumarate levels showed similar trends to those found with *S. pneumoniae.*

Concentrations of succinate increased at higher doses of bacteria. Fumarate showed a biphasic curve with an increase at low doses and decrease at high doses of bacteria.

2.4.2. Metabolism of amino acids

Concentrations of the amino acids isoleucine and threonine decreased, while the levels of tartrate increased in a dose-dependent manner in the supernatants of A549 cells infected with *S. aureus* (Figure 2.10 A). Concentrations of isoleucine and threonine in DMEM alone with *S. aureus* did not vary significantly (Figure 2.10 B). Tartrate concentrations were undetectable in DMEM alone with all concentrations of *S. aureus* (results not shown).

2.4.3. Energy metabolism

Higher concentrations of *S. aureus* were associated with lower concentrations of glucose and higher concentrations of lactate and pyruvate when incubated with A549 cells. *S. auresus* on its own had no effect on glucose and lactate levels (Figure 2.11).

2.4.4. Bacterial-derived metabolites

Increased concentrations of all bacteria were associated with gradual increases in acetate and formate, 2-hydroxyvalerate isovalerate, and propionate (Figure 2.12 (A)), as well as 3-phenyllactate, 4-hydroxyphenyllactate, isobutyrate, and 2-hydroxyisovalerate (results not shown).

2.5. Conclusions

Infection of A549 cells with *S. pneumoniae* and *S. aureus* was associated with a characteristic pattern of changes in TCA cycle metabolites, amino acids, intermediates of energy production, bacterial-derived metabolites, death of a large fraction of cells, decreased mitochondrial potential, and changes in cell morphology.

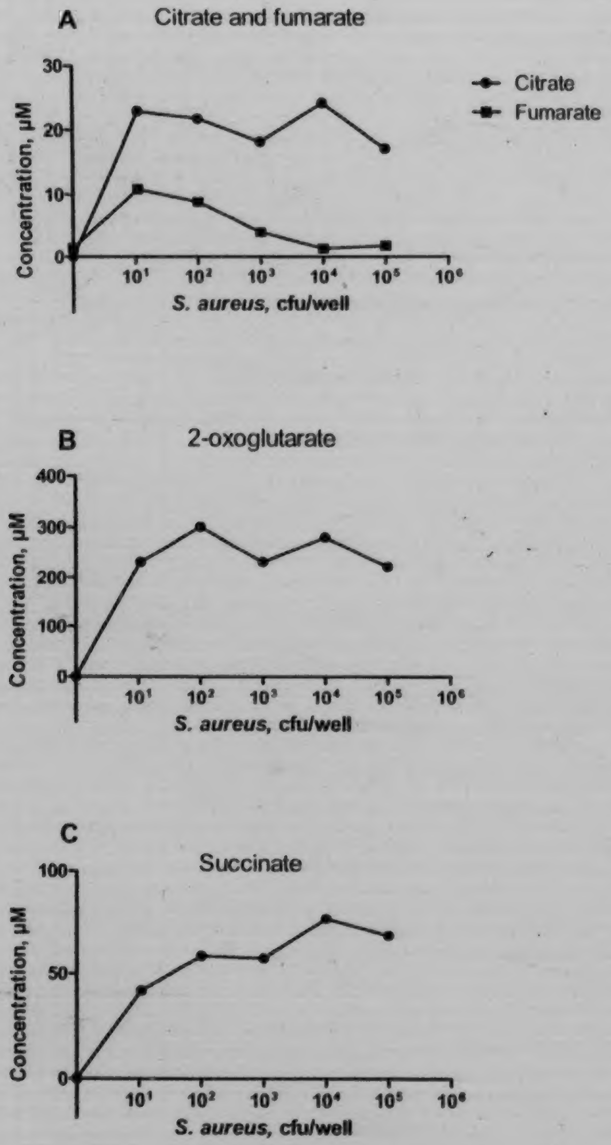

Figure 2.9. TCA cycle intermediates in the supernatants of A549 cells infected with increasing doses of *S. aureus* (A) Concentrations of citrate and fumarate. (B) Concentrations of 2-oxoglutarate. (C) Concentrations of succinate ($n = 1$).

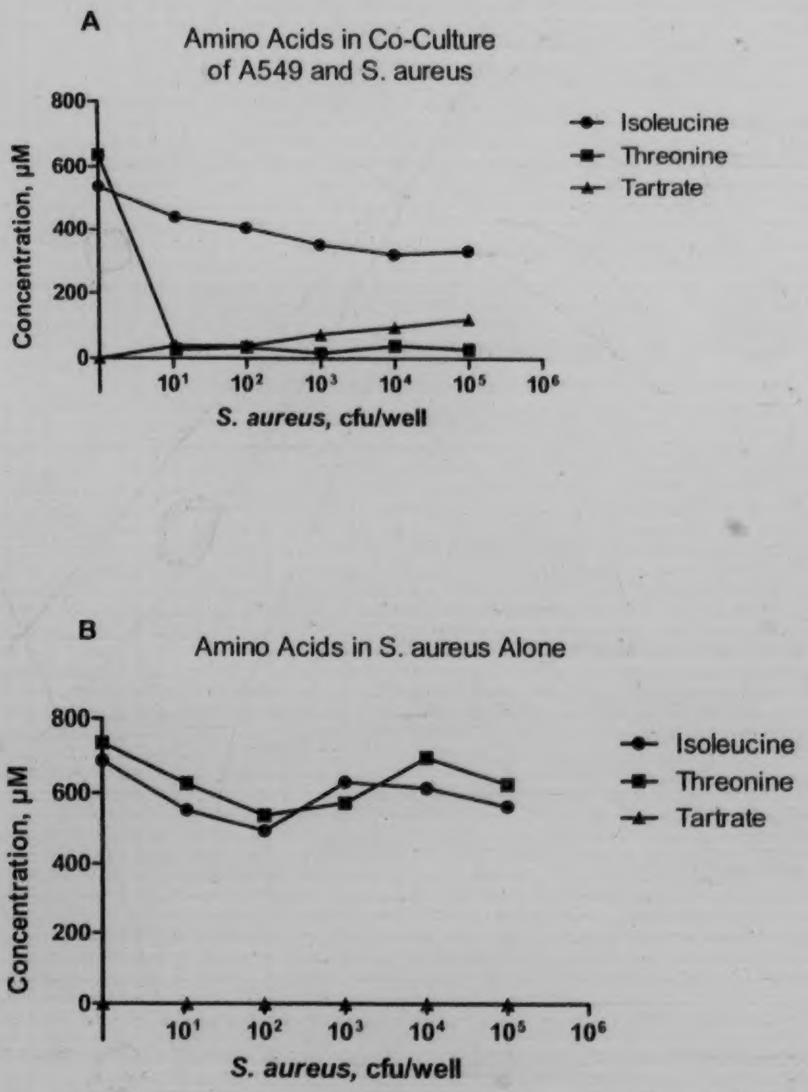

Figure 2.10. Metabolism of amino acids isoleucine, threonine, and amino acids' derivative tartrate in supernatant of A549 cells infected with different doses of *S. aureus*. Consumption of isoleucine, threonine, and production of tartrate in DMEM by *S. aureus*. (A) Metabolism of amino acids isoleucine, threonine, and derivative tartrate in supernatants of A549 cells infected with different doses of *S. aureus* (*n* = 1). (B) Consumption of isoleucine, threonine, and production of tartrate in DMEM by *S. aureus* (*n* = 1).

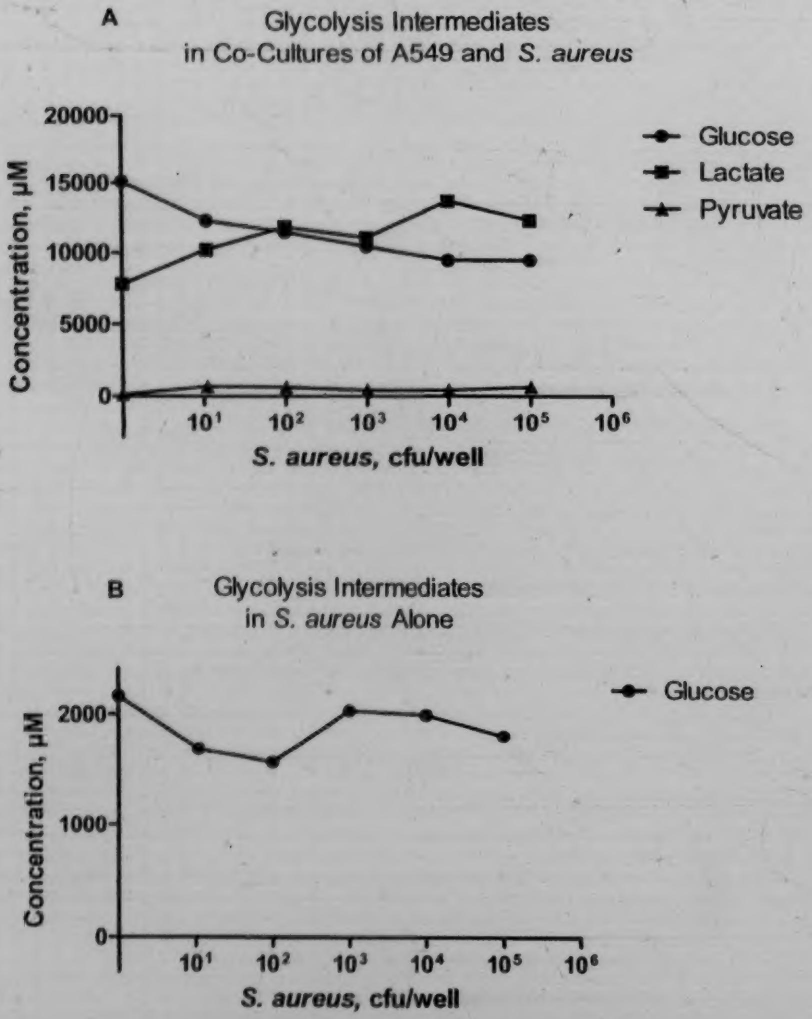

Figure 2.11. Glycolysis intermediate concentrations in supernatants of *S. aureus* – infected A549 cells. (A) Metabolism of glucose, lactate, and pyruvate in supernatants of A549 cells infected with different doses of *S. aureus* (*n* = 1). (B) Consumption of glucose and production of lactate by *S. aureus* in DMEM (*n* = 1).

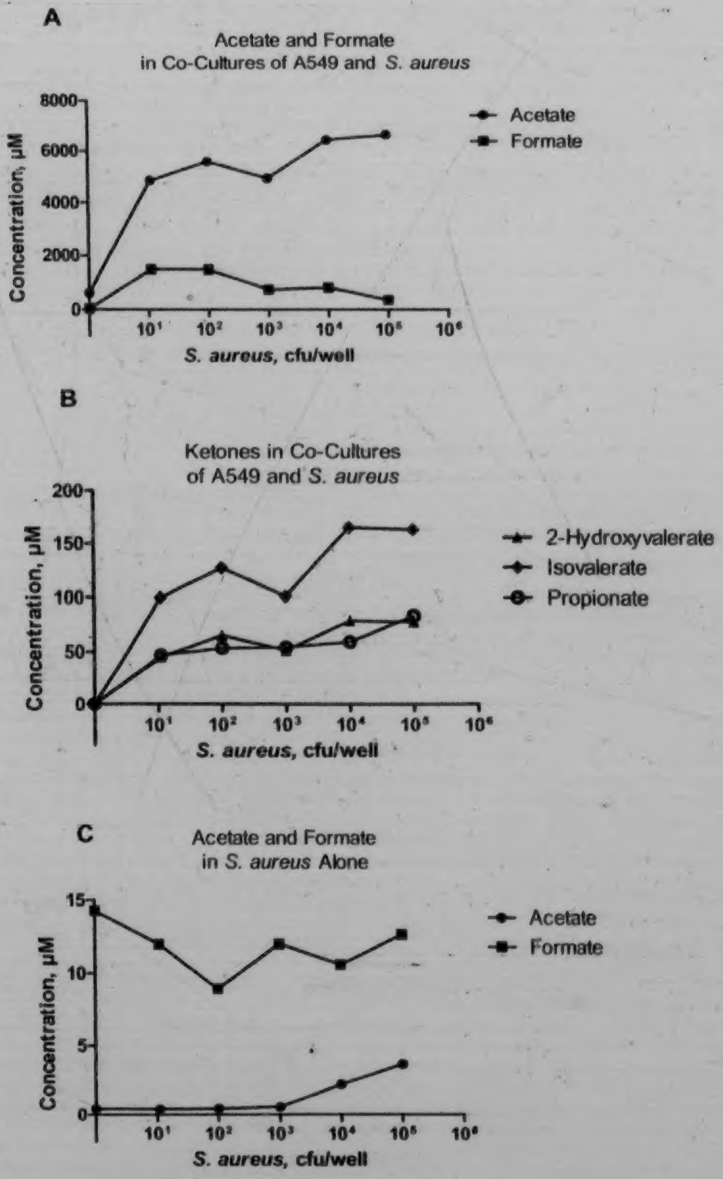

Figure 2.12. Ketones and small organic acid concentrations in supernatants of *S. aureus* – infected A549 cells. (A) Production of acetate and formate by *S. aureus* in supernatants of A549 cells. *(n* = 1). (B) Production of ketones by *S. aureus* in supernatants of A549 cells *(n* = 1). (C) Production of acetate and formate by *S. aureus* in DMEM.

The TCA cycle intermediate fumarate showed a biphasic curve of increase and subsequent decrease with increasing bacterial concentrations, while succinate steadily increased synchronously with an increased degree of cell damage and presence of dead cells. This association was observed in both *S. pneumoniae* and *S. aureus* experiments, taking into account that *S. aureus* experiments were done in the absence of added NEAA, which slowed the growth of bacteria and damage of cells.This resulted in 10^5 cfu of *S. aureus* causing the same level of cell death as 10^3-10^4 cfu of *S. pneumoniae*. Decreased concentrations of the ranges of amino acids and increasing levels of bacterial-derived metabolites correlated with dose of bacteria, both initially and after 24 h of incubation (which in turn depends on the presence or absence of NEAA).

We expect that future studies will show an association between damage of mitochondria, increased membrane permeability by bacterial virulence factors, and changes in levels of TCA intermediates. We expect that initial cytotoxic influences cause the release of the intermediates and increased concentrations, while subsequent damage of mitochondria and cell death leads to decreased TCA cycle intermediates. We also expect that studies of bacterial metabolism will quantitatively describe consumption and release of metabolites by bacteria at different phases of growth during different stages of bacterial-cell interaction.

Chapter 3

Mouse pneumonia model

3.1. Introduction

The metabolic response of an organism to bacterial infection is a poorly understood area of research. While normal metabolic profiles of urine and serum have been determined using NMR in earlier studies (Zuppi, 1997; Parfentjev, 1936), no studies have indicated changes in mouse metabolites during lung infection.

We hypothesized that definitive metabolic changes can be detected by NMR analysis of samples of biofluids (urine, serum, and bronchoalveolar lavage) of mice infected with pathogenic bacteria. We further propose that these changes can be differentiated from sham-treated animals. To test this hypothesis, the metabolomics of pneumonia in a mouse model of infection with two Gram-positive bacteria, *S. pneumoniae* and *S. aureus*, were studied (Figures 3.1 and 3.2). Each experiment also included sham-treated mice which were handled in the same manner as infected mice, except they were injected with the same volume of bacterial growth medium (Todd-Hewitt broth). These studies provided definitive evidence that a specific, highly differentiated metabolic response to infection occurs in mice, and that this response can be detected by analysis of multiple urinary metabolites.

Metabolomics of the mouse pneumonia model includes a cross-sectional study of metabolites in biological fluids of *S. pneumoniae*- and *S. aureus*-infected mice and a longitudinal study of the metabolites found in the urine of mice infected with *S. pneumoniae.* Each study included sham-treated mice, which were handled exactly as infected mice except that they injected with the same volume of bacteria growth media. Dr. Lacy designed the cross-sectional study; Dr. Slupsky designed the longitudinal study in mouse pneumonia model experiments.

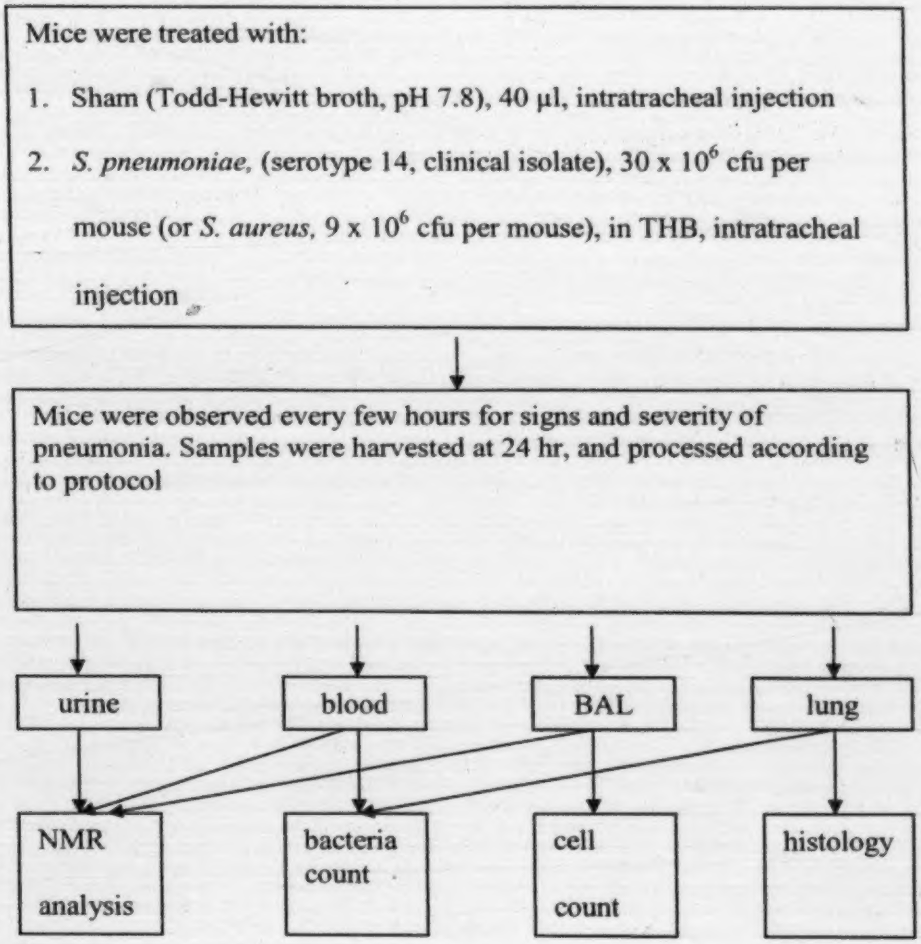

Mice were treated with:

1. Sham (Todd-Hewitt broth, pH 7.8), 40 µl, intratracheal injection
2. *S. pneumoniae,* (serotype 14, clinical isolate), 30 x 10^6 cfu per mouse (or *S. aureus,* 9 x 10^6 cfu per mouse), in THB, intratracheal injection

Mice were observed every few hours for signs and severity of pneumonia. Samples were harvested at 24 hr, and processed according to protocol

Figure 3.1. Design of cross-sectional study of mouse pneumonia model

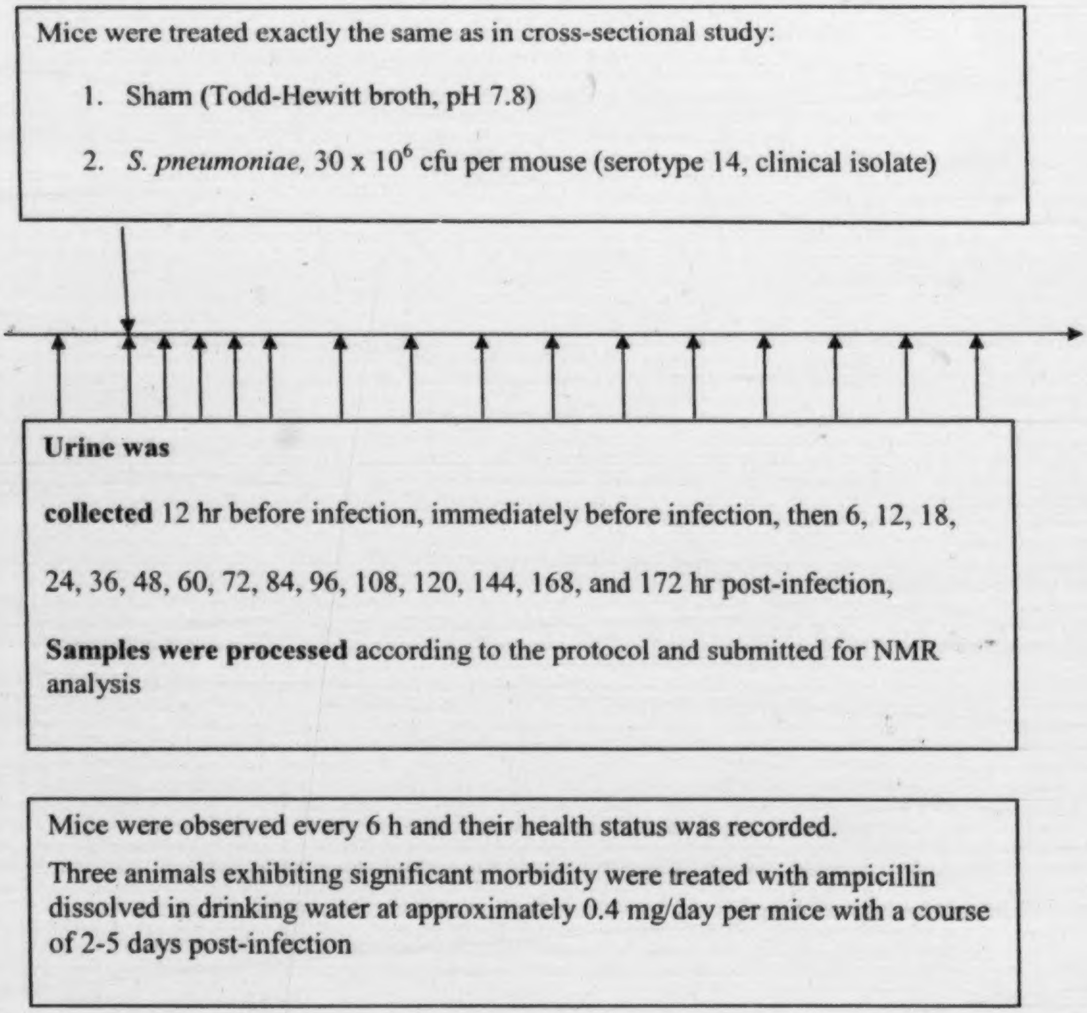

Mice were treated exactly the same as in cross-sectional study:

1. Sham (Todd-Hewitt broth, pH 7.8)
2. *S. pneumoniae,* 30 x 10^6 cfu per mouse (serotype 14, clinical isolate)

Urine was

collected 12 hr before infection, immediately before infection, then 6, 12, 18,

24, 36, 48, 60, 72, 84, 96, 108, 120, 144, 168, and 172 hr post-infection,

Samples were processed according to the protocol and submitted for NMR analysis

Mice were observed every 6 h and their health status was recorded.

Three animals exhibiting significant morbidity were treated with ampicillin dissolved in drinking water at approximately 0.4 mg/day per mice with a course of 2-5 days post-infection

Figure 3.2. Design of longitudinal study

3.2. Materials and methods

Materials. All general chemicals used were obtained from Sigma-Aldrich and Invitrogen (Carlsbad, California).

Bacteria. Todd-Hewitt broth (THB), 5 % sheep blood agar plates (BAP), and strains of *S. pneumoniae* and *S. aureus* were gifts from Dr. Gregory Tyrrell and Ms. Sandy Shokoples of the Northern Alberta Provincial Laboratory. For experiments with *S. aureus*-infected mice (and for sham-treated mice in the same experiments) THB was used, which caused a marginal degree of peribronchial infiltration in two bronchi of sham mouse, probably due to proteins in the broth (results are not shown). For experiments with *S. pneumoniae* (and for sham-treated mice in the same experiments) THB was diluted with 30 % DMEM to adjust the osmolality of the growth media to a normal range of 260-270 mOsm and subsequently to decrease the observed death of pneumococci due to osmotic stress and decrease the antigenic load of proteins in sham mice. Work with bacteria was done according to biohazard safety regulations at the University of Alberta. Using a conventional invasion assay, *S. pneumoniae* (strain 04SR2228) was selected by Sandy Shokoples as the most invasive strain among the collection of clinical isolates available, and was typed as serotype 14. The strain *S. aureus* used in this study was a clinical isolate, methicillin-resistant, Panton-Valentine leukocidin (PVL) positive and α-toxin positive (as suggested by β-haemolysis of erythrocytes of BAP). Bacterial suspensions for mouse infection were prepared as described in Chapter 2. The bacterial doses for infection per mouse (that induced disease without causing severe morbidity or a moribund state in the animal) were 30×10^6 cfu *S. pneumoniae* in 40 μl of THB, and 9×10^6 cfu *S. aureus* in 40 μl of THB. Bacterial inocula for *S. pneumoniae* were prepared using Beckman DU-640 spectrophotometer. *S. aureus* suspensions were prepared with a Vitek colorimeter (bioMérieux Inc., USA). Precautions were taken in preparing similar bacterial doses as described in Chapter 2.

Concentrations of bacteria were checked by colony count after plating inocula on BAP before and after mouse infection to check the dose of bacteria per mouse in 40 µl of broth. During infection experiments, the doses of viable *S. pneumoniae* in inoculum in cross-sectional and longitudinal studies decreased by 50 – 70 % from 30 x 10^6 cfu per mouse (probably due to confluence-dependent bacteria death because of activation of autolysin of cell wall (Brock, 1984) at high densities of *S. pneumoniae*, for instance, 7.50 x 10^8 cfu/ml in these experiments. *S. aureus* in the inoculum multiplied by 50% during infection experiments.

Prior to the described experiments, bacteria were passaged through the mice (data not shown) by inoculating into mouse lungs and recovering bacteria from the blood 24 h later (once for *S. pneumoniae* and three times for *S. aureus*). The strain of *S. pneumoniae* we used was sensitive to ampicillin, and this was determined prior to infection experiments by the disk diffusion technique (Jorgensen, 1994), with more than 25 mm growth inhibition zone around paper disk Whatman # 1 (Fisher Scientific, USA) and with a potency 100 µg of ampicillin.

Mice. C57Bl/6 male mice (8-10 weeks old) were obtained from Charles River Laboratory, Canada or NCI Frederick Laboratory (USA), for *S. pneumoniae* and *S. aureus* infection experiments. They were housed and handled according to approved protocols of the University of Alberta Health Sciences Animal Policy and Welfare

Committee (HSAPWC), kept under artificial light on 12:12-h light/dark cycle, and had access to water and food *ad libitum*.

Filters. Nanosep Omega 3 kDa molecular weight cut-off filters (Pall Life Sciences, USA) were prepared according to the protocol in Chapter 2.

Mouse infection. Mice were subjected to inhalational narcosis with 4 % isoflurane and 96 % oxygen with a flow rate 0.5 L/min. Mice developed deep anaesthesia and were infected with bacterial inoculum by intratracheal injection. Trachea was accessed by cutting skin on the middle line of the neck, moving salivary glands to the sides from middle line and cutting fascia and muscles on the middle line. Injection of bacterial inoculum in THB for infected mice or THB alone for control mice was done with a 50 μl syringe (Hamilton, USA) and 26 G needle, inserted between 2nd and 3rd tracheal cartilages and directed toward the bifurcation of trachea. Care was taken to direct bacterial inoculum to the alveoli. Mice entered a surgical plane of narcosis determined by loss of pinch, corneal and other reflexes. Injection was done during a time period of 2 seconds before and until the end of inspiration. Mice were held at 45° during injection and 10 min after to facilitate movement of inoculum toward the lungs. In a separate experiment, injection of dye into trachea showed that more than 90 % of Evan's blue dye was distributed into the lung alveoli (results are not shown) as described in literature (Su, 2004).

After injection, the skin was sealed with 3-4 surgical sutures. Care was taken to decrease trauma, bleeding and inflammation during surgery by using small cuts, carefully handling soft tissues with forceps, and careful application of sutures. After mice were resuscitated from narcosis, they were placed into pre-labeled cages and monitored every

6 h; their health status and signs of disease were evaluated according to extended HSLAS criteria (from 0 to 3). Changes in activity ranged from 0 in the case of a mouse spending most of its time outside of the nest, being alert, and investigating the cage or fighting with neighbours, to 3 in the case of the mammal spending all its time in its nest with a hunched back. Regular grooming led to shiny and smooth hair coat (signed 0), absence of grooming - to severe piloerection (3). A decrease in mobility ranged from 0 level when the mouse rose in the cage and investigated when human appeared, to 3 in the case of sitting with hunched back and being reluctant to move even if prodded gently. Healthy mice usually had normal food and water intake (marked as 0), while ill ones showed decreased food and water intake. Mice with severe pneumonia partially closed their eyes most of the time, even if taken out of the cage (evaluated as 3), while healthy ones spent most of the time with eyes wide open (evaluated as 0). Healthy mice had normal rapid and shallow breathing (marked as 0) while infected had slow and laboured breathing (3).

Blood. For the cross-sectional study, mice were sacrificed at 24 h and blood samples were collected. Mice were euthanized with an overdose of ketamin/rompun 3:1 v/v mixture and by cardiac puncture with exsanguination. Blood was collected in Eppendorf tubes and serum was prepared by allowing clot formation and subsequent centrifugation. A few drops of blood were collected separately and 10 µl of blood were spread on BAP to determine bacteremia. Serum samples were stored at -80° C, quickly thawed, and filtered through pre-washed Nanosep filters.

Urine. Urine was collected from euthanized animals in the cross-sectional study by opening the abdominal cavity and puncturing the base of the bladder with a 26 G needle and suctioning urine with a syringe. In the longitudinal study, urine samples were collected by holding mice above a weighing boat. The samples were stored at -80° C, prepared, and analysed by NMR analysis as described above.

Bronchoalveolar lavage. After urine collection, mice were either subjected to bronchoalveolar lavage (BAL), or lungs were excised for either histology or homogenised for bacterial counts. BAL samples were centrifuged, pellets were characterised by cell count, and supernatants were analyzed by NMR. For lavage, the trachea was accessed as described before: the trachea was cut halfway through and a plastic tube was inserted toward the bifurcation; 1 ml of ice-cold HBSS was injected into the trachea by syringe. BAL was collected into new syringe while the chest was massaged. Care was taken to avoid excessive pulling on the syringe to prevent damage to the lung tissue resulting in the appearance of bronchial epithelial cells in the BAL. BAL samples were centrifuged at 300 *g* at 4° C for 10 min to pellet cells and at 14,000 *g* at 4°C to pellet bacteria. Supernatants were frozen and stored at -80° C for NMR analysis. Samples of cell pellets were resuspended, the total number of cells was counted by hemocytometer, and the ratio of live to dead cells was calculated with Trypan blue exclusion assay. Results were normalized to the volume of each cell pellet sample. Differential cell counts were done on Diff-Quick stained slides prepared on a Shandon Cytospin 4 (Fisher Scientific, USA). After a total cell count in the cell pellet, a volume containing 10,000 cells was calculated for each sample and the total volume was adjusted to 100 µl. Samples were loaded into cytofunnels (Thermo Scientific, USA) with pre-labeled slides and filter cards (Thermo Scientific, USA). Cytofunnels were centrifuged at 400 *g* for 15 min to allow binding of cells to the slides and absorption of liquid. Slides were air-dried for 12-18 h in the dark and stained in Diff-Quick stain as described in

Chapter 2. Stained slides were air-dried for a few hours and all cells were counted (neutrophils, macrophages, eosinophils, basophils, lymphocytes) until the total cell number reached 200. Supernatant samples of BAL were filtered through Nanosep filters and analysed by NMR.

Histology. Lungs for histology were fixed with formalin, embedded, sliced, stained with hematoxylin eosin stain (H/E), evaluated for the presence and severity of inflammation, and photographed. For collection, a plastic tube was inserted into the trachea, after which fixative (10% v/v formalin) was injected. The syringe and extra tubing was kept 25 cm above the lung for 5 min to ensure equal and careful fixation. Lungs were excised and placed into tubes with formalin. Lung samples were then transported to Dr. Lakshmi Puttagunta, Department of Laboratory Medicine and Pathology, who embedded the lungs in paraffin wax, sectioned and stained tissues with H/E. Sections were observed by microscopy to estimate the severity of pneumonia by an Olympus CX31 (Olympus, Japan) microscope. The severity of pneumonia was scored on a scale of zero (no lesion) to four (severe inflammation) according to the following criteria: exudate, presence of macrophages and PMN, pneumocyte shedding, and perivascular edema. Areas with different degrees of inflammation were approximated. Slides were photographed with a Nikon E600 microscope and a Nikon DXN 1200 digital camera controlled by Nikon Act-1 software. Mr. Tom Turner (Department of Laboratory Medicine and Pathology) processed images using Adobe Photoshop 9.

Bacterial counts. Lungs for bacterial counts were collected by excision of chest cavity, diaphragm, and neck as described above. Lungs were washed in 5 ml of HBSS to remove excess blood, weighed, and immediately homogenized in 1 ml of THB to maintain bacterial viability with a manual glass homogeniser. Serial dilutions with a 1:10 ratio were prepared, 100 µl of each were plated in duplicates on BAP and colonies were calculated, normalised to the dilution ratio, and reported as the number of bacteria per mg of lung weight.

NMR experiments. The volume of each sample was adjusted to 585 µL with distilled water and 65 µL of internal standard (Chenomx, Edmonton, Canada), and the pH was adjusted to 6.8; samples were acquired with a 600 MHz NMR spectrometer by Shana Regush, Kathryn Rankin and analyzed by Hao Fu at the Magnetic Resonance Diagnostic Centre, University of Alberta. Targeted profiling was carried out using the Chenomx NMR Suite version 4.6 software by Hao Fu and myself to simultaneously determine the identities and concentrations of specific metabolites. Metabolites with very low concentrations, or very complex spectra, which overlapped significantly with other metabolites or noise, were ignored during analysis to decrease the probability of false-positive results.

Data analysis. Concentrations of metabolites were exported and metabolite patterns were analysed and visualised by principal component analysis (PCA) with SIMCA-P software (version 11, Umetrics, Umeå, Sweden). Quantities of metabolites were plotted as mean, standard error of mean, and statistical significance using two-tailed Mann-Whitney non-parametric test by GraphPad Prism v 5.0 (demo-version, GraphPad Software, San Diego, USA) and Microsoft Excel 2007 (Redmond, USA). Metabolites of vastly different concentration were scaled down by an order for plotting purposes. Metabolites were grouped according to the most significant known physiological function, biochemical pathway, localization in cells or organs, according to the known or hypothetical role and origin.

In some cases, a lower than detectable concentration of some metabolites in some biofluids led to additional complications in comparative analysis. On the graphs below, undetectable metabolites were shown on plots to allow visual comparison with other biofluids, where metabolites were detectable.

3.3. Results

3.3.1. Severity of pneumonia of infected mice

3.3.1.1. Cross-sectional study with *S. pneumoniae*-infection. A group of 28 male C57Bl/6 mice aged 8-10 weeks were used in the study: 13 mice were sham-treated and 15 mice were infected with 3.0 x 10^7 cfu of *S. pneumoniae*. Infected mice developed mild-severe or severe pneumonia 24 h after infection; disease progression was assessed with changes in their appearance and behaviour. Infected mice were less motile, with half-closed eyes and reduced motility. They also spent less time eating, drinking, and cleaning their fur. Their fur was dull and stood out, indicating increased morbidity. Larger, stronger mice with a tendency to fight before infection were observed to fight less post infection; these mice were apparently less ill than smaller and more peaceful animals post-infection.

There was a 5-10-fold increase in macrophage and neutrophil counts in BAL, as well as bacteremia in 20 % of infected mice (Figures 3.3, 3.4). Additionally, the BAL of infected mice contained substantial cell debris, bacteria, and fibrin-like particles.

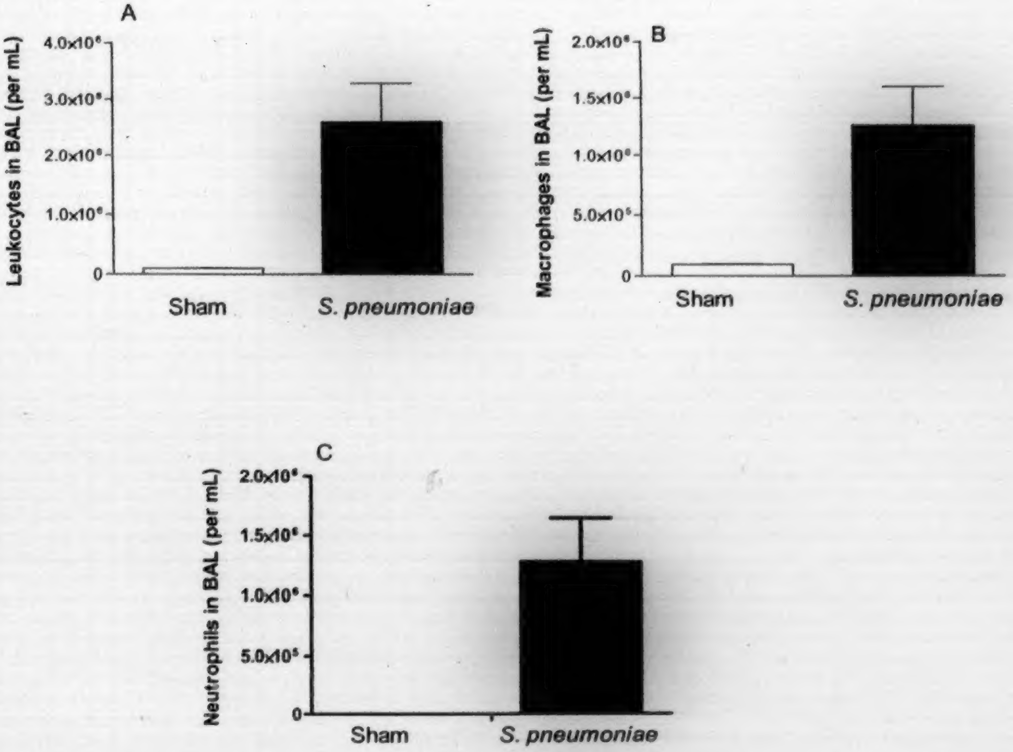

Figure 3.3. Total cell counts (macrophages and neutrophils) in BAL 24 h post-infection with *S. pneumoniae*. Mice were injected with 40 µl THB (sham) or 3 x 10^7 cfu/mouse *S. pneumoniae* (serotype 14). Values represent mean and error bars indicate standard error of the mean. Sham, *n* = 5, *S. pneumoniae*, *n* = 8.

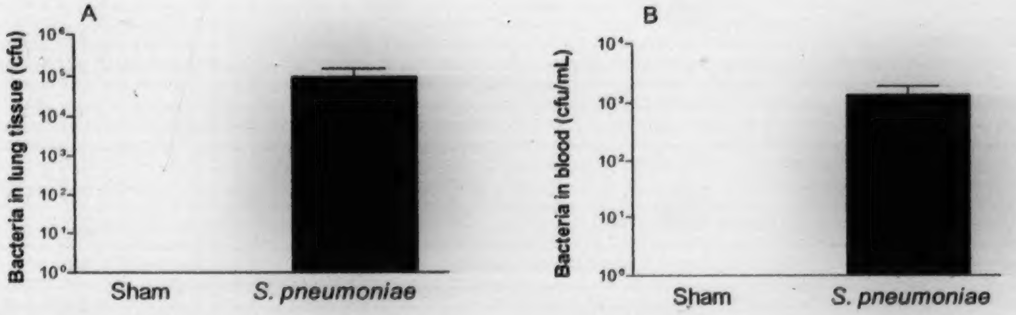

Figure 3.4. Bacterial counts in lung tissue and blood 24 h post-infection with *S. pneumoniae*. (A) Bacterial counts in excised lungs 24 h post-infection with *S. pneumoniae*. Mice were injected with 40 µl THB (Sham) or 3 x 10^7 cfu/mouse *S. pneumoniae* (serotype 14). Values represent mean and error bars indicate standard error of the mean. Sham, *n* = 5, *S. pneumoniae, n* = 4. (B) Number of *S. pneumoniae* per 1 ml of blood 24 h post-infection. Mice were injected with 40 µl THB (Sham) or 3 x 10^7 cfu/mouse *S. pneumoniae* (serotype 14). Values represent mean and error bars indicate standard error of the mean. Sham, *n* = 13, *S. pneumoniae, n* = 15.

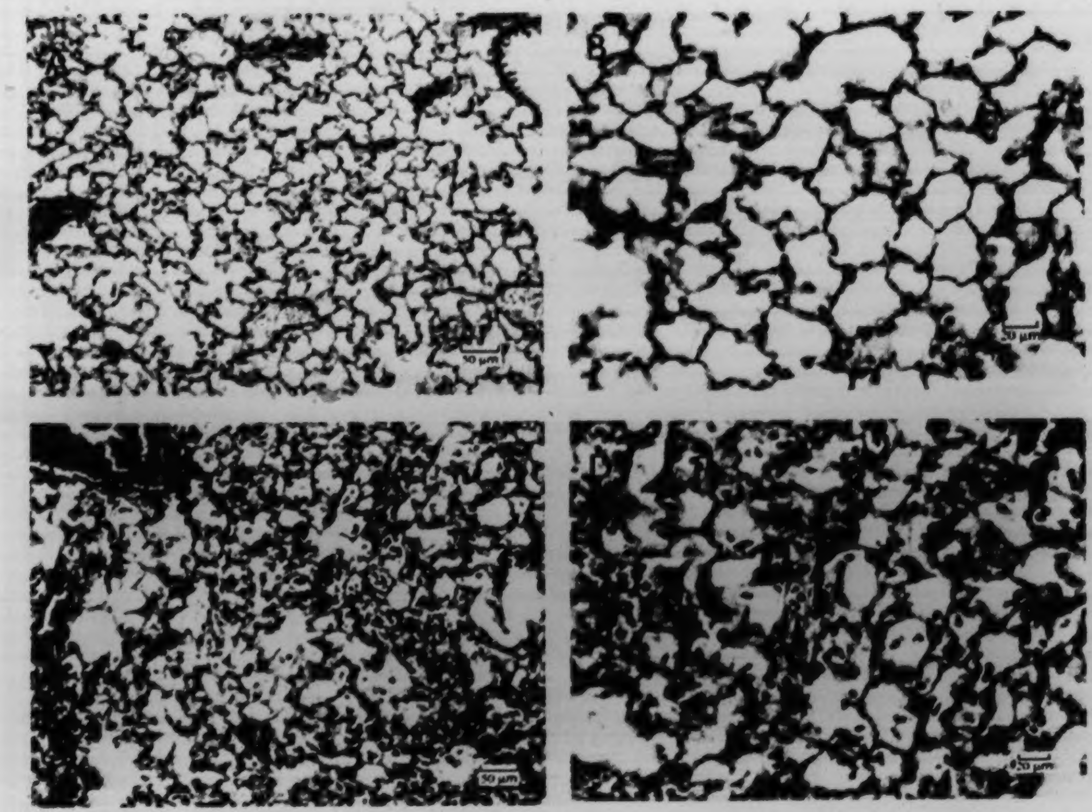

Figure 3.5. Lungs of sham and *S. pneumoniae*-infected mice. (A) Sham, H/E, 20X magnification. Normal architecture of the lung: alveoli have normal size, erythrocytes and white blood cells of blood are present only in blood vessels, while the lumenal side of bronchi have small amounts of mucus. (B) Sham, H/E, 40X magnification. Normal architecture of the lung: alveoli have preserved numbers and structure of type I and type II pneumocytes with few alveolar macrophages, and the basal lamina is filled with cells. (C) *S. pneumoniae* infection, H/E, 40X magnification: peribronchiolar, bronchial, and perivascular infiltrates, edema, hemorrhage, and damage of alveolar architecture. (D) *S. pneumoniae* infection, H/E, 20X magnification: consolidation, massive infiltration of alveoli with neutrophils and macrophages, hemorrhage, alveolar edema with proteinaceous fibrin and sloughed epithelial cells. Sham, $n = 3$, *S. pneumoniae,* $n = 3$.

As well, histological observations showed a severe inflammation in 25-30% of a lung lobe or 15-20% of two lobes (Figure 3.5).

3.3.1.2. Longitudinal study of *S. pneumoniae*-infection. A group of 13 male C57Bl/6 mice aged 10 weeks were used in this study: 3 mice were sham-treated and 10 mice were infected with 3.0 x 10^7 cfu of *S. pneumoniae* using the same protocol as used for the cross-sectional study. Infected mice developed mild-severe or severe pneumonia with a peak at 24-36 h for most mice and 36-42 h for 3 of the most severely ill mice (as assessed with changes in mouse behaviour). These severely ill mice were treated with ampicillin (0.4 mg/mouse/day at 2-5 days post-infection).

3.3.2. Metabolomics of blood, urine and BAL of *S. pneumoniae*-infected mice

Metabolomic analysis of samples of mouse biofluids revealed changes in a range of metabolites from many biochemical pathways with the most profound changes in intermediates of tricarboxylic acid cycle (TCA cycle), amino acids and their metabolism, as well as metabolites from the glycolysis pathway, exogenous (food-derived) metabolites, by-products of bacterial metabolism, and metabolites with unknown physiological functions.

Precise measurements of daily urine production and their influences on the concentrations of metabolites were problematic. However, the amount of urine from control mice was statistically not different from the amount of urine of infected mice (Figure 3.6 A). The method and data shown in Figure 3.6 A are not precise; however, they give an overall idea about the dynamics of urine production. Figure 3.6 B shows the number of urine samples used for analysis. During the longitudinal study, mice urinated actively at the beginning (after infection), and less as they became accustomed to

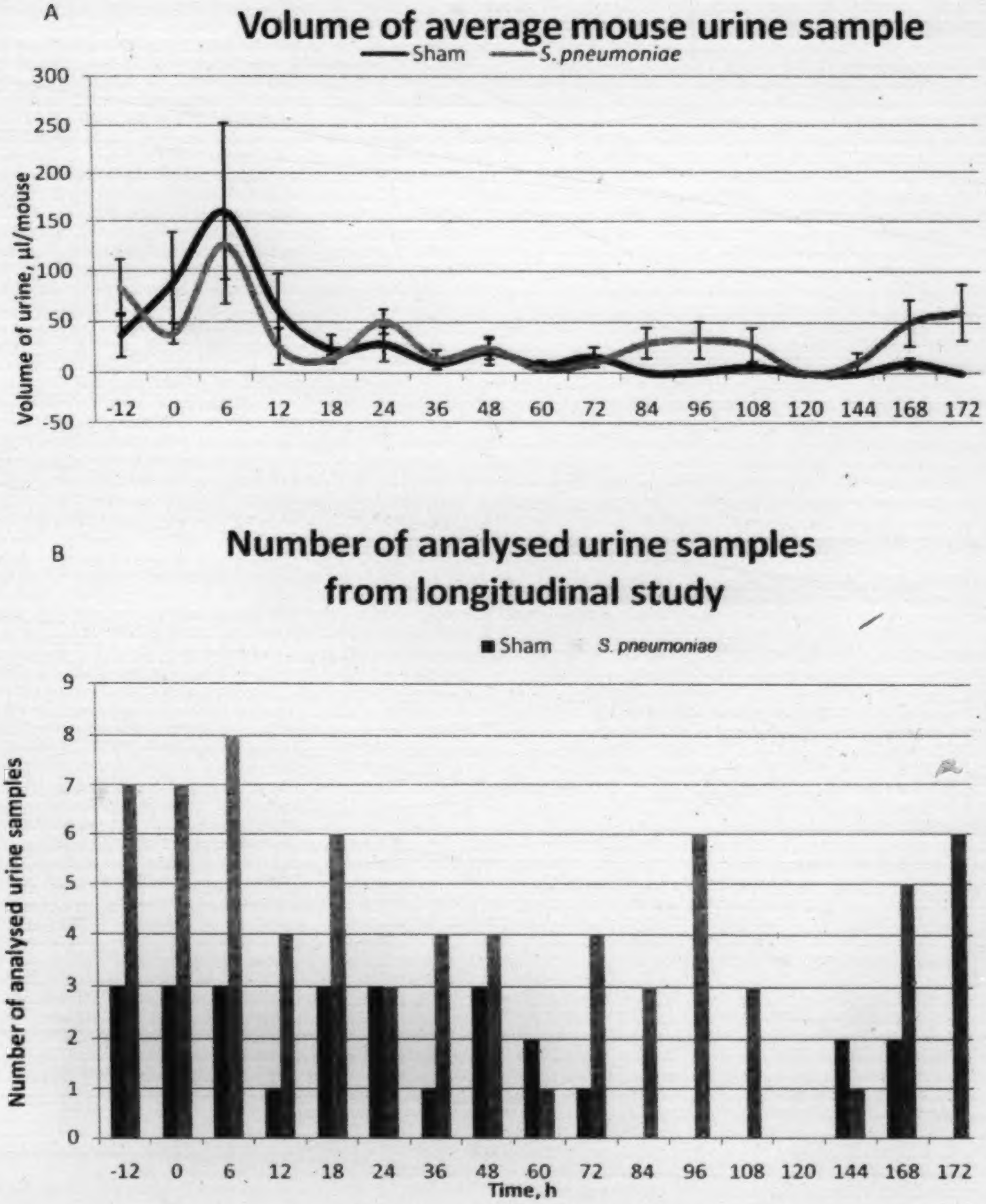

Figure 3.6. Production of urine by *S. pneumoniae*-infected and sham mice in the longitudinal study. (A) Average volumes of collected mouse urine. (B) Number of analysed urine samples from mice used in longitudinal study. Total sham, $n = 3$; *S. pneumoniae*, $n = 9$.

handling. The last collection of urine was done with a syringe on euthanized animals using the same protocol as the cross-sectional study.

3.3.2.1. Concentrations of TCA cycle intermediates in blood, urine and BAL of *S. pneumoniae*-infected mice

The levels of most TCA cycle intermediates decreased significantly in the biofluids of infected mice. More specifically, at 24 h post-infection the Krebs cycle intermediates decreased approximately by 50 % in serum (Figure 3.7 B), and by 50-97 % in urine (Figure 3.7 C). All metabolites showed progressively increasing concentrations of metabolites from BAL through serum to urine, which was most concentrated. Figures 3.8-3.10 show concentrations of the metabolites during the longitudinal study. Metabolites gradually decreased their concentrations during first 24-30 h after infection, and returned to normal values in the next 100 h with an increase in subsequent hours in some cases (see results of longitudinal study in Figures 3.8-3.10 respectively). These changes were synchronous with the development of pneumonia (according to the other methods in cross-sectional study) and peaks of changes were close to the climax of disease (according to observations of mouse health status in the longitudinal study).

3.3.2.2. Metabolism of amino acids. *S. pneumoniae*-infected mice had lower concentrations of many amino acids and their derivatives in biofluids. Most of the measured amino acids in serum decreased during infection (from a few to 50 %), except for arginine, asparagine, glutamine, serine, and tyrosine, which showed no change

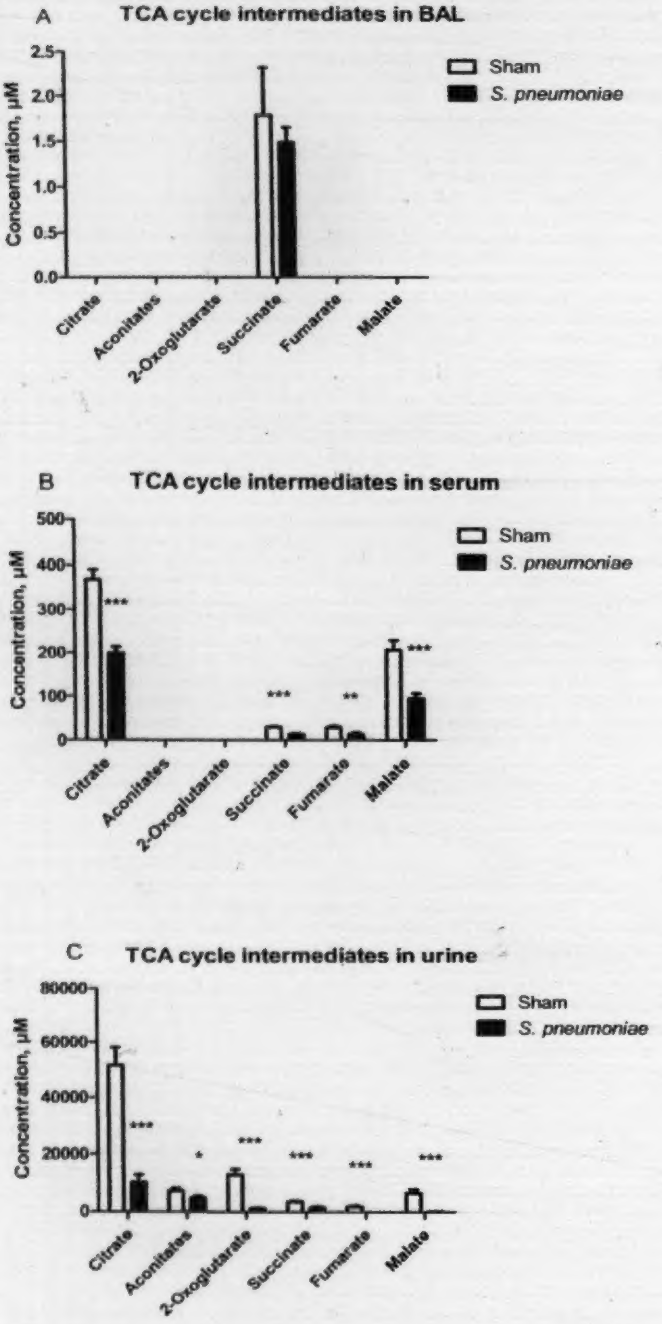

Figure 3.7. Concentrations of TCA cycle intermediates in biofluids of mice from cross-sectional study 24 h post-infection with *S. pneumoniae* or sham-treatment.

Figure 3.7 (continued). (A) BAL samples, sham, $n = 4$, *S. pneumoniae*, $n = 7$. (B) Serum samples, sham, $n = 8$, *S. pneumoniae*, $n = 8$. (C) Urine samples, sham, $n = 12$, *S. pneumoniae*, $n = 13$. Aconitates refers to both cis- and trans-aconitate * $p < 0.05$; ** $p < 0.01$; *** $p < 0.001$.

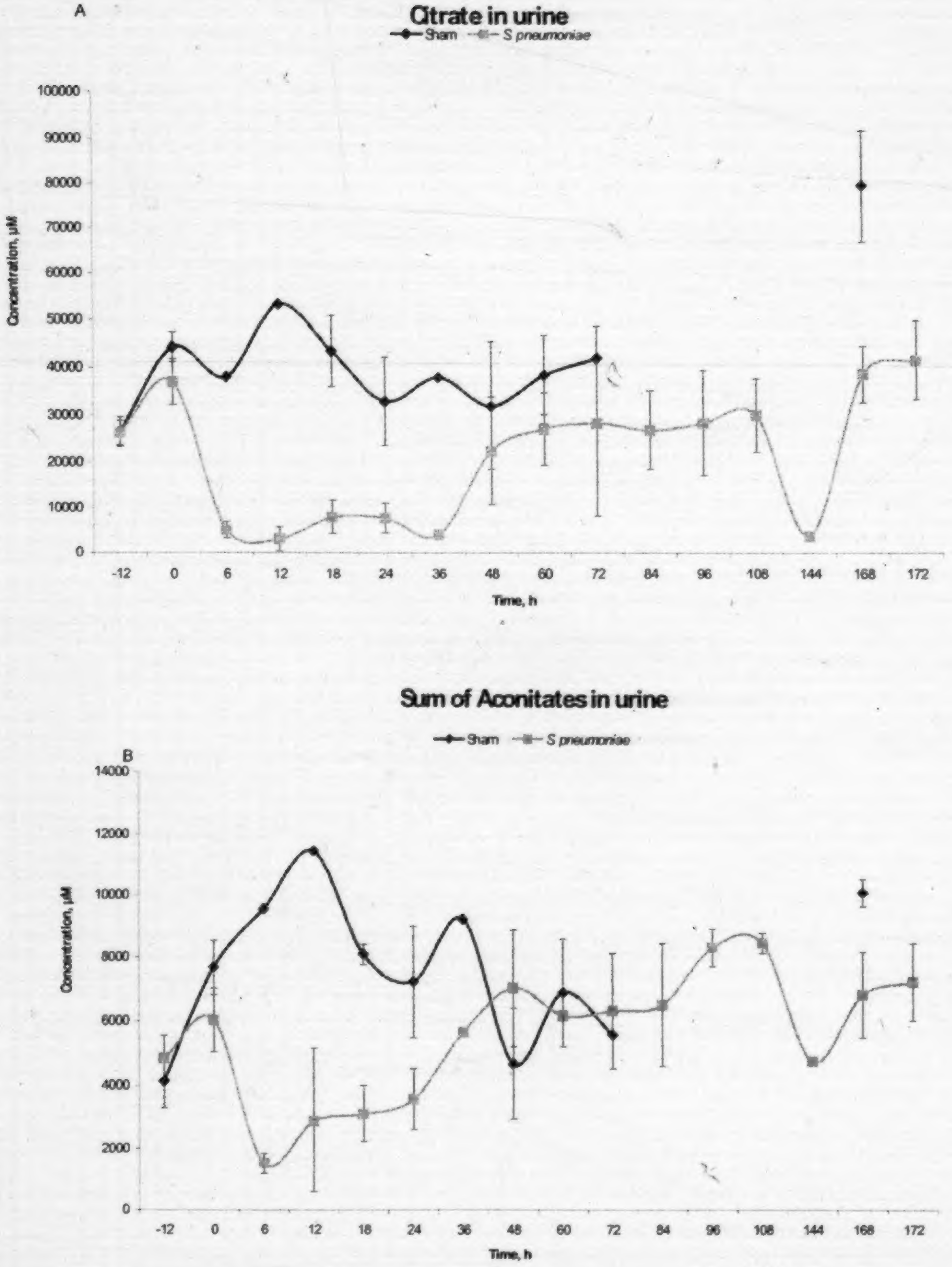

Figure 3.8. Concentrations of TCA cycle intermediates in *S. pneumoniae*-infected mouse urine in the longitudinal study. (A) Citrate. (B) Cis- and trans-aconitates in urine samples. See the numbers of sham and infected samples at different time points in Figure 3.6 (B).

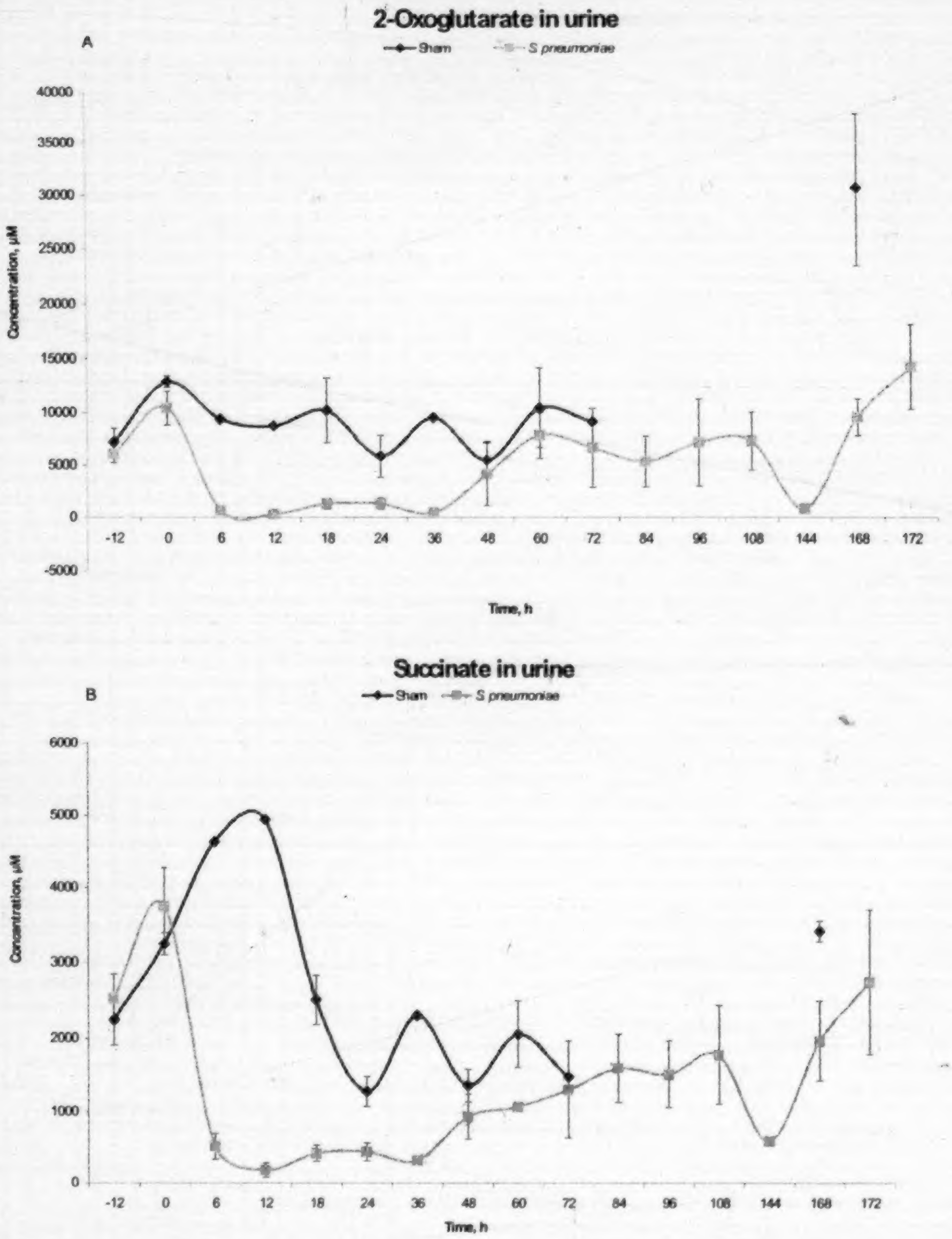

Figure 3.9. Concentrations of TCA cycle intermediates *S. pneumoniae*-infected mouse urine in the longitudinal study. (A) 2-Oxoglutarate. (B) Succinate in urine. See the number of sham and infected samples at different time points in Figure 3.6 (B).

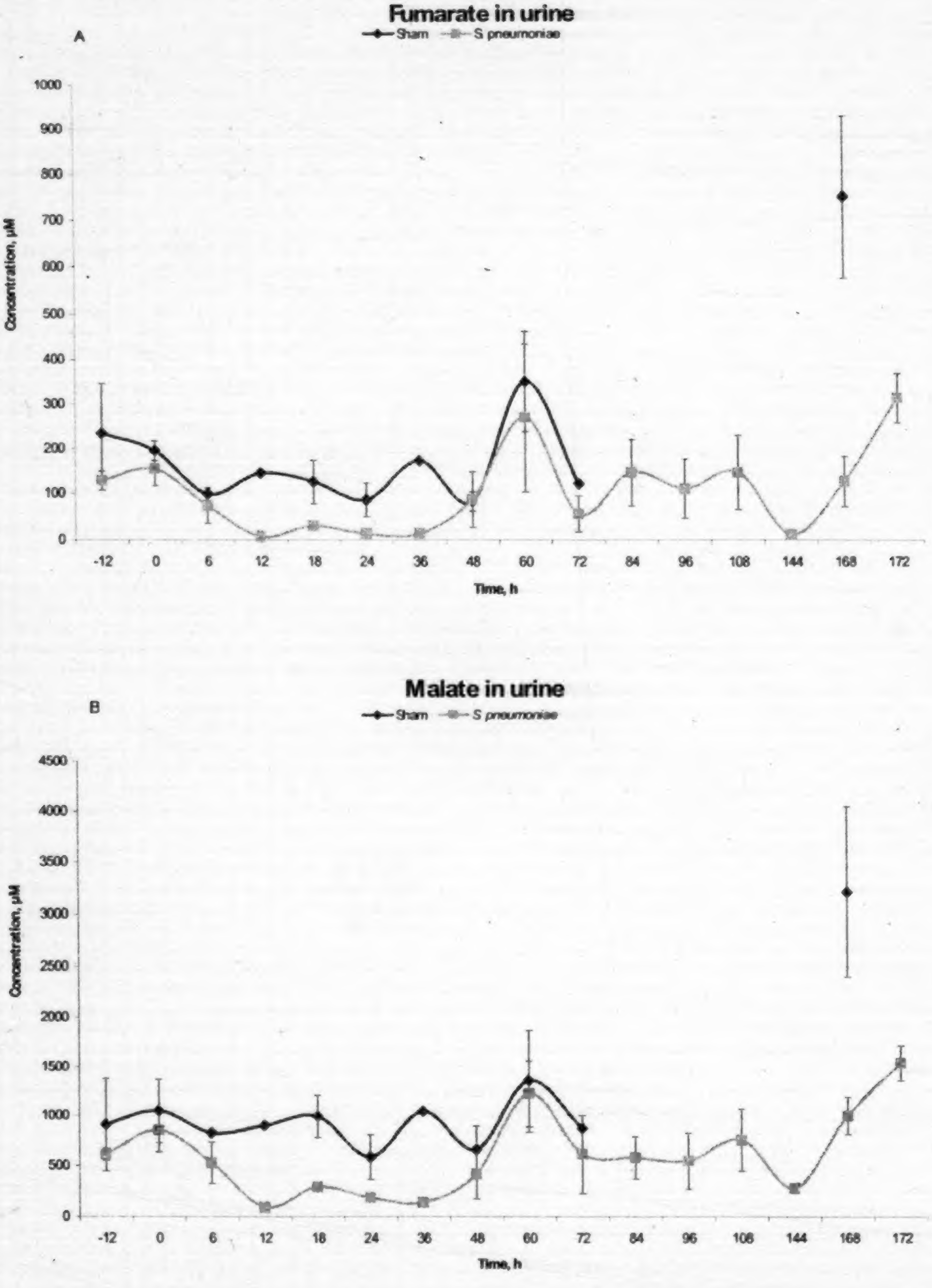

Figure 3.10. Concentrations of TCA cycle intermediates in *S. pneumoniae*-infected mouse urine in the longitudinal study. (A) Fumarate. (B) Malate in urine samples. See the number of sham and infected samples at different time points in Figure 3.6 (B).

(Figure 3.11-3.12). Similarly, amino acids decreased in urine and BAL with the exception of increased lysine in BAL. Concentrations of branched chain amino acids (BCAAs) leucine, isoleucine, valine decreased by 45-65% in the serum of infected mice. Levels of the leucine derivative 2-oxoisocaproate in urine and the urea cycle intermediate ornithine in the serum of infected mice decreased by 30-40%. Levels of alanine in serum decreased in a similar manner to BCAAs or slightly less (Figure 3.12). Infection of mice did not change the concentration of the leucine derivative N-isovalerylglycine in urine. The concentration of tryptophan was decreased by approximately 50-60% in urine samples, while the concentration of its derivative 3-indoxylsulfate decreased by 60-70%.

Urea decreased by approximately 20% serum and BAL of infected mice. Figure 3.11 shows the concentrations of essential amino acids and derivatives of amino acid metabolism in the cross-sectional study. Figure 3.12 shows concentrations of nonessential amino acids. Figure 3.13 shows glycine and tryptophan dynamics in the longitudinal study that represents changes in other amino acids in urine during pneumonia.

3.3.2.3. Energy metabolism

Concentrations of lactate increased in BAL and decreased in serum and, particularly, urine. Levels of ketone bodies in serum were altered in both directions. Figure 3.14 shows concentrations of these metabolites in the cross-sectional study; Figure 3.15 shows dynamics of glucose and lactate in the longitudinal study. We observed a transient increase in lactate in urine at 6 h and of glucose at 6 and 36 h in infected animals.

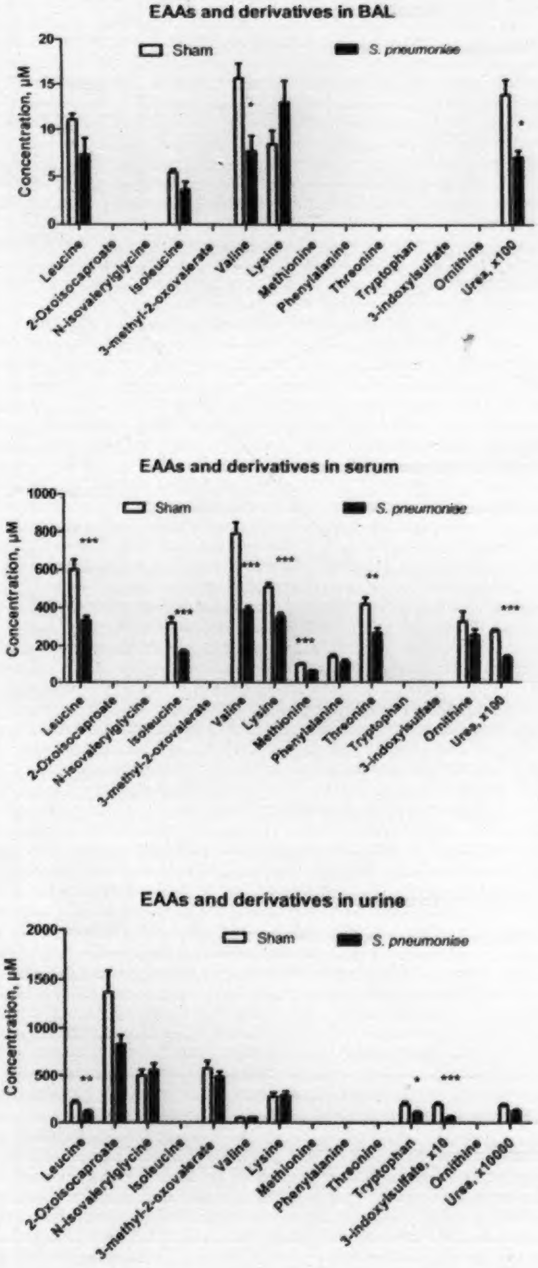

Figure 3.11. Concentrations of essential amino acids in biofluids of mice from cross-sectional study 24 h post-infection with *S. pneumoniae* or sham-treatment. (A) BAL samples, sham *n* = 4, *S. pneumoniae n* = 7. (B) Serum samples, sham *n* = 8, *S. pneumoniae, n* = 8. (C). Urine samples sham *n* = 12, (*S. pneumoniae*) *n* = 13.

Figure 3.11 (continued). * $p < 0.05$; ** $p < 0.01$; *** $p < 0.001$. Concentrations of urea were scaled down by 100 (A) and (B), and 10,000-fold (C) to fit the scale on this graph.

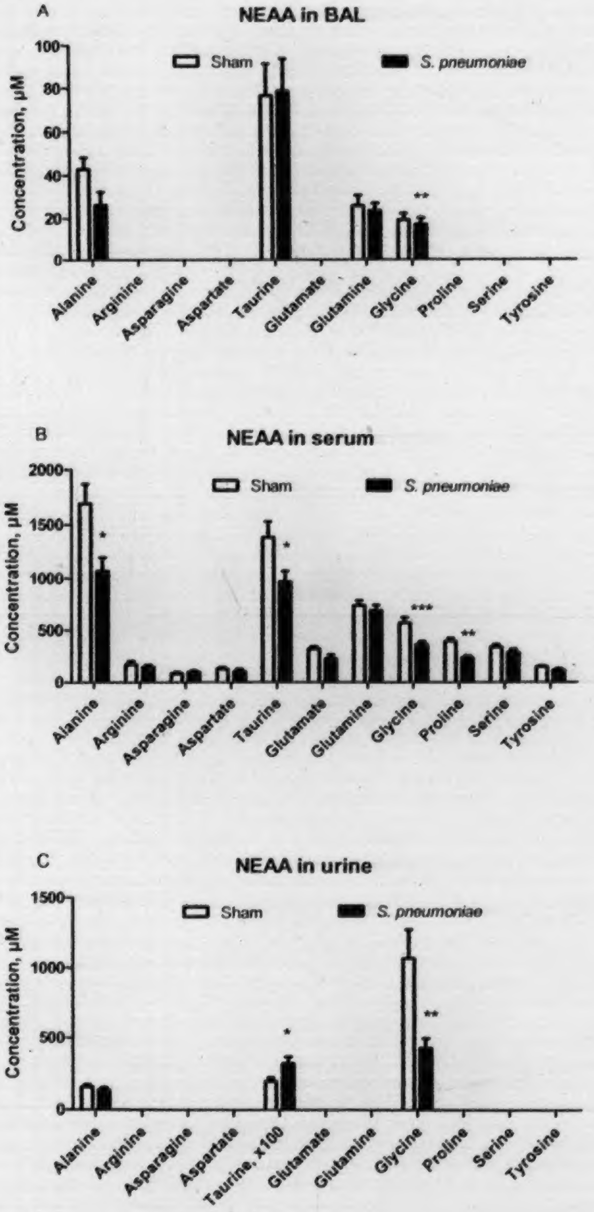

Figure 3.12. Concentrations of nonessential amino acids in biofluids of mice from cross-sectional study 24 h post-infection with *S. pneumoniae* or sham-treatment. (A) BAL samples, sham $n = 4$, *S. pneumonia* $n = 7$. (B) Serum samples, sham $n = 8$, *S. pneumoniae*, $n = 8$. (C) Urine samples, sham $n = 12$, *S. pneumoniae* $n = 13$. * $p < 0.05$; ** $p < 0.01$; *** $p < 0.001$. The concentration of taurine was scaled down by 100-fold to fit the scale on graph (C).

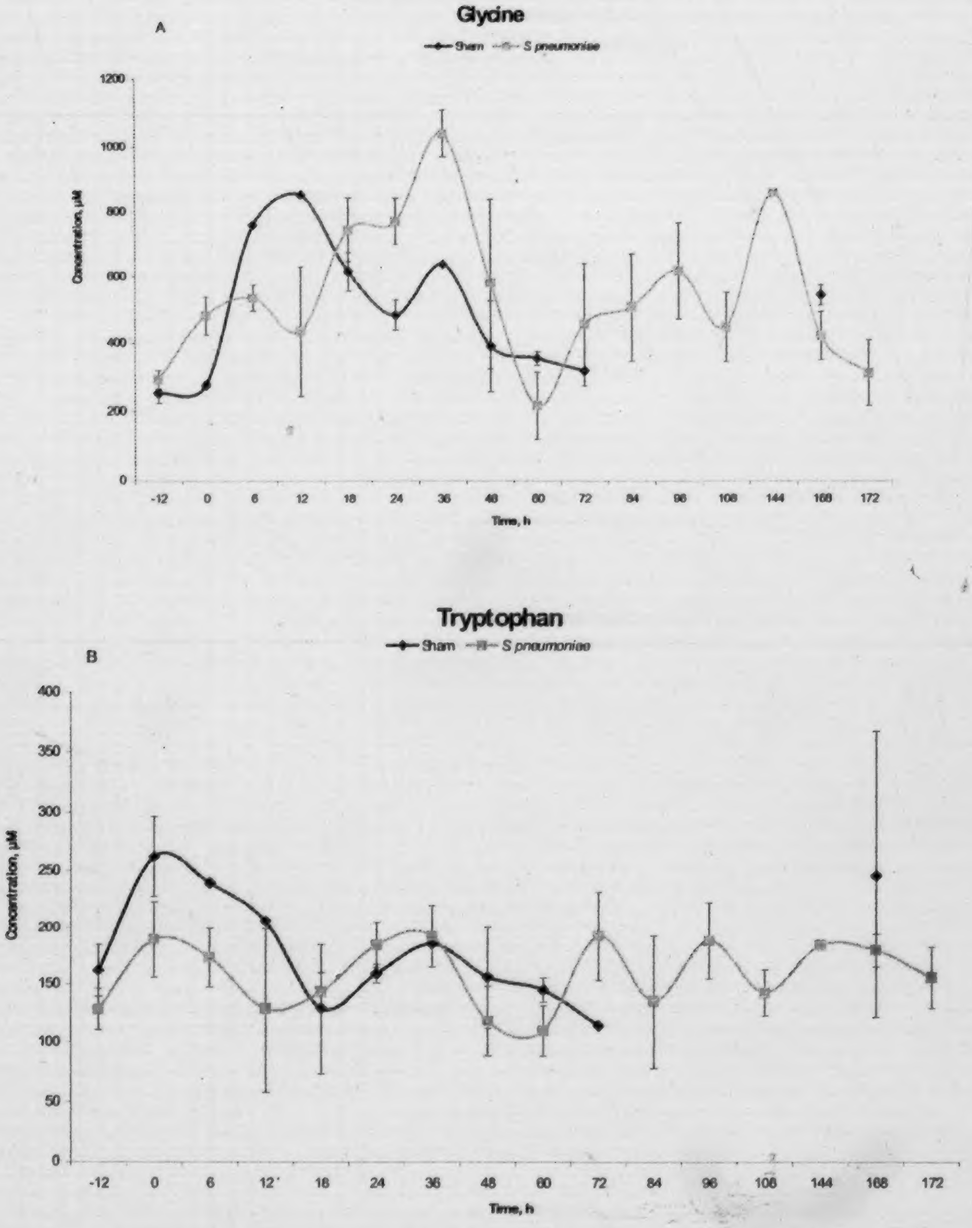

Figure 3.13. Levels of glycine (A) and tryptophan (B) in mouse urine in the longitudinal study of *S. pneumoniae*-infected mice. See the number of sham and infected samples at different time points in Figure 3.6 (B).

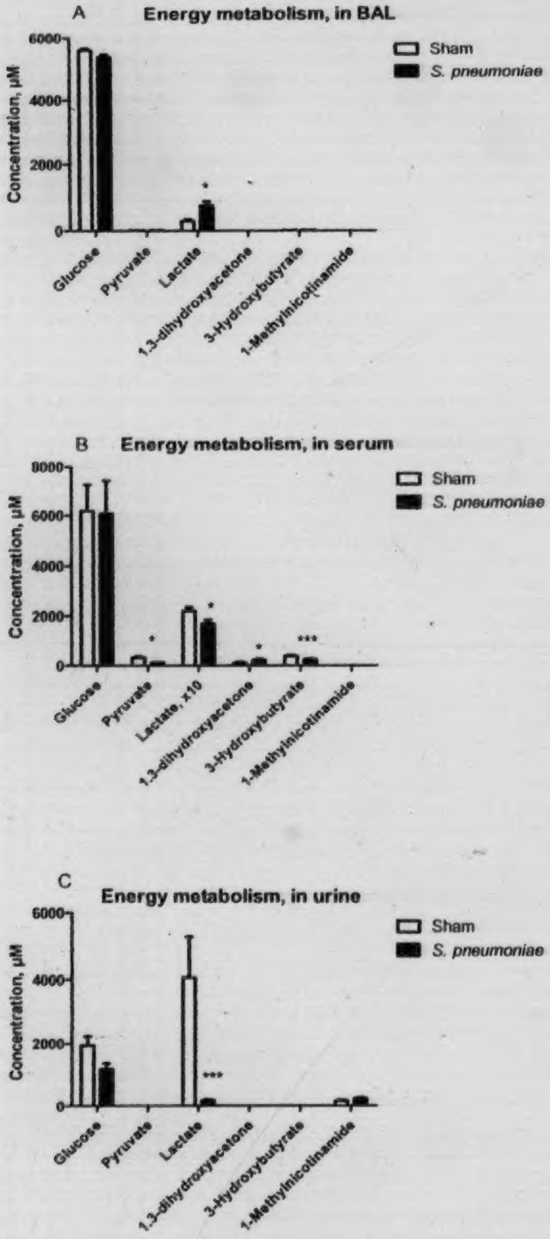

Figure 3.14 Concentrations of energy metabolism intermediates in biofluids of mice from cross-sectional study 24 h post-infection with *S. pneumoniae*. (A) BAL samples, sham *n* = 4, *S. pneumoniae, n* = 7. (B) Serum samples, sham *n* = 8, *S. pneumoniae*, *n* = 8. (C). Urine samples sham, *n* = 12, *S. pneumoniae, n* = 13. * $p < 0.05$; ** $p < 0.01$;

*** $p < 0.001$. The concentration of lactate was scaled down by 10-fold to fit the scale on graph (B).

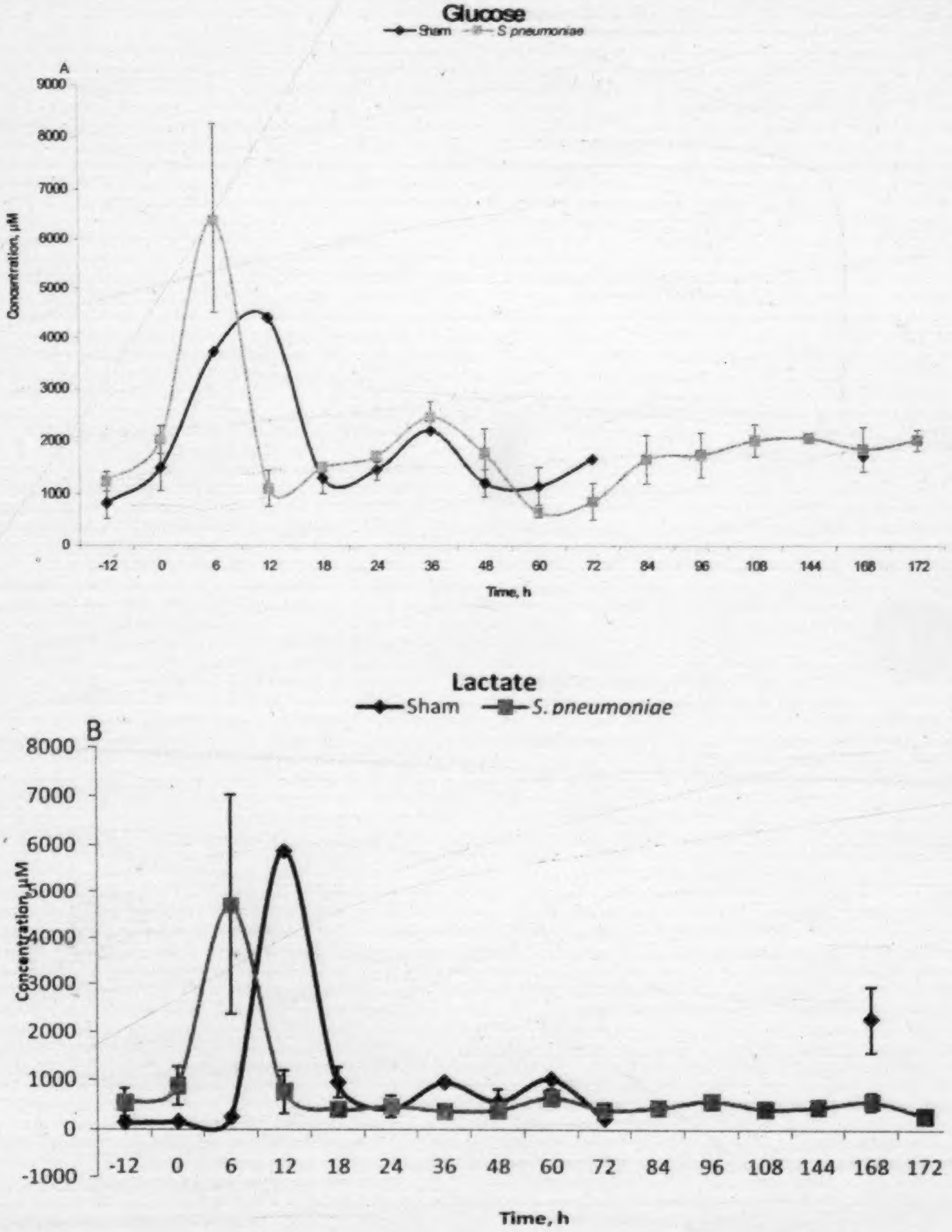

Figure 3.15. Concentrations of glucose (A) and lactate (B) in urine in the longitudinal study of *S. pneumoniae*-infected mice. See the number of sham and infected samples at different time points in Figure 3.6 (B).

3.3.2.4. Osmolytes, membrane constituents, nucleotides, and derivatives

Concentrations of osmolytes with metabolic functions, such as carnitine, decreased while its derivative, O-acetylcarnitine, increased in urine (Figures 3.14-3.15). Choline (as well as compounds of its catabolism N, N-dimethylglycine, O-phosphocholine and betaine) decreased in biofluids where measurable (except for choline's concentration in urine which did not change). Additionally, choline and betaine primarily derive from food, but they are also synthesised by liver and kidney and constitute phospholipids of cell membranes (Chapter 1). Ethanolamine (another constituent of phospholipids) and phenylacetyglycine (a putative marker of phospholipidosis) in urine increased (Figure 3.16 C). Fucose levels increased two-fold while xylose did not change in the urine of infected mice (Figure 3.16 C).

Levels of the pyrimidine uracil increased; while its derivative N-carbamoyl-β-alanine decreased in the urine of infected mice (Figure 3.16).

3.3.2.5. Metabolism of creatine

Average creatine levels in urine of infected mice increased two-fold 24 h after infection. Creatine concentrations in BAL of infected mice appear to be slightly increased (statistically not significant). Levels of creatine in blood of infected mice were not changed. In the urine of infected mice 24 h post-infection, levels of the creatine precursor, guanidoacetic acid, and its derivative creatinine appear to be slightly increased (not significant) (Figure 3.20). Elevation of creatine in urine of infected mice reflects progression of pneumonia and ceases after 36 h post infection, while creatinine and guanidoacetate were not changed significantly (Figures 3.21 and 3.22).

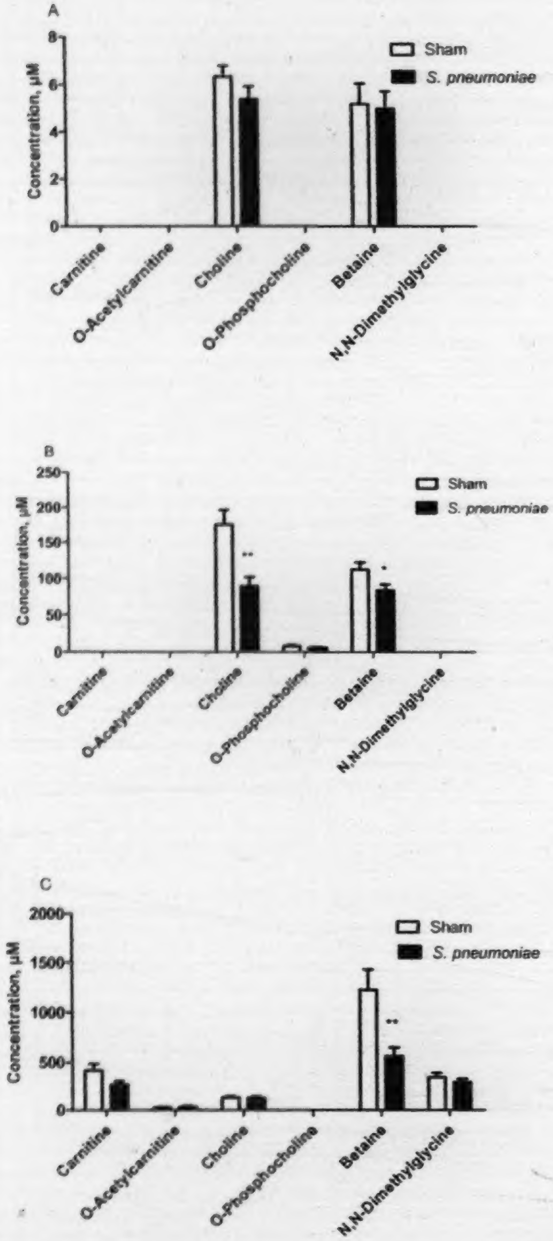

Figure 3.16. Concentrations of osmolytes, constituents of host cell membranes, and their derivatives in biofluids of mice 24 h post-infection with *S. pneumoniae*. (A) BAL samples, sham $n = 4$, *S. pneumoniae*, $n = 7$. (B) Serum samples, sham, $n = 8$, *S. pneumoniae*, $n = 8$. (C) Urine samples sham $n = 12$, *S. pneumoniae*, $n = 13$. * $p < 0.05$; ** $p < 0.01$; *** $p < 0.001$.

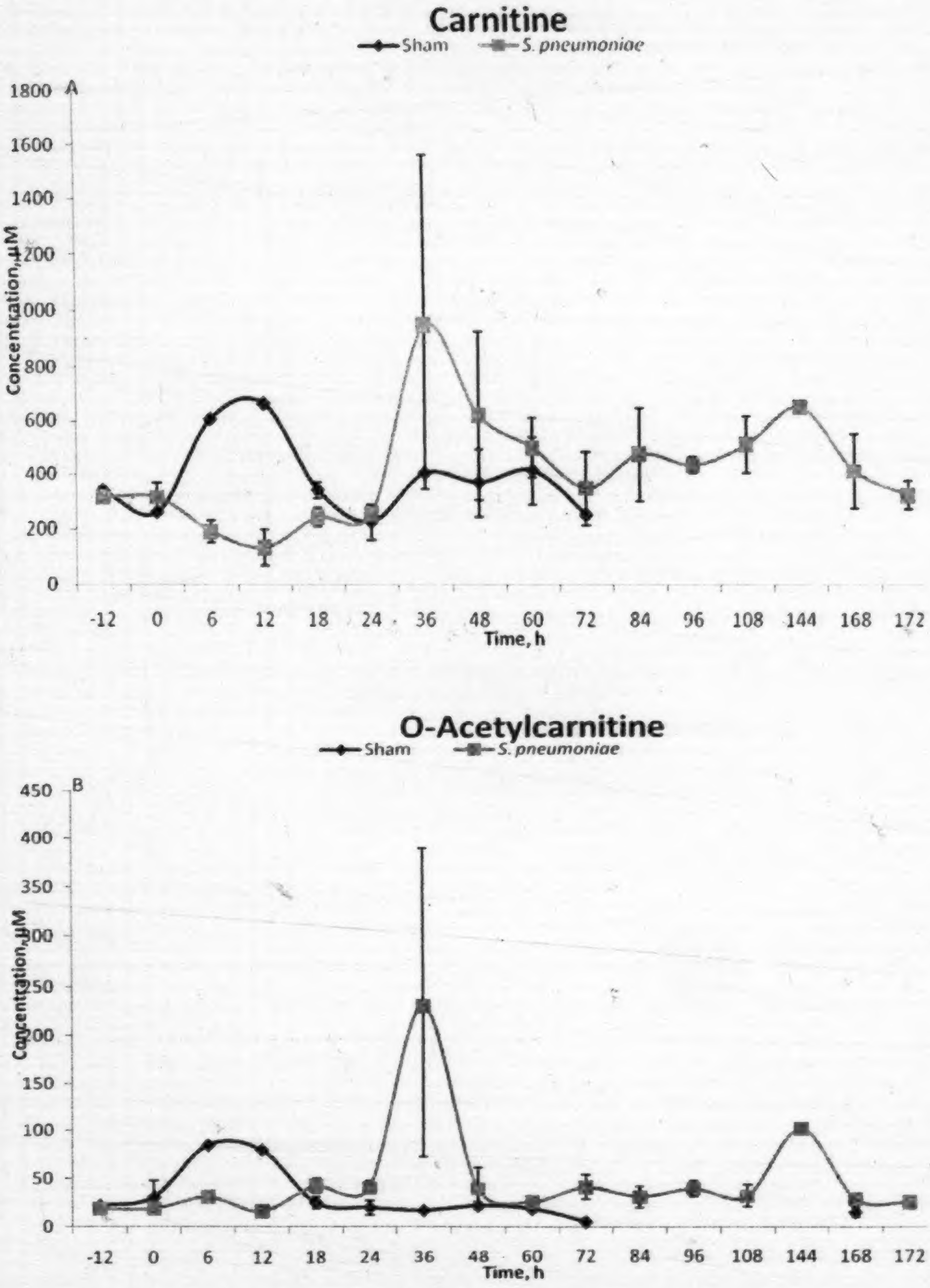

Figure 3.17. Concentrations of carnitine (A) and O-acetylcarnitine (B) in mouse urine in the longitudinal study in *S. pneumoniae*-infected mice. See the number of sham and infected samples at different time points in Figure 3.6.

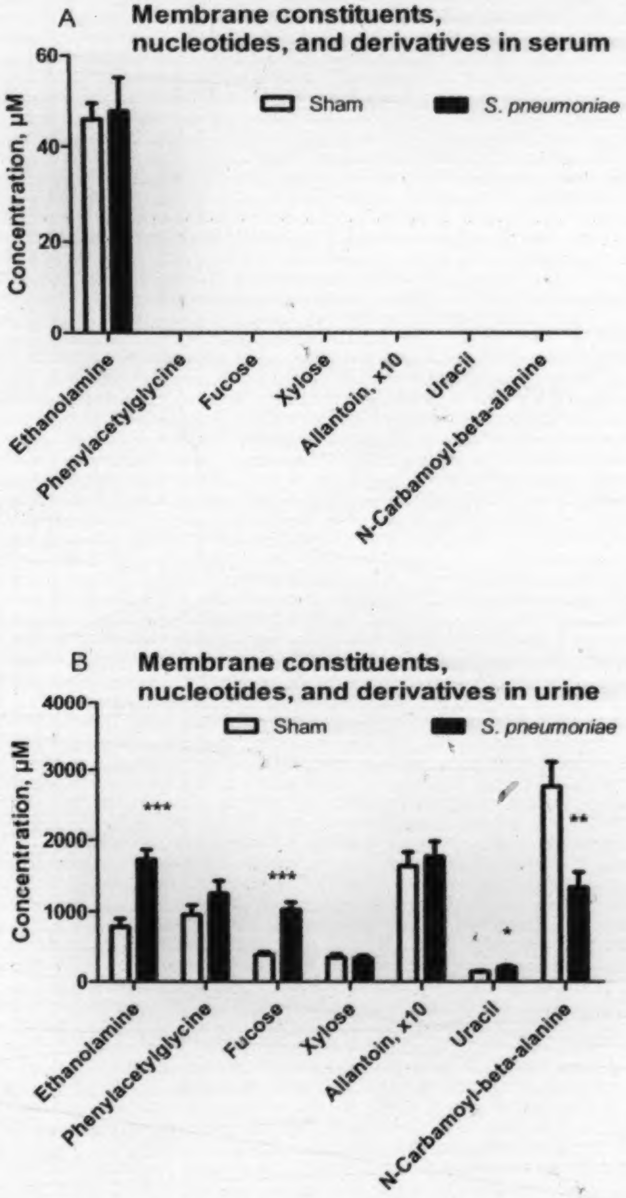

Figure 3.18. Concentrations of osmolytes, membrane constituents, nucleotides, and derivatives in biofluids of mice from cross-sectional study 24 h post-infection with *S. pneumoniae* or sham-treatment. (A) BAL samples, sham $n = 4$, *S. pneumoniae* , $n = 7$. (B) Serum samples, sham, $n = 8$, *S. pneumoniae*, $n = 8$. (C). Urine samples *sham*, $n = 12$, *S. pneumoniae*, $n = 13$. *: $p < 0.05$; **: $p < 0.01$; ***: $p <0.001$. The concentration of allantoin was scaled down by 10-fold to fit the scale on this graph.

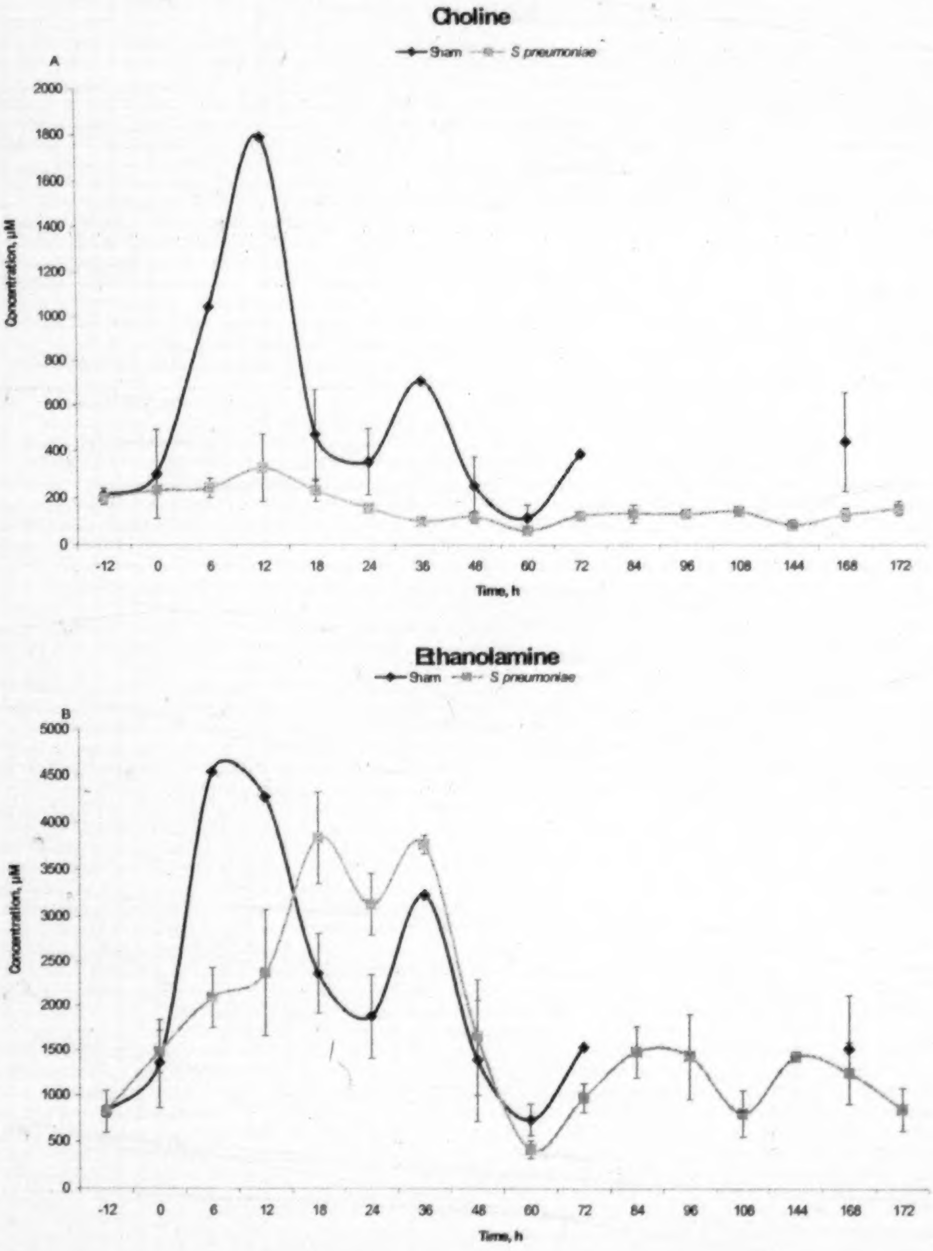

Figure 3. 19. Concentrations of choline (A) and ethanolamine (B) in *S. pneumoniae*-infected mouse urine in the longitudinal study. See the number of sham and infected samples at different time points in Figure 3.6.

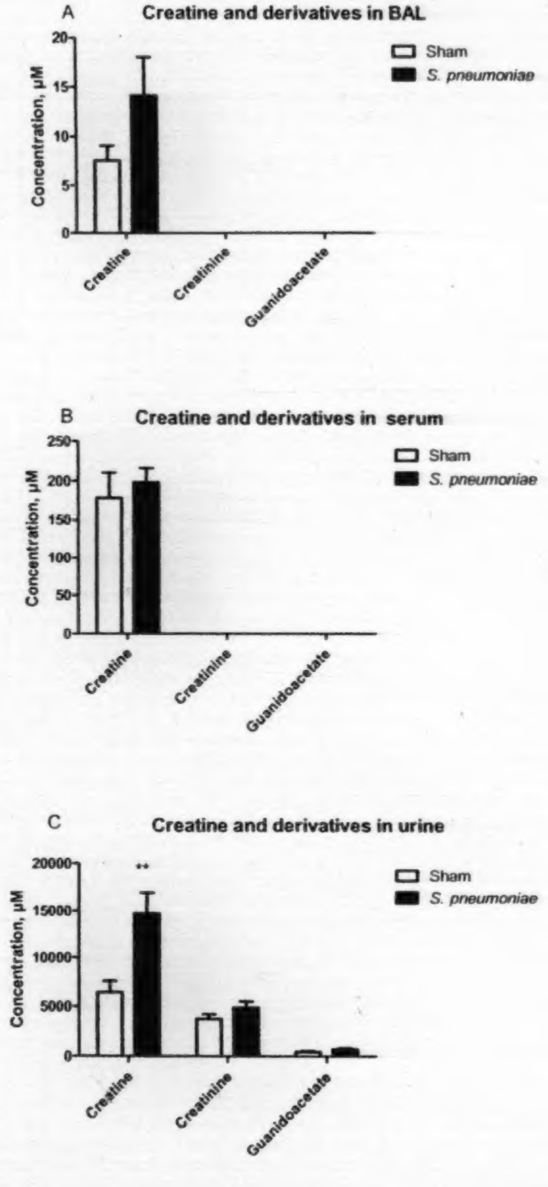

Figure 3.20. Concentrations of creatine and derivatives in biofluids of mice from the cross-sectional study 24 h post-infection with *S. pneumoniae*. (A) BAL samples, sham, $n = 4$, *S. pneumoniae,* $n = 7$. (B) Serum samples, sham, $n = 8$, *S. pneumoniae,* $n = 8$. (C). Urine samples, sham, $n = 12$, *S. pneumoniae,* $n = 13$. * $p < 0.05$; ** $p < 0.01$; *** $p < 0.001$.

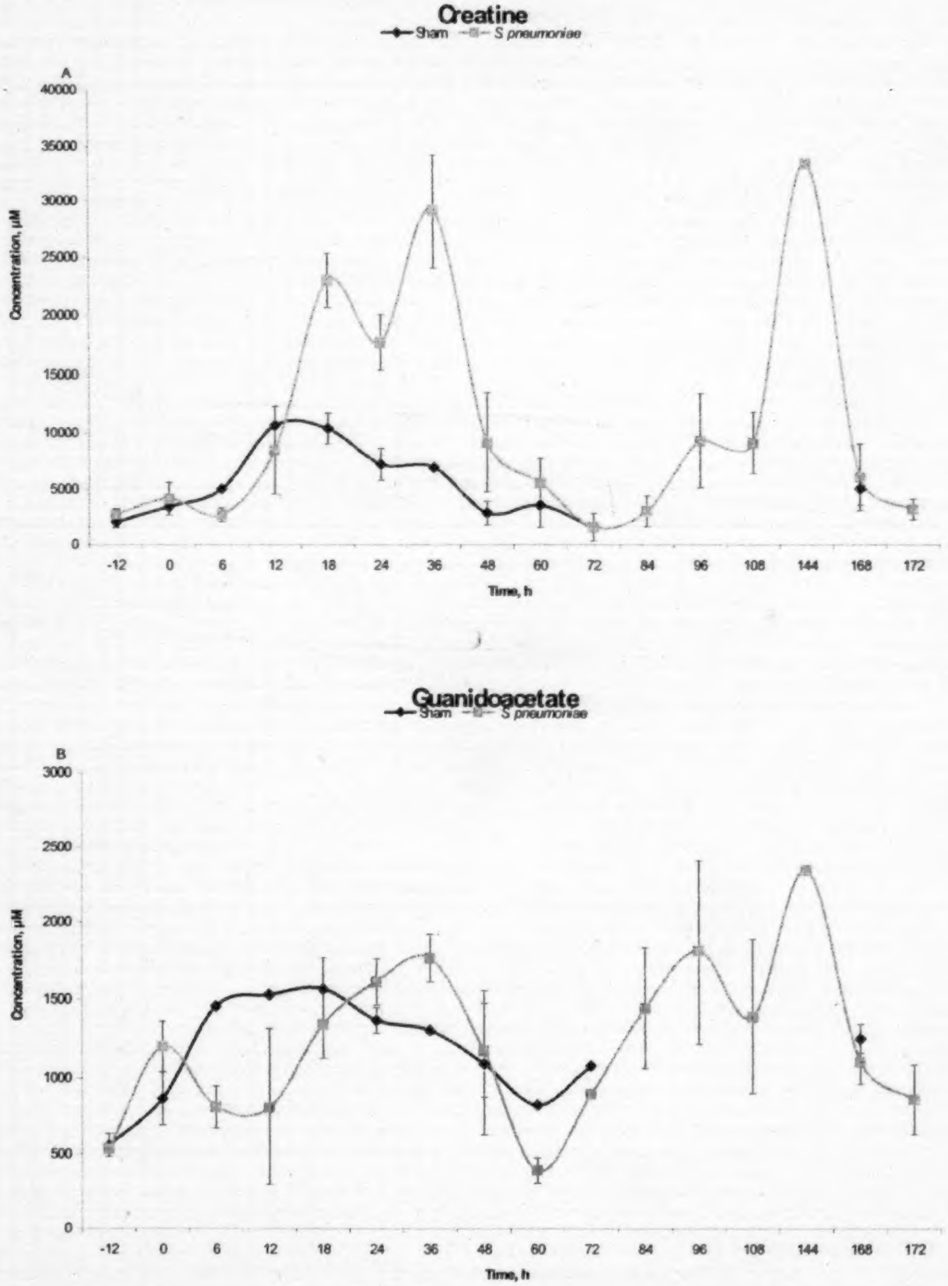

Figure 3.21. Concentrations of creatine (A) and guanidoacetate (B) in urine samples from *S. pneumoniae*-infected mice in the longitudinal study. See number of sham and infected samples at different time points in Figure 3.6 (B).

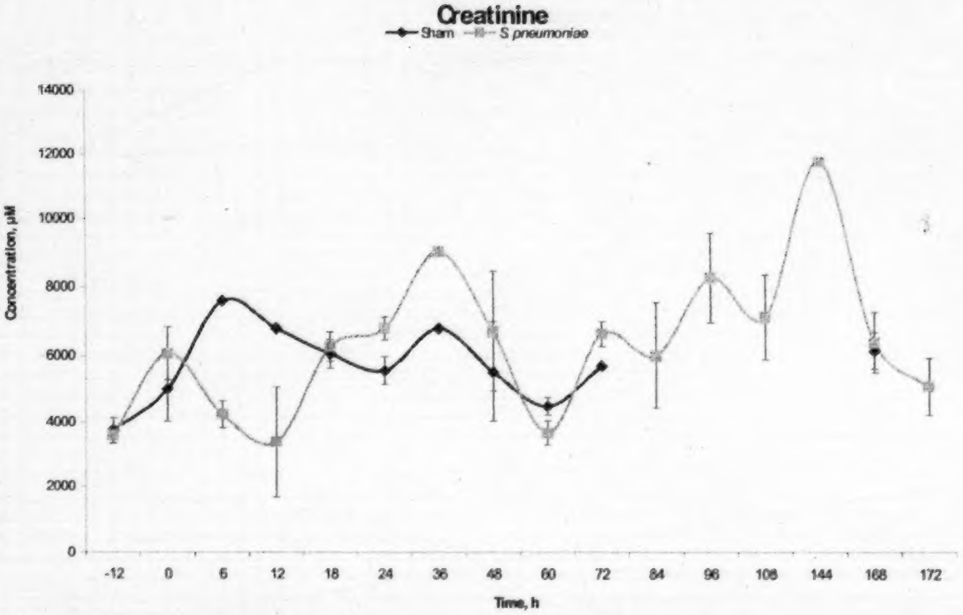

Figure 3.22. Concentrations of creatinine in urine samples from *S. pneumoniae*-infected mice in the longitudinal study. See number of sham and infected samples at different time points in Figure 3.6 (B).

3.3.2.6. Bacteria- and food-derived compounds

Concentrations of bacterial-derived metabolites (predominantly gut microflora), acetate, formate, and hippurate, decreased in urine and in serum by 30-50% of their respective concentrations in sham mice 24 h post infection (Figures 3.23 and 3.24 A). Concentrations of acetate in BAL increased, but decreased in serum.

The concentrations of mainly food-derived components trigonelline and glycolate, as well as of mainly food- and bacteria-derived trimethylamine decreased to 50-60% of concentration in urine of infected mice 24 h post infection (Egert, 2006) (Figure 3.23); the decrease in concentration reflected the stage of pneumonia (Figure 3.24).

3.3.2.7. Conclusion. Metabolomics data of biofluids of the mouse pneumonia model caused by *S. pneumoniae* (cross-sectional and longitudinal studies). We observed local and systemic decreases in concentrations of TCA cycle intermediates in biofluids of infected mice, with dynamics similar to progression of disease. Increased energy production is exemplified by intensified glycolysis (decreased glucose in urine and increased lactate and pyruvate in BAL), by apparently higher turnover of nicotinamide (increased excretion of 1-methylnicotinamide, not shown) and increased excretion of creatine. Decreased food intake is accompanied by decreased levels of most of amino acids, and amino acid derivatives, and decreased synthesis of gut bacterial-derived metabolites. Amino acid metabolism was shifted towards its catabolism.

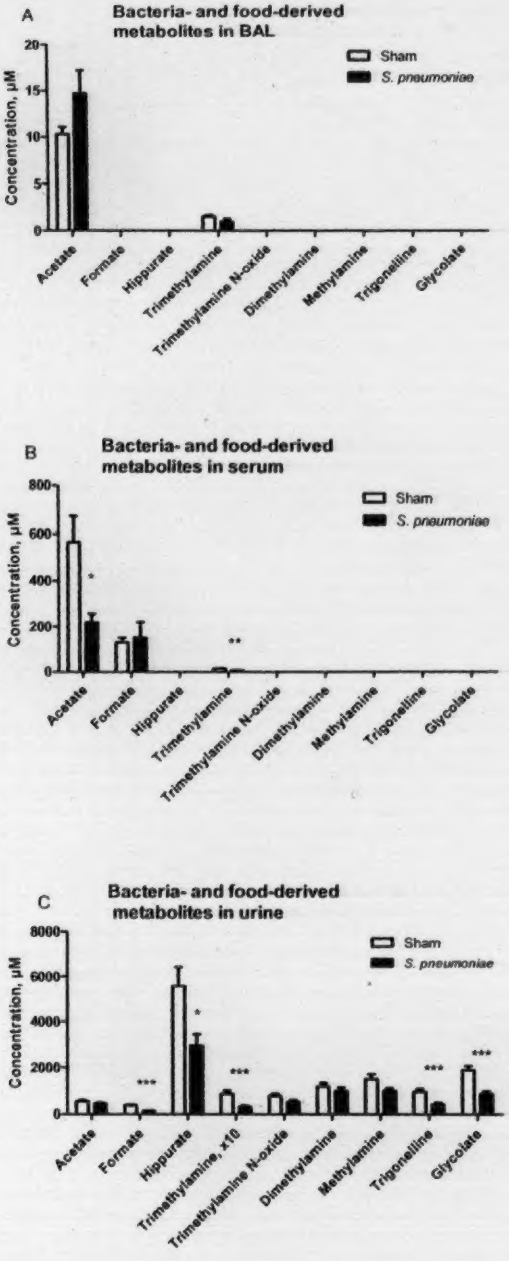

Figure 3.23. Concentrations of bacteria- and food-derived metabolites in biofluids of mice from cross-sectional study 24 h post-infection with *S. pneumoniae*. (A) BAL samples, sham $n = 4$, *S. pneumoniae*, n = 7. (B) Serum samples, sham, $n = 8$, *S. pneumoniae,* $n = 8$. (C). Urine samples sham, $n = 12$, *S. pneumoniae*, $n = 13$. * $p < 0.05$; ** $p < 0.01$; *** $p <0.001$.

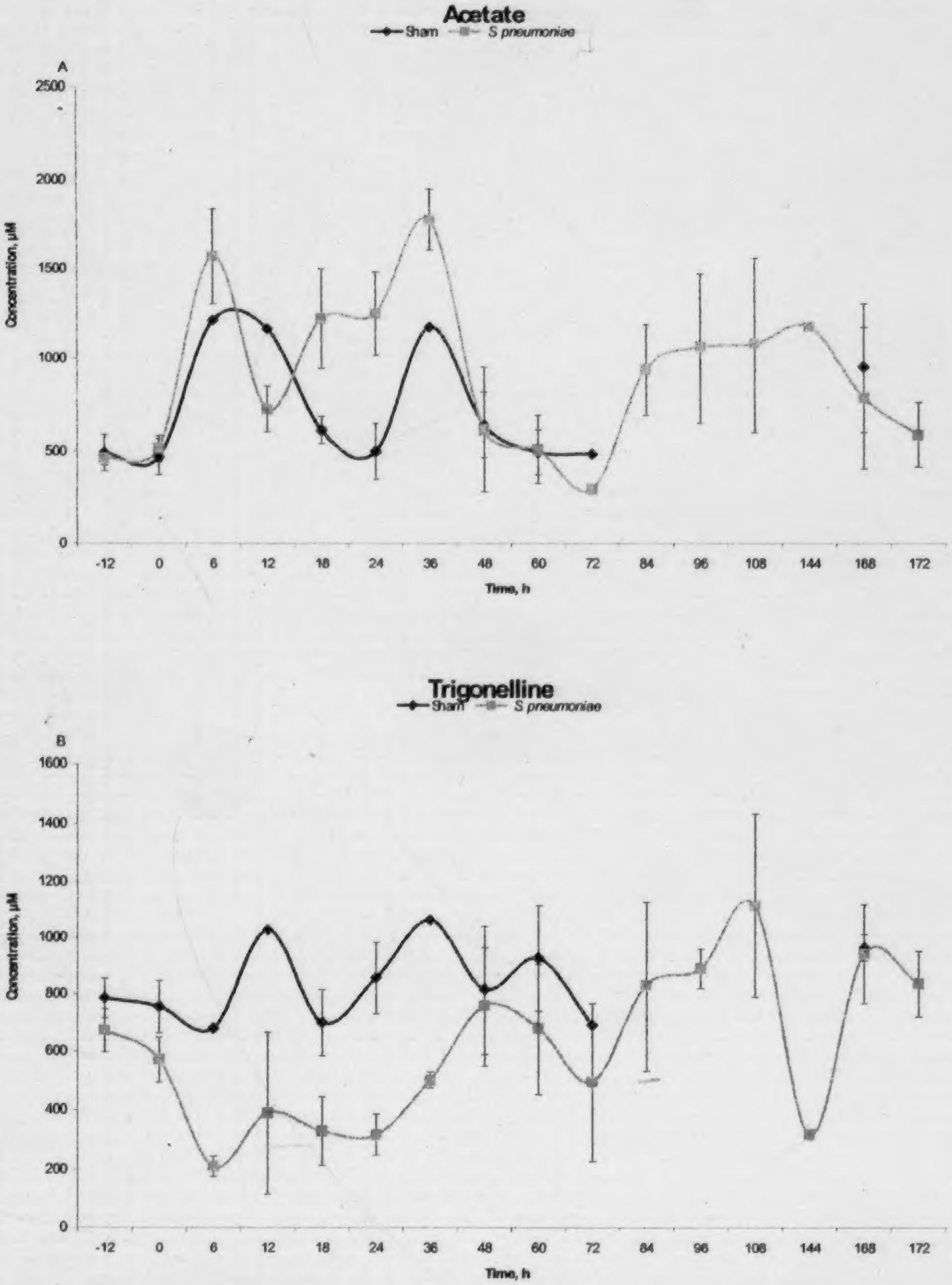

Figure 3.24. Concentrations of acetate (A) and trigonelline (B) in urine from *S. pneumoniae*-infected mice in the longitudinal study. See number of sham and infected samples at different time points in Figure 3.6 (B).

3.3.2.8. PCA analysis of urine of *S. pneumonia*-infected mice

The pattern of the metabolites in the urine samples in cross-sectional study with *S. pneumoniae*-infected mice was analysed with the multivariate analysis tool, PCA. The plot shows a clear separation between sham and *S. pneumoniae*-infected mice (Figure 3.25). This confirms that metabolic patterns of sham and *S. pneumoniae*-infected mice are different. The patterns of the metabolites in the urine samples in longitudinal study with *S. pneumoniae*-infected mice have shown dynamics of this separation (Figure 3.26). Separation between these groups appears early at 6 h post-infection, reached the maximum at 36 h post-infection for most of the mice and disappeared later in next days post-infection (Figure 3.26). The dynamics of changes reflected the severity of disease, as assessed by observation of health status of mice. Treatment of a group of infected mice with ampicillin ($n = 3$) did not result in separation between these two groups of infected mice.

3.3.3. Cross-sectional study with *S. aureus* infection. A group of 25 male C57Bl/6 mice 9-10 weeks old were used in this study: 13 mice were infected with 9×10^6 cfu of *S. aureus* and 12 sham mice were injected with THB. Mice were sacrificed at 24 h post-infection as done in the cross-sectional study with *S. pneumoniae* infection.

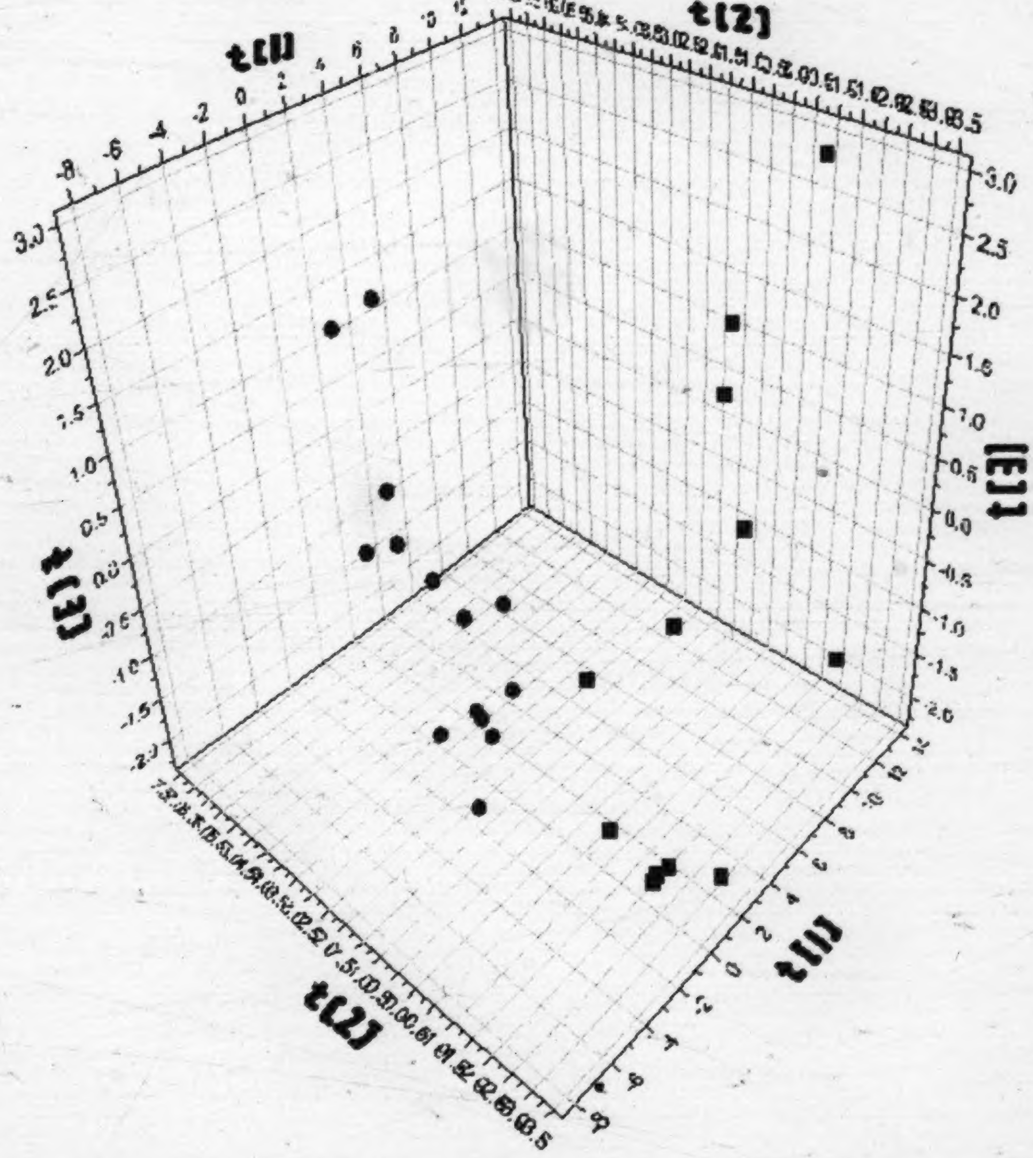

Figure 3.25. PCA plot of urine metabolites of sham and *S. pneumoniae*-infected mice in the cross-sectional study. Red dots indicate *S. pneumoniae*-infected mice, black squares – sham mice (*S. pneumoniae, n* = 14, sham, *n* = 12).

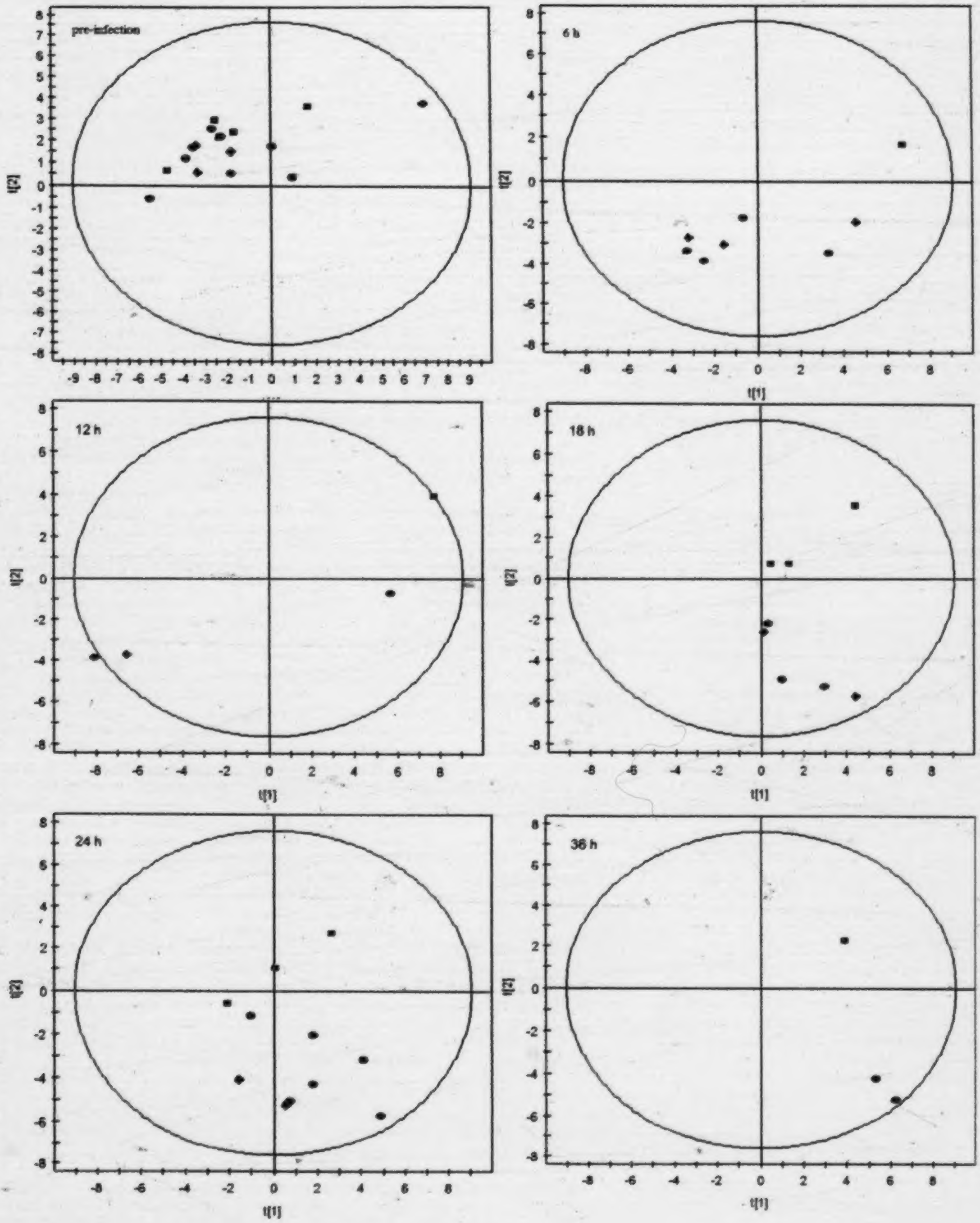
pre-infection
6 h
12 h
18 h
24 h
36 h
t[1]
t[2]

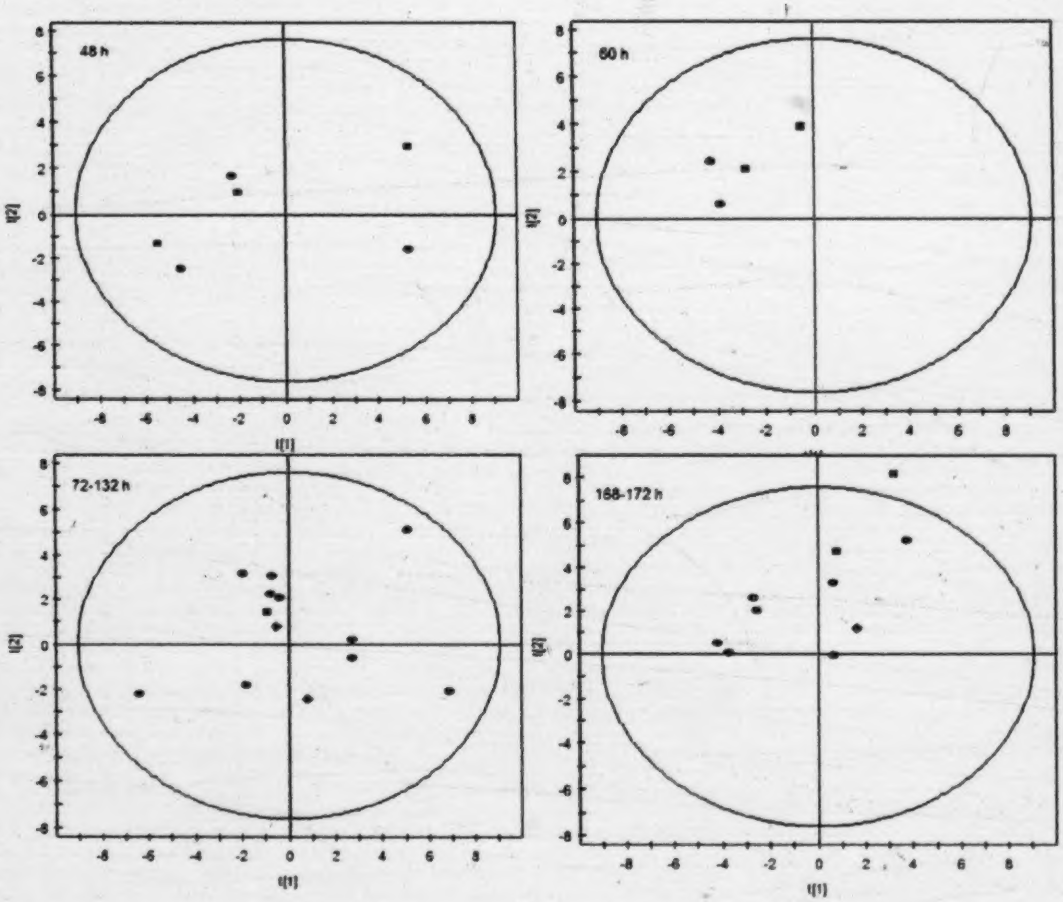

Figure 3.26. PCA plot of urine metabolites of sham and *S. pneumoniae*-infected mice in the longitudinal study. Red dots indicate *S. pneumoniae*-infected mice, blue diamonds - *S. pneumoniae*-infected ampicillin-treated mice, black squares – sham mice.

Infected mice developed mild pneumonia (as described by changes in mouse behaviour, assigned by one in each category, 2-3 fold increase in macrophages and neutrophils count in BAL, bacteremia in most of the infected mice, and mild local inflammation according to histology), (Figure 3.27).

Infected mice cleared part of their inoculum at 24 h (Figure 3.28) and most of them developed bacteremia (bacterial count in blood was assayed by plating blood clots due to an insufficient amount of heparin per tube).

Macroscopic and microscopic investigation of BAL of *S. aureus*-infected mice showed a higher content of neutrophils and macrophages in BAL than sham-treated animals, as well as more cell debris, bacteria, and fibrin (Figure 3.29).

In general, these findings showed that MRSA-infected mice developed much less severe pneumonia than *S. pneumoniae*-infected mice, likely due to a smaller dose of inoculum.

3.3.4. Metabolomics of urine *S. aureus*–infected mice

In our experiments with *S. aureus*-induced pneumonia, the mice developed mild pneumonia. Thus, metabolic changes appeared to be small (they did not increase above background in many cases). Analysis suggests some similarities and differences when compared with *S. pneumoniae*-infected mice. Similarities included a decrease at the level of amino acids and amino acid derivatives. For TCA cycle intermediates, citrate, malate, 2-oxoglutarate, and succinate in the urine of infected mice were decreased by 25-30 % at 24 h post-infection (results not shown).

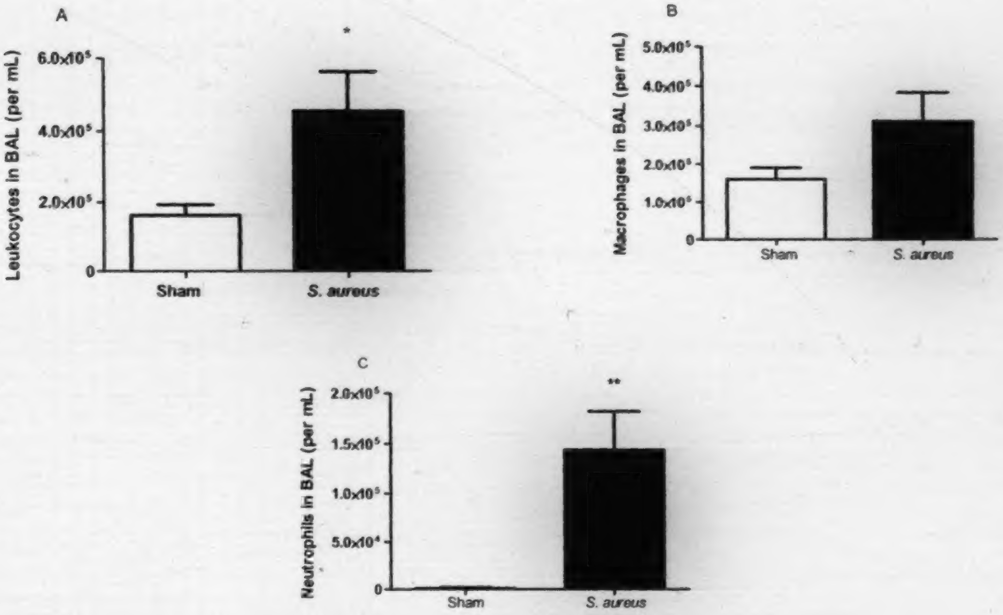

Figure 3.27. Cell counts in BAL 24 h post-infection with *S. aureus*. Sham, $n = 4$; *S. aureus*, $n = 3$. Mice were injected with 40 µl THB (sham) or 9 x 10^6 cfu/mouse *S. aureus* (methicillin-resistant PVL-positive *S. aureus*). Values represent mean and error bars indicate standard error of the mean. (A) Total cell counts. (B) Macrophage counts. (C) Neutrophil counts. * $p<0.05$, ** $p < 0.01$

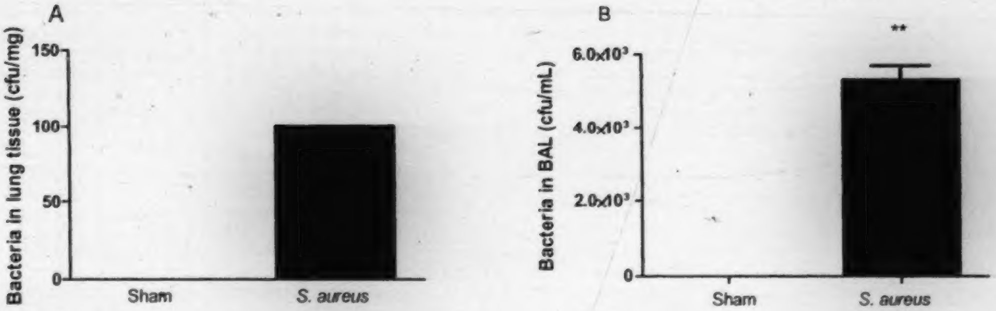

Figure 3.28. Bacterial counts in lung tissue and BAL 24 h post-infection with *S. aureus*. Mice were injected with 40 µl THB (sham) or 9 x 10^6 cfu/mouse *S. aureus*. Values represent mean and error bars indicate standard error of the mean. (A) Bacterial counts in lung tissue (cfu/mg), Sham, *n* = 1; *S. aureus*, *n* = 1. (B) Bacteria counts in BAL (cfu/mL), Sham, *n* = 1; *S. aureus*, *n* = 1.

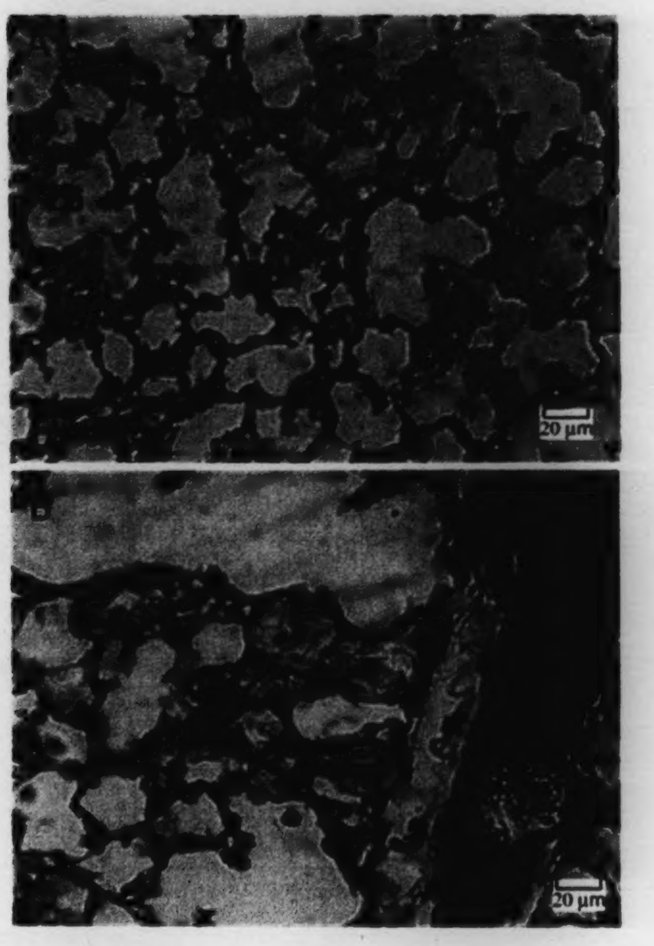

Figure 3.29. Histology of mouse lungs 24 h post-infection with *S. aureus.* Mice were injected with (A) 40 µl THB (sham) or (B) 9 x 10^6 cfu/mouse *S. aureus*. In the lungs of the sham-treated mouse, there was normal architecture of the lung: alveoli have preserved relative numbers and the structure of type I and type II pneumocytes is intact with few alveolar macrophages, while the basal lamina is covered with cells. Infected lungs show a modest increase in infiltration by leukocytes. Sham, *n* = 1; *S. aureus, n* = 2. H/E, 40X magnification.

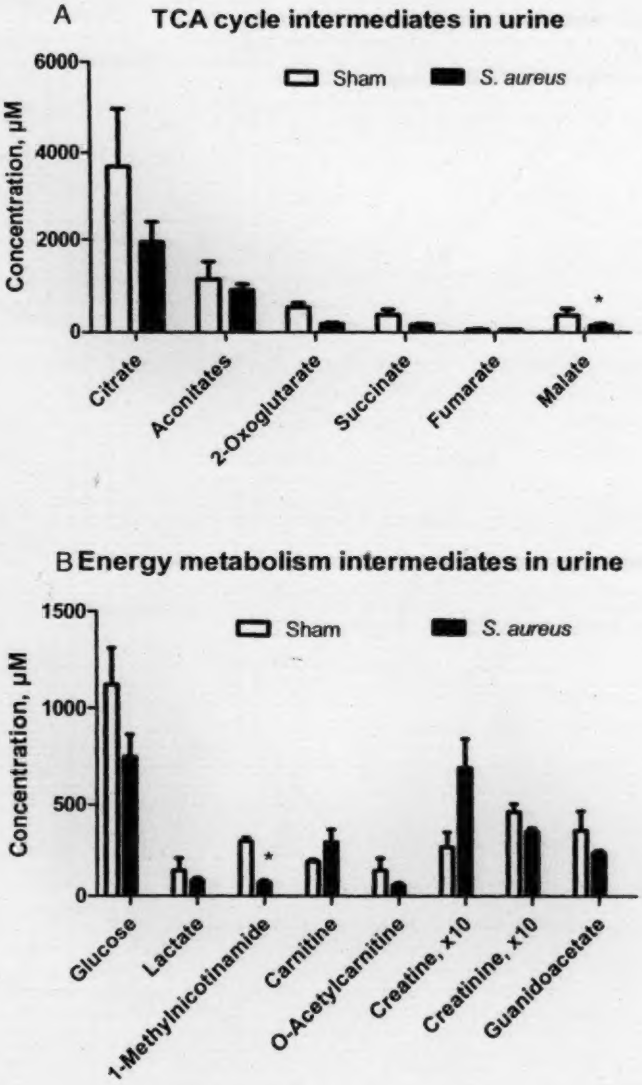

Figure 3.30. Concentrations of TCA cycle intermediates (A) and intermediates of energy metabolism (B) in urine of mice from cross-sectional study 24 h post-infection with *S. aureus*. Concentrations of creatine and creatinine were scaled down by 10-fold to fit the scale on this graph. Sham, $n = 3$, *S. aureus*, $n = 6$. * $p < 0.05$.

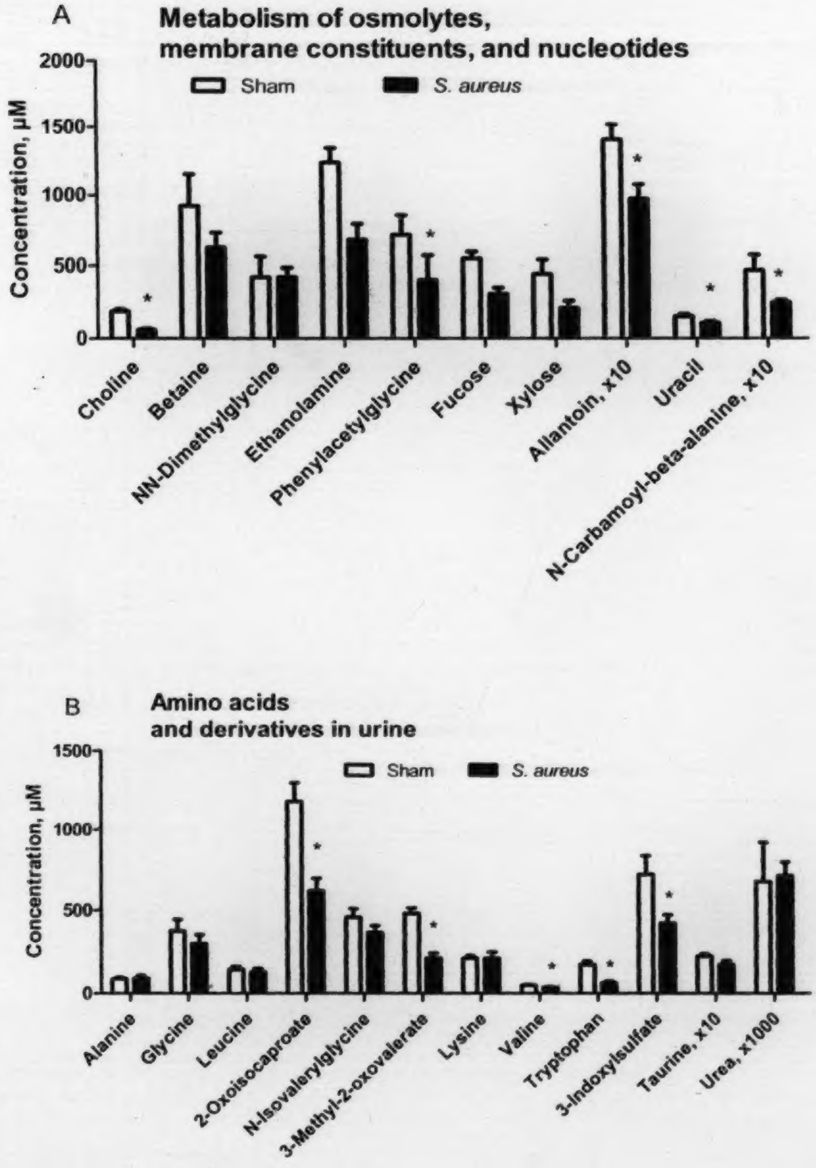

Figure 3.31. Concentrations of osmolytes, membrane constituents, and nucleotides (A) and amino acids and derivatives (B) in urine of mice from cross-sectional study 24 h post-infection with *S. aureus*. Concentrations of allantoin, N-carbomyl-beta-alanine, and taurine were scaled down by 10-fold; the concentration of urea was scaled down by 1,000-fold to fit the scale on this graph. Sham, $n = 3$, *S. aureus*, $n = 6$. *: $p < 0.05$.

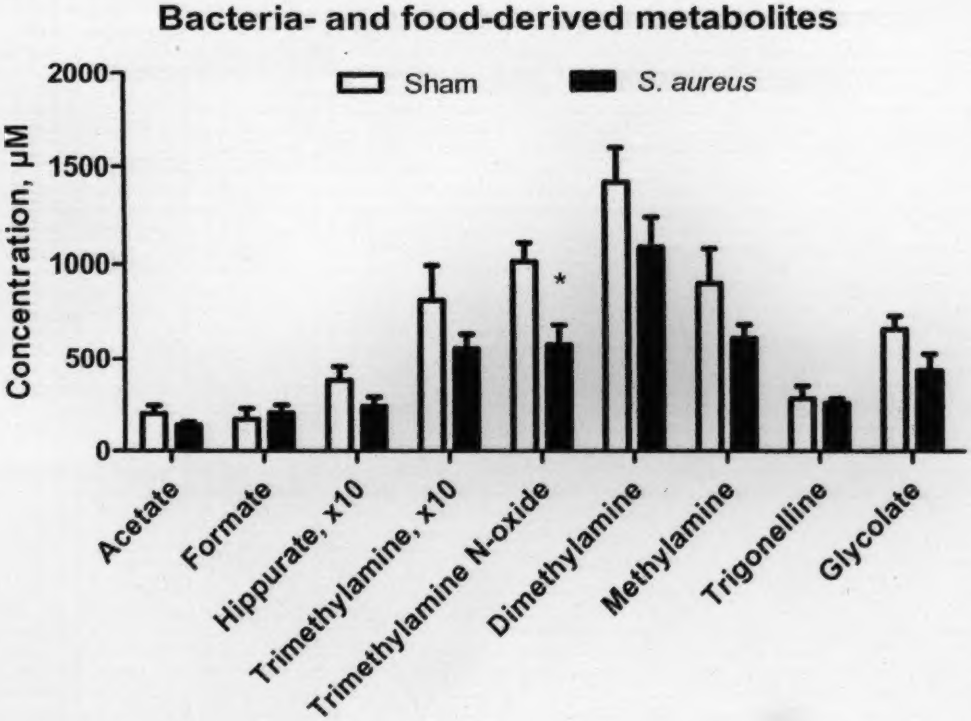

Figure 3.32. Concentrations of bacteria- and food-derived metabolites in urine of mice from cross-sectional study 24 h post-infection with *S. aureus*. Concentrations of hippurate and trimethylamine were scaled down by 10-fold to fit the scale on this graph. Sham, $n = 3$, *S. aureus*, $n = 6$. *: $p < 0.05$.

Fumarate, cis- aconitate and trans-aconitate were not significantly changed (Figure 3.30 (A). These changes were accompanied by the development of mild pneumonia-like disease according to the other methods in cross-sectional study.

We observed decreased concentrations of allantoin, choline, and uracil (Figures 3.31-3.32). These changes may reflect mild staphylococcal pneumonia in our experiments; however, the changes have to be interpreted carefully, as these are preliminary data. For instance, a lower level of allantoin during staphylococcal pneumonia may be the result of lower concentrations of ROS in the lung, since *S. aureus* produces catalase that decreases ROS levels in lungs, while *S. pneumonia* produces H_2O_2 contributing to oxidative stress in the lungs.

3.4. Conclusion

We observed different urinary metabolite patterns in samples of *S. pneumoniae*- and *S. aureus*-infected mice (the latter are preliminary data). The study described a pattern of metabolic changes during pneumococcal pneumonia in different biofluids. Similar to other metabolomic findings, the metabolic pattern may be used for diagnostics and may help in generating hypotheses regarding the roles and mechanisms of specific metabolites during infection.

We observed changes in TCA cycle as an early attribute of bacterial pneumonia. Disease, decreased food intake and catabolism of amino acids were accompanied by increases in creatine, creatinine, and guanidoacetate. Specific changes in metabolism of glucose, lactate, osmolytes, and carbohydrates also contributed to the establishment of the metabolic pattern.

It is tempting to conclude that some of these changes are characteristic for inflammation in the lung, while the others are caused by specific bacterial influence (toxins and other factors of virulence; absorption of host metabolites by bacteria; activation of the immune system induced by bacterial factors of pathogenicity, and others). Therefore, we may speculate that this pattern may inform us more about the particular type of pneumonia and specific diagnostic pattern of metabolites during the course of disease (diagnostic marker) and help to evaluate the gravity of disease (prognostic marker).

Chapter 4

Summary of Data and Discussion

4.1. Infection of lung cells

The infection of lung cells in culture by either *S. pneumoniae* or *S. aureus* was accompanied by changes in cell homeostasis (decreased mitochondrial potential), cell death, and bacterial multiplication. Measurements taken during lung cell infection also showed changes in concentrations of TCA cycle intermediates, amino acids, bacterial-derived products, and metabolites of energy production. A decreased concentration of glucose and increased concentrations of lactate suggested increased glycolysis. Low doses of bacteria (10^1 -10^2 cfu per well) caused increased concentrations of TCA cycle intermediates compared to uninfected cells and relatively insignificant cell death. Low doses of bacteria also caused small changes in mitochondrial potential and high doses of bacteria (10^4 -10^5 cfu per well) caused significant decrease of mitochondrial potential according to fluorescent microscopy.

4.1.1. Microbiological processes in cell cultures

These results suggested increased permeability of cell and mitochondrial membranes at low doses of bacteria and low cell death and decreased function of mitochondria at high doses of bacteria. Pneumolysin, a primary membrane toxin, has been found to directly bind and damage mitochondria (Rubins, 1993; Braun, 2002). The relative distribution between cellular and mitochondrial membranes of these toxins, and the relative contribution of such a distribution to death of cells *in vitro* and *in vivo* are currently unknown. The higher cytotoxicity and virulence of more invasive strains of *S. aureus* and *S. pneumoniae* (Krut, 2003) and the increased cell death during internalisation of *S. pneumoniae* and *S. aureus* may be attributable partially to the appearance of toxin inside the cells and to a higher degree of mitochondrial damage

(Dockrell, 2001; Menzies, 1998). Pneumolysin from *S. pneumoniae* creates water permeable channels in cell membranes allowing free movement of metabolites smaller than maltose, as well as potassium, sodium, and calcium ions (Tilley, 2005); while α-toxin from *S. aureus* creates channels for sodium and potassium ions in cell membranes (Alouf, 2006). These (as well as other yet unknown) mechanisms cause sublethal damage at low doses and cell death at high doses. Theses effects are due to apoptosis in the case of pneumolysin and necrosis, in case of α-toxin (Tweten, 1991; Alouf, 2006).

An increase in the permeability of cell and mitochondrial membranes can lead to numerous changes in homeostasis and metabolism, both known and hypothetical. After treatment with pneumolysin, pores in membranes with an internal diameter 30 nm allow passage of metabolites smaller than maltose (Tilley, 2005). After application of α-toxin, which induces pores with an internal diameter of 20 nm, cells undergo necrosis and subsequent increase of cell membrane permeability. Increased permeability of cell and mitochondrial membranes lead to changes in cell compartmentalization, osmolality, concentrations of ions, and intracellular pH.Other effects include: activation of phospholipase A_2 (Rubbins, 1994), opening of mitochondrial permeability transition pores, calcium influx, increase in mitochondrial pH, and decoupling of oxidative respiration (Papa, 1999; Mergner, 1990). These processes can lead to facilitated diffusion of metabolites from the affected cells, changes in activity of cytoplasmic and mitochondrial enzymes, and thus changes in production and consumption of metabolites. Damage to mitochondria can cause cell death and subsequent metabolic changes such as low Krebs cycle intermediates at high doses of bacteria.

The role of pneumolysin and other factors of pathogenicity of *S. pneumoniae* (hydrogen peroxide, secreted bacterial proteases, components of the cell wall, capsule, neuraminidase, glucosidase, and adherence receptors) on metabolic changes are unknown. Since pneumolysin causes the most significant changes in homeostasis and cell death, it is likely to be the cause of the most significant changes in metabolism. Since pneumolysin is released from dead pneumococci, it would be important to measure bacterial death. Preliminary data of counts of dead pneumococci (Chapter 2) suggest increased death of pneumococci at high doses, which may be partially due to the observed build-up of lactate. More precise methods, such as differential staining of live and dead bacteria, or direct measurement of pneumolysin, may be useful for determining bacterial death (Roth, 1997). The effects of pneumolysin are usually studied by culturing eukaryotic cells with pneumolysin and with a pneumolysin-negative mutant. The role of hydrogen peroxide may also be studied by the addition of catalase to a mixture of pneumococci and cells, and by use of an SpxB mutant. A549 cell cultures can synthesize the cytokines TNF, IL-1β, and IL-6 in response to components of the bacterial cell wall and pneumolysin, and can further promote apoptosis of host cells (Chapter 1). A preliminary study of culturing of A549 cells with sterile-filtered supernatants of bacterial culture and of sterile-filtered supernatants of A549 cells infected with 10^3 cfu *S. pneumoniae* revealed changes in cell viability and morphology similar to that observed in the same cells infected with 10^3 cfu of *S. pneumoniae,* described above (results not shown).

It may be important to consider the influence of pH on changes in production of metabolites as bacterial infection is accompanied by an observed lowering of pH in a dose-dependent manner. A preliminary study with infection of HepG-2 cell line showed changes in cell viability and morphology similar to A549 cells (results not shown).

4.1.2. TCA cycle intermediates

Changes in the concentrations of TCA cycle intermediates may have resulted in efforts within the cell to replenish these to normal levels. This can involve shifts into alternate biochemical pathways. Replenishing of TCA cycle intermediates is done mainly by carboxylation of pyruvate to oxaloacetate by mitochondrial pyruvate carboxylase, and to a certain extent by deamination of glutamate to α-ketoglutarate and aspartate to fumarate (Coffee, 1998). We observed decreased levels of pyruvate in media of infected cells, which may be related to an increase in oxaloacetate. However, it could have been the result of conversion of pyruvate by other metabolic pathways or consumption by bacteria. Decreased pyruvate carboxylation due to inhibition of pyruvate carboxylase by citrate is unlikely, since the observed citrate concentrations were low.

A decrease in TCA cycle intermediates may also be the result of facilitated synthesis of amino acids and lipids. For example, 2-oxoglutarate is a precursor for glutamate, oxaloacetate is a precursor for aspartate and glucose (gluconeogenesis), succinyl-CoA is a precursor for the heme group of hemoglobin, and citrate is a precursor for fatty acids (and, indirectly, for many nonessential amino acids [McMurray, 1983]). We observed increased aspartate and glutamate in the media, which may have been derived from these, as well as many other processes. One may argue that increased glutamate concentration results from increased activity of mitochondrial glutaminase; since a decrease in concentrations of glutamine corresponded to increases in glutamate (Lowenstein, 1969). However, glutamine degrades spontaneously to pyruvate under the conditions of our experiments, and it is also used by cells in cell culture as an energy source (Freshney, 2000), and consumed by *S. pneumoniae* (Chapter 1).

Conversion of oxaloacetate to aspartate could account for the observed decrease in the concentrations of Krebs cycle intermediates and increases in aspartate concentrations. Alternatively, a rise in aspartate concentration may be due to released intracellular aspartate. We could not measure concentrations of oxaloacetate (since it decomposes quickly to pyruvate), but increases or decreases in one metabolite of the mitochondrial TCA cycle usually causes similar changes in all of them (McMurray, 1983). Therefore, the concentration of oxaloacetate probably decreases in line with the concentrations of other TCA cycle intermediates.

Consumption of TCA intermediates by *S. pneumoniae* and by *S. aureus* is possible and needs to be investigated, but this may not be the only reason for such dramatic noncompensated decreases of citric acid cycle intermediates (Chapter 1). *S. pneumoniae* does not have a TCA cycle, and instead produces energy by glycolysis. *S. pneumoniae* and *S aureus* may absorb aspartate and other amino acids instead of having to produce them from citric acid cycle intermediates to facilitate bacterial growth (Chapter 1). *S. pneumoniae* and *S. aureus* do not have enzymes capable of catabolising citrate. For example, Rhizobium species consume TCA cycle intermediates rather than glucose if both are present in the media and consume glucose in the absence of TCA cycle intermediates (White, 2007).

Similar changes in levels of TCA cycle intermediates were observed in *S. pneumoniae* serotype 3 (data not shown) and *S. aureus* infections in our preliminary data; this suggest a common basis of bacterial infection changes in host cell metabolism and potential markers of cell damage and death. Changes in TCA cycle intermediates and cell death in *S. pneumoniae* serotype 3 and *S. aureus* infections are reminiscent of changes in *S. pneumoniae* serotype 14 infections if the final concentrations of bacteria are compared. The absence of nonessential amino acids is speculated to have decreased the speed of growth of *S. aureus* and slowed cell death.

In all experiments, changes in TCA intermediates corresponded to cell death and to final rather than initial doses of bacteria (determined by colony count); this suggests a commonality for bacterial infection-induced changes in host cell metabolism and potential markers of cell damage and death.

4.1.4. Amino acids

Bacterial infections were accompanied by a decrease in amino acids in the media. *S. pneumoniae* serotype 14 infection caused a decrease of most amino acids and their derivatives. However, increased concentrations of aspartate, glutamate, and alanine were observed. These changes may be the result of concomitant release of intracellular amino acids due to cell damage, altered production and consumption of amino acids and by A549 cells, and consumption of amino acids by bacteria. *S. aureus* infection resulted in decreased concentrations of arginine, isoleucine, leucine, valine, glutamate, and threonine, and increased concentrations of lysine and taurine. Such decreases probably reflect consumption of amino acids by bacteria. Consumption of amino acids during *in vitro* experiments may not completely reflect processes *in vivo* (Chapter 1). Additionally, the metabolic profile of a particular bacterial species is complicated by presence of mutants with slightly different metabolic requirements (Chapter 1). Classical studies of bacterial metabolism used artificial media with chemical compositions different from those of animal fluids and tissues (Blazevic, 1975). Todd-Hewitt broth, used in our experiments, has a complex chemical composition since it contains extracts of yeast and beef meat, pepsin digest of casein, glucose, and sodium carbonate (Atlas, 2006). Precise chemical composition of this media was not studied in our experiments. It is very unlikely that metabolites from the media appear in measurable quantities in the samples of A549 cells since bacteria were washed three times with DMEM before adding to A549 cultures (Chapter 2).

4.1.5. Bacterial-derived metabolites

Some metabolites are likely bacterial-derived and have been described as gut microflora derivatives in metabolic studies of animals (Egert, 2006); examples are acetate, formate, and isovalerate in infections of *S. pneumoniae* and *S. aureus*, the unknown metabolite in *S. pneumoniae* infections, and propionate in *S. aureus* infections. However, these metabolites are not easily detected in animal biofluids because their concentrations are low and they are mixed with metabolites derived from gut microflora.

4.1.6. Other metabolites

These results suggest that *S. pneumoniae* serotype 14 and *S. aureus* infections are accompanied by some common metabolomic changes: increased and decreased levels of TCA intermediates at low and high degrees of cell damage respectively; changes in concentrations of amino acids and ketone bodies were more specific. More studies with similar experimental conditions need to be conducted to describe metabolic profiles of bacteria and lung cells infection and mechanisms of metabolic alterations.

4.2. Mouse pneumonia model

Mouse pneumonia model experiments show different (as visualized by PCA plot) patterns of metabolites in the urine of *S. pneumoniae*-infected mice and sham mice; the dynamics of *S. pneumoniae*-infected mice reflected differences of health status. Differences were insignificant at the time of infection; they progressed up to 24–36 h and disappeared after recovery. Some metabolites derive from different sources (for example, from food or synthesized endogenously), can be synthesized by different pathways (pathways crossing), and have many functions in homeostasis.

The distribution of metabolites in different biofluids and tissues suggest potential sources due to increased production, consumption, or excretion. However, such analyses are complicated by several processes, such as different dynamics of metabolites in normal or disease states, or changes in biofluids leading to, for example, potential changes in urine production. Table 4.2 summarizes metabolic changes, observed in biofluids of *S. pneumoniae*-infected mice in cross-sectional study and grouped according to known or hypothetical biochemical pathways.

4.2.1. TCA cycle intermediates

A decrease in TCA cycle intermediates may be a result of mitochondrial damage due to bacterial factors of pathogenicity, host defence factors (ROS and proteases), and cell death due to a local increase of cytokines. We observed decreased concentrations of TCA cycle intermediates, most amino acids and their derivatives, food-derived and bacterial-derived products, and other metabolites. These changes were accompanied by the development of pneumonia-like disease (assessed by other methods) and returned to normal or higher values when signs of disease disappeared (in the longitudinal study with

S. *pneumoniae* infection). We hypothesize that the observed changes resulted from several conditions: sublethal damage to cells by bacterial toxins, cell death due to apoptosis or necrosis, consumption of metabolites by bacteria, changes in metabolism and cell death due to inflammation (respiratory burst, edema, local and systemic hypoxia), systemic changes (Chapter 1). Complement activation due to pneumolysin release from *S. pneumoniae* and subsequent cell damage can contribute to these changes. The pattern of decreased levels of TCA intermediates alone (without consideration of other metabolites and without PCA) is a potential marker of bacterial pneumonia and may be used to monitor the progress of disease.

Concentrations of succinate at 6 h post-infection were relatively high and decreased between 6 and 36 h post-infection. The decrease in mouse BAL, blood, and urine may reflect impaired function or damage to the mitochondria due to infection; for example, by bacterial toxins (pneumolysin and α-toxin) which are membrane- and mitochondria-damaging toxins. The timing of such changes (when bacteria multiply and start to damage lung cells) reflects the start of infection (Chapter 1). The release and role of pneumolysin at early stages of S. *pneumoniae* pneumonia are important factors for development of the disease (Rubins, 1995). If certain types of cell damage and death are associated with a decrease in TCA cycle intermediates, then death of host cells due to immune defence factors (ROS and proteases produced by neutrophils and macrophages) 24–36 h post-infection (Chapter 1) may be another reason for the decrease in TCA intermediates.

Other factors that can contribute to changes in TCA cycle intermediates include: inhibition of replenishment because of decreased synthesis from pyruvate and aspartate as a consequence of infection, hypoxia (with activated glycolysis as main source of energy), systemic acidosis, increased body temperature (and change in enzyme kinetics), and decreased food uptake.

Metabolites	BAL (%), (statistical significance)	Serum (%), (statistical significance)	Urine (%), (statistical significance)
TCA cycle intermediates			
citrate	n/a	54 (***)	27 (***)
malate	n/a	46 (***)	3 (***)
fumarate	n/a	47 (**)	1 (***)
2-oxoglutarate	n/a	n/a	9 (***)
succinate	84	43 (***)	44 (***)
total aconitates	n/a	n/a	27 (**)
Amino acid metabolism			
leucine	66	56 (***)	53 (**)
2-oxoisocaproate	n/a	n/a	61
isoleucine	50	68 (***)	53
phenylalanine	n/a	80	n/a
tyrosine	n/a	77	n/a
phenylalanine : tyrosine ratio		0.97 (sham), 1.18 (*S. pneumoniae*)	
threonine	n/a	65 (**)	n/a
tryptophan	n/a	n/a	53 (*)
3-indoxylsulfate	n/a	n/a	32 (***)

Metabolites	BAL (%), (statistical significance)	Serum (%), (statistical significance)	Urine (%), (statistical significance)
alanine	61	63 (*)	83
lysine	155	70 (**)	103
glycine	40 (**)	63 (***)	88 (**)
proline	n/a	59 (**)	n/a
methionine	n/a	62 (***)	n/a
urea	50 (*)	50 (***)	68
Energy metabolism			
lactate	262 (*)	76 (*)	5 (***)
1,3-dihydroxyacetone	n/a	217 (*)	n/a
3-hydroxybutyrate	105	68 (***)	n/a
Osmolytes and membrane constituents			
carnitine	n/a	n/a	63
O-acetylcarnitine	n/a	n/a	131
choline	85	51 (**)	99
betaine	96	65 (*)	46 (**)
ethanolamine	n/a	104	219 (***)
fucose	n/a	n/a	266 (***)
xylose	n/a	n/a	97
taurine	103	70 (*)	164 (*)

Metabolites	BAL (%), (statistical significance)	Serum (%), (statistical significance)	Urine (%), (statistical significance)
Metabolism of nucleotides			
uracil	n/a	n/a	145 (*)
N-carbamoyl-β-alanine	n/a	n/a	49 (**)
Creatine metabolism			
creatine	186	111	228 (**)
creatinine	n/a	n/a	131
guanidoacetate	n/a	n/a	155
Metabolites, potentially derived from metabolism of bacteria and from food			
acetate	142	39 (**)	82
formate	n/a	116	36 (**)
hippurate	n/a	n/a	53 (*)
trimethylamine	61	46 (**)	36 (***)
trigonelline	n/a	n/a	43 (***)
glycolate	n/a	n/a	46 (***)

Table 4.1. Concentrations of metabolites in the biofluids of mice, infected with *S. pneumoniae,* normalised to respective concentrations in the respective biofluids of sham. Data are the percentage (average concentration of each metabolite in each biofluid of control mice is assumed to be equal 100% and the average concentration of the metabolite in infected mice as percentage of value of sham mice is listed for each metabolite). Statistical significance, calculated using the non-parametric Mann-Whitney test, *** p<0.001, ** p<0.01, * p<0.05, no indication of significance: not significant).

Metabolites	Urine 6-48 h post-infection (%), (statistical significance)	Urine 60-96 h post-infection (%), (statistical significance)	Urine 144-172 h post-infection (%)[1]
TCA cycle intermediates			
citrate	21 (***)	70	46
malate	38 (***)	56	35
fumarate	36 (***)	51	26
2-oxoglutarate	13 (***)	67	35
succinate	21(***)	76	63
total aconitates	38 (***)	109	68
Amino acid metabolism			
2-oxoisocaproate	62 (**)	87	69
urea	75 (*)	102	74
Energy metabolism			
lactate	60	84	19
Osmolytes and membrane constituents			
carnitine	61 (*)	123	98
O-acetylcarnitine	116	240 (*)	243
choline	36 (*)	58	31
betaine	28 (***)	69	39
phenylacetylglycine	185 (*)	116	142

Metabolites	**Urine 6-48 h post-infection (%), (statistical significance)**	**Urine 60-96 h post-infection (%), (statistical significance)**	**Urine 144-172 h post-infection (%)**
fucose	130 (*)	185	130
Metabolism of nucleotides			
N-carbamoyl-β-alanine	53 (***)	85	56
Creatine metabolism			
creatine	193	197	156
creatinine	97	135	104
guanidoacetate	91	132	90
Metabolites, potentially derived from metabolism of bacteria and from food			
acetate	171 (*)	159	78
formate	37 (**)	169	190
hippurate	53 (***)	94	68
trimethylamine	46 (***)	80	60
trimethylamine N-oxide	53 (***)	81	112
trigonelline	44 (***)	90	86

Table 4.2. Concentrations of metabolites in urine of mice infected with *S. pneumoniae* in the longitudinal study (presented as relative percent of concentrations from sham-treated mice). The average concentration of each metabolite in urine of control mice is assumed to be equal to 100%, and average concentrations of metabolites in infected mice were calculated as well as statistical significance, calculated using non-parametric Mann-Whitney test, *** $p<0.001$, ** $p<0.01$, * $p<0.05$, no indication of significance: not significant). Urine 6-48 h, sham, *n* = 12, *S.pneumoniae, n* =28. Urine 60-96 h, sham, *n* = 3, *S.pneumoniae, n* = 14 Urine 144-172 h sham, *n* = 2, *S.pneumoniae, n* = 9.
[1]Statistical significance was not calculated because of small number of samples.

4.2.2. Energy metabolism

Decreased concentrations of glucose in the BAL and increased concentrations of the products of glycolysis, pyruvate, and lactate in the BAL of infected animals may be due to several conditions: local hypoxia due to edema, respiratory burst of neutrophils, increased metabolic rate due to fever, and consumption of glucose by bacteria. Blood glucose levels were close to normal in infected animals. Since glucose level in blood is such an important factor in homeostasis it is unlikely to be changed during pneumonia. An increased level of glucose in urine of infected mice 6 h after infection could be due to a stress response and/or cytokine response (Chapter 1). Low levels of lactate and pyruvate in mouse blood may be explained by increased gluconeogenesis in liver as a result of decreased food uptake, which is stimulated by action of cytokines (Coffee, 1998). Increased pyruvate levels in mouse BAL indicate either inhibition of mitochondrial pyruvate dehydrogenase or increased glycolysis with a relative insufficiency of NADH (to reduce pyruvate to lactate) (Coffee, 1998). Increased levels of 1,3-dihydroxyacetone in mouse serum may also indicate increased glycolysis. Concentrations of 1-methylnicotinamide in mouse urine increased insignificantly, which could be explained by a faster turnover of mitochondrial NAD^+ and NADH or cytoplasmic $NADP^+$ and NADPH (Coffee, 1998).

4.2.3. Metabolism of amino acids

Decreased concentrations of amino acids in the biofluids of *S. pneumoniae*-infected mice may be the result of catabolism of amino acids for gluconeogenesis (due to decreased food intake and fever) and consumption of amino acids by pneumococci (Chapter 1). Concentrations of glutamine (unlike most amino acids) in the serum of infected mice did not change, probably since its consumption by gluconeogenesis was compensated by increased production by fasting muscles (Wannemacher, 1977). Concentrations of alanine, branched chain amino acids leucine, isoleucine, and valine in serum of infected mice decreased by approximately 40-50%. Alanine (as well as glutamine) is released by fasting skeletal muscles for gluconeogenesis in liver (Wannemacher, 1977). Branched chain amino acids are important sources of amino groups for production of alanine in muscles using branched chain amino acids aminotransferase (Salway, 1994). Other products of the process, such as keto acids 2-oxoisocaproate and 3-methyl-2-oxovalerate, are catabolised in the liver to acetyl-CoA using mitochondrial branched chain amino acids dehydrogenase, which is inhibited by low concentrations of TCA cycle intermediates and low ADP (Hinsbergh, 1979). Relative decrease of these keto acids in serum samples appeared to be greater than the relative decrease of corresponding amino acids. These differences may be due to observed decrease in citrate concentrations in the biofluids of infected mice. On the other hand, the distribution of some enzymes of intermediary metabolism in different organs and tissues in the mouse is not completely understood, thus other mechanisms could be causing these changes. Concentrations of the leucine derivative, N-isovalerylglycine, did not change in urine, which may indicate differential activation of the catabolic pathways of leucine during pneumonia or other unknown reasons. For example, an important step in the formation of N-isovalerylglycine is conjugation of glycine and keto acid isovaleric acid by liver mitochondrial glycine N-acylase (which resembles production of hippurate [Schachter, 1954]). The concentration of tryptophan, and especially its derivative 3-indoxylsulfate, was significantly decreased, unlike the reported increased tryptophan (as well as phenylalanine) in serum of people with infectious diseases (Wannemacher, 1977) due to release from fasting muscles.

In humans, the urea concentration in biofluids largely depends on the amount of consumed proteins and catabolism of amino acids, and is an important part of the nitrogen balance, which is negative during progression of disease and positive in recovery from disease (Hartmann, 2007; McMurray, 1983). Increased secretion of ammonia salts in urine (due to increased catabolism of amino acids during disease), increased angiotensin II production, and systemic acidosis (Chapter 1) and can contribute to a negative nitrogen balance and decreased excretion of sodium in human and mouse (McMurray, 1983; Knepper, 1989; Nagami, 1995, 2002). An increase in ammonium salts in urine decreases the relative contribution of urea to removal of nitrogen from the organism and can hypothetically explain a decreased concentration of the urea cycle intermediate ornithine in the serum of infected mice. A slightly increased urea concentration in the urine of S. *pneumoniae*-infected mice at the climax of disease (36 – 60 h, longitudinal study) may be due to intensification of amino acid catabolism by liver or in kidney during inflammation (Chapter 1). However, this increase in mouse urea concentration appeared to be a temporary restoration to a healthy level and may be used as a part of principal component analysis rather than as a single marker. In general, the decrease in concentrations of amino acid intermediates is less prominent than the decrease of other food-derived compounds such as trigonelline, which can reflect a slower, more complex and interconnected catabolism of amino acids (McMurray, 1983) and the contribution of amino acids, released from extracellular matrix

4.2.4. Osmolytes with metabolic function and their derivatives

The slightly decreased carnitine during the first 30 h post-infection may occur due to several reasons, such as decreased consumption of food carnitine, increased absorption by cells from biofluids (due to somotic shock, caused with pneumolysin or due to possible salt retention [Chapter 1]). Increased concentrations of carnitine 36-60 h post-infection may indicate its release from damaged lung cells (Chapter 1), increased synthesis in kidney and liver (Peluso, 2000), or potential redistribution from tissues to biofluids due to decreased serum osmolality after climax of the disease (Chapter 1). Decreased concentrations of other osmolytes betaine and trimethylamine N-oxide may be explained by similar reasoning: changes in osmolality during pneumonia may lead to changes in osmolyte concentrations in tissues and biofluids (Chapter 1). We have to account for the theory that mammalian carnitine is mostly derived from food and is only partially synthesized in kidney and liver (Peluso, 2000). Increased production of O-acetylcarnitine 36-60 h post-infection may indicate its release from damaged lung cells (Chapter 1) or increased catabolism of fatty acids during starvation (McMurray, 1983).

4.2.5. Creatine metabolism

The concentration of creatine in serum of infected mice was increased, which could occur during infection for several reasons. Damage to skeletal and smooth muscles leads to release of creatine and creatinine into serum (Hartmann, 2002) (Chapter 1). Increase of creatine and creatinine levels can happens due to damage of bronchial smooth muscles or skeletal muscles due to inflammation in the lung. Such changes in tissues and organs located distant from the alveoli may occur due to released bacterial toxins (from infected alveoli and from bacteria in mouse blood), cytokine action, and released intracellular enzymes and metabolites (with subsequent generation of ROS, Chapter 1). Increase of creatine in mouse BAL and serum may suggest that the main source of creatine is bronchial smooth muscles. On the other hand, higher concentration of creatine in skeletal muscles and small mass of bronchial muscles increases probability that skeletal muscles are a source for elevated creatine and creatinine (Chapter 1). Other possible source of increased creatine and guanidoacetate is liver (Chapter 1). More studies must be done to address these possibilities.

Elevated serum creatinine concentrations may be the result of damaged kidney glomeruli, hypotension, and other diseases, and serum urea : creatinine ratio may be important in distinguishing between these states (Hartmann, 2002). The chemical structure of creatine resembles that of the methylamines with osmolytic function as well as carnitine, betaine, and trimethylamine N-oxide (TMAO), however, no such function of creatine has been described (Peluso, 2000).

4.2.6. Food-derived and bacterial-derived compounds

Decreased levels of food-derived compounds in urine, such as trimethylamine (TMA), TMAO, trigonelline, and glycolate may be expected following decreased food uptake. Mice were fed Rodent Diet 5001 (Purina Mills (PMI) Nutrition International Company, USA), which contains "ground corn, dehulled soybean meal, dried beet pulp, fish meal, ground oats, brewer's dried yeast, cane molasses, dehydrated alfalfa meal, dried whey, wheat germ, porcine animal fat preserved with BHA, porcine meat meal, meat middlings," vitamins, and microelements (LabDiet, 2007). Trigonelline (N-methylnicotinic acid), present in plant food (Zwarta, 2003; Joshi, 1960), is an endogenous derivative of nicotinic acid; its decrease in biofluids may be associated with decreased food uptake. Precursors of TMA—choline, carnitine, and TMNO—are present in fish and in plant food. Bacterial microflora release TMA, TMNO, dimethylamine, and methylamine (Tsikas, 2007; Dumas, 2006) from food; therefore, decreased concentrations of these metabolites in biofluids of infected mice indicate decreased food uptake. We hypothesize that decreases in acetate, formate, and hippurate are similarly due to decreased bacterial production of these substances as a result of decreased food uptake. A decrease in the number of gut bacteria and death from pneumococcal virulence factors due to swallowing a small part of the inoculum is unlikely. Only a small part of the inoculum can enter the stomach (Chapter 3), and most of streptococci should be destroyed by the acidic pH in the stomach and by bile in the gut. Released intracellular compounds, capsule, and cell wall compounds are typical bacterial constituents and cannot damage gut microflora. Pneumolysin attacks cholesterol-containing host cell membranes only and cannot damage bacteria (Andrew, 2000). We also have to consider decreased absorption of substances from the gut due to stress and centralization of blood flow. However, the probability of such a process is low and no such significant changes during pneumonia have been described.

Concentrations of acetate, formate, and hippurate in the urine of infected antibiotic-treated mice from the longitudinal study tended to be slightly lower compared to untreated mice (this may be either a result of treatment and changes in gut microflora or a statistical error, or a reflection of the slightly higher severity of disease of treated mice).

The increased concentration of acetate in BAL from infected mice is hypothetically derived from the metabolism of streptococci. It is possible that increased acetate in BAL is derived from acetyl-CoA due to damage of mitochondria with impaired entrance of acetyl-CoA into mitochondria, and citrate cleavage in cytoplasm with release of acetyl-CoA. The increased lysine in mouse BAL may be due to released from Gram-positive bacterial cell walls (Boyd, 1988) or from endogenous metabolism of amino acids (Coffee, 1999).

4.2.7. Carbohydrates

Increased concentrations of fucose at 12–36 h post-infection cannot be explained based on previously known information. It is tempting to speculate that sources of fucose are glycosylated proteins of cell membranes, mucins, and glycolipids of eukaryotes (Ma, 2006; Chan, 1979). This sugar may be released from the proteins due to action of pneumococcal neuraminidase during the first few days of infection. The increase of fucose later may derive from apoptotic and phagocytosed host cells or from the bacterial capsule. Rats and apparently mice absorb fucose from food and utilise it for glycosylation; while humans utilise food-derived fucose partially for gluconeogenesis (Shull, 1960; Chan, 1979). It is unlikely that fucose has derived from pneumococcal polysaccharide capsule, since pneumococci contain N-acetyl-α-L-fucosamine and other sugars, rather than fucose itself (Kamerling, 2000). Increased fucose intake from food during pneumonia is unlikely, since food consumption was apparently decreased as assessed by observations and decreased concentrations of food-derived metabolites. On the other hand, an increase of fucose in mouse urine could be due to decreased reabsorption in kidney. Additionally, the normal levels of xylose in urine of infected mice and difficulties in measuring other sugars and acetyl sugars of the glycocalyx make this unlikely. In general, staphylococci do not contain neuraminidase, and staphylococcal pneumonia was not accompanied by an increase in fucose concentration. Further research is needed to elucidate the mechanism of the increase of fucose in urine.

4.2.8. Components of the cell membrane and nucleotides

Choline and betaine are mostly derived from food, but are also synthesized in liver and kidney (Zwarta, 2003; Joshi, 1960). The 50% decrease in the level of choline in serum of infected animals resembles the significant decrease in food-derived metabolites trigonelline, trimethylamine, etc. However, betaine concentrations decreased more slowly which can indicate either slower catabolism or increased compensatory endogenous synthesis. *In vitro* studies of apoptosis revealed no changes in choline concentration in cells during apoptosis, a decrease during necrosis, and an increase in phosphocholine early in apoptosis (Valonen, 2004); however, *in vivo* studies of the mouse pneumonia model are complicated by decreased food-intake. Ethanolamine is synthesized from serine and may be a precursor of choline (Arthur, 1991). Its serum and urine concentrations were increased at the peak of inflammation, which can be explained by phospholipid damage and catabolism or *de novo* synthesis for membrane reparation. A decreased ratio of choline-containing versus ethanolamine-containing phospholipids is associated with an increased resistance to apoptosis; an increased ethanolamine level is found in some tumors (Lutz, 2005).

Slightly increased concentrations of allantoin 24–36 h post-infection may be a result of its increased production from uric acid due to ROS release or intensified metabolism of purines (Chapter 1).

4.2.9. Distribution of metabolites in biofluids

The concentrations of most measured metabolites changed approximatelly equally and synchronously in all biofluids of infected mice. Concentrations of each compound in urine, serum, and BAL differed by several orders of magnitude, but the relative changes of the same compound as a percent of normal values tended to be similar in all biofluids. The exceptions to this common rule were more significantly decreased concentrations of citrate (and other TCA cycle intermediates), glucose, lactate, and glycine in urine than in serum (Chapter 3), possibly because of increased reabsorption in kidney. For example, increased reabsorption of citrate in the kidney was reported in response to low pH in kidney (Brennan 1988); low pH is observed during pneumonia (Chapter 1).

Decreased glucose concentrations in mouse urine may be explained by increased reabsorption in the kidney by SGLT1-3 transporters (Frayn, 2003) due to increased sodium reabsorption. Sodium reabsorption increases with increased ammonia production and secretion (McMurray, 1983), increased angiotensin II production (Henger, 2000; Geibel, 1990), and acidosis which is characteristic of pneumonia (Chapter 1). Further experiments may substantiate this view since reabsorption and secretion of many metabolites may be different in health and disease (Weinstein, 2003).

Many of amino acids in mouse urine could not be measured since they were present at concentrations below detection limits, and the spectra of some amino acids (for example, arginine, lysine, proline, and others) overlapped considerably with spectra of other compounds present in the mice urine samples.

4.3. Summary

In this thesis, a pattern of metabolites different from control mice was discovered in the biofluids of mice with pneumonia caused by *S. pneumoniae*. This pattern may be useful for diagnostic purposes. The dynamics of compound concentrations in mouse urine during the course of moderate and severe pneumonia strengthen the possibility that metabolomics may be applied to diagnosis of *S. pneumoniae*. Thess dynamics could potentially be used for monitoring and prognostic purposes. Since metabolomic methods generate large amount of data and generate hypotheses, we hypothesized about some of the potential mechanisms of metabolic changes. Similar metabolites can originate from distinct biochemical pathways; thus, the precise mechanism of metabolic changes are hypothetical at our current understanding of metabolomics in pneumonia.

New research on metabolic trajectories with different doses of pneumococci, leading to different outcomes, would strengthen the application of metabolic profiling for prognostic purposes. This thesis has also demonstrated a pattern of metabolites in staphylococcal mild pneumonia. This pattern may be useful for future studies of metabolic profiling as a diagnostic, monitoring, and prognostic method in mild cases of pneumonia (Chapter 1). Metabolic profiling of infected lung cells also showed metabolic changes at different stages of host cell death. We observed synchronous changes in mitochondrial potential and hypothesize causative relationships between mitochondrial (and cell) damage and changes in the Krebs cycle. These results may assist in determining some of the mechanisms leading to metabolic changes in the lung during pneumonia. Further studies on the influence of bacterial factors of pathogenicity on host cell and bacterial metabolism will strengthen metabolic profiling.

4.4. References

Alouf, J.E., Popoff, M.R. (2006). *The comprehensive sourcebook of bacterial protein toxins*. (3rd ed.). Burlington, MA: Elsevier.

Amano, A., Nakagawa, I., Yoshimori, T. (2006). Autophagy in innate immunity against intracellular bacteria. *J Biochem.* 140, 161-166.

An, Y., Friedman, R. J. (1997). Concise review of mechanisms of bacterial adhesion to biomaterial surfaces. *J Biomed Mat Res.* 43 (3), 338-348.

An, H. Y., Friedman, R.J. (Eds). (2000). Handbook of bacterial adhesion. Principles, methods, and applications. Totowa, NJ: *Humana Press*.

Anderson, R., Smith, B. (2005). Deaths: Leading causes for 2002. National Vital Statistics Reports, 53(17): 1-90.

Andrew, P., Mitchell, T., Morgan, P., Gilbert, R. (2000). Relationship of structure to function in pneumolysin. In Tomasz, A. (Ed.), *Streptococcus pneumoniae: Molecular biology and mechanisms of disease*. New York: Mary Ann Liebert Inc.

Armstrong, L., Medford, A., Uppington, K., Robertson, J., Witherden I., Tetley, T., Millar, A. (2004). Expression of functional Toll-like receptor (TLR-)2 and TLR-4 on alveolar epithelial cells. *Am J Respir Cell Mol Biol,* 31: pp. 241-245.

Arthur, G., Page, L. (1991). Synthesis of phosphatidylethanolamine and ethanolamine plasmalogen by the CDP-ethanolamine and decarboxylase pathways in rat heart, kidney and liver. *Biochem J.* 273(*1*): 121–125.

ATCC. "A549". Retrieved from <http://atcc.org/catalog/numSearch/numResults.cfm?atccNum=CCL-185>, July 25, 2007.

Atlas, R. (2006). *Handbook of microbiological media for the examination of food.* Boca Raton: Taylor & Francis.

Atkinson, B. F., Silverman, J. (1998). *Atlas of difficult diagnoses in cytopathology.* Philadelphia: W.B. Saunders.

Austrian, R. (2000). The enduring pneumococcus: unfinished business and opportunities for the future. In Tomasz, A. (Ed.), *Streptococcus pneumoniae: Molecular biology and mechanisms of disease.* New York: Mary Ann Liebert Inc.

Bae, S.M., Yeon, S.M., Kim, T.S., Lee, K.J. (2006). The effect of protein expression of Streptococcus pneumoniae by blood. *J Biochem Mol Biol.* 39(6): 703-8.

Bantel, H., Sinha, B., Domschke, W., Peters, G., Schulze-Osthoff, K., Jänicke, RU. (2001). α –toxin is a mediator of *Staphylococcus aureus*-induced cell death and activates caspases via the intrinsic death pathway independently of death receptor signalling. *J Cell Biol.* 155 (4), 637-647.

Bates, J.H., Campbell, G.D., Barron, A.L., McCracken, G.A., Morgan, P,N, Moses, E,B,, Davis, C.M. (1992). Microbial etiology of acute pneumonia in hospitalized patients. *Chest* 101: 1005-1012.

Baum, G.L. (Ed.) (1998). *Textbook of pulmonary diseases.* (Vol. 1). 6th ed. Philadelphia: Lippincott –Raven.

Bayles, K., Wesson, C., Liou, L., Fox, L., Bohach, G., Trumble, W. (1998). Intracellular *Staphylococcus aureus* escapes the endosome and induces apoptosis in epithelial cells. *Infect Immun.* 66 (1): 336-342.

Becker, B. (1993). Towards the physiological function of uric acid. *Free Radic Biol Med.* 14(6):615-31.

Becker, S., Palsson, B. (2005). Genome-scale reconstruction of the metabolic network in *Staphylococcus aureus* N315: an initial draft to the two-dimensional annotation. *BMC Microbiology.* 5:8.

Becker, B. (1993). Towards the physiological function of uric acid. *Free Radic Biol Med.* 14(6):615-31.

Behnia, M. Robertson, K., Martin, W. (2006). Lung infections: role of apoptosis in host defence and pathogenesis of disease. *Chest.*117, 1771-1777.

Belanger, A., Clague, M., Glass, j., LeBlanc, J. (2004). Pyruvate Oxidase Is a Determinant of Avery's Rough Morphology. *J Bacteriol.* 186 (24):8164-8171.

Benton, K. A., M. P. Everson, and D. E. Briles. 1995. A pneumolysin-negative mutant of Streptococcus pneumoniae causes chronic bacteremia rather than acute sepsis in mice. *Infect. Immun.* 63:448-455.

Berger, J., Johnson, M., Peterson, W. (1938). The proteolytic enzymes of bacteria II. The peptidases of some common bacteria. *J Bacteriol.* 36(5):521-545.

Bergeron, Y., Ouellet, N., Deslauriers, A., Simard, M., Olivier, M., Bergeron, M. (1998). Cytokine kinetics and other host factors in response to pneumococcal pulmonary infection in mice. *Infect Immun. 66*(3), 912-922.

Bezabeh, T., Mowat, M., Jarolim, L., Greenberg, A., Smith, I. (2001). Detection of drug-induced apoptosis and necrosis in human cervical carcinoma cells using ^{1}H NMR spectroscopy. *Nature.* 8, 219 – 224.

Blazevic, D, Ederer, G. (1975). *Principles of biochemical tests in diagnostic microbiology.* New York: Wiley. pp. xi, 15-17.

Blasi, F., Tarsia, P., Aliberti, S. (2005). Strategic targets of essential host-pathogen interactions. *Respiration.* 72: 9-25.

Boyd, R. (1988). *General microbiology.* St. Louis: Times Mirror. Pp. 103-110.

Brandenburg, J., Marrie, T., Coley,C., Singer, D., Obrosky, D., Kapoor, W. (2000). Clinical presentation, processes and outcomes of care for patients with pneumococcal pneumonia. *J Gen Inter Med. 15*(9): 638-646.

Braun, J. S., Hoffmann, O., Schickhaus, M., Freyer, D., Dagand, E., Bermpohl, D., Mitchell, T. J., Bechmann, I., Weber, J. R. (2007). Pneumolysin causes neuronal cell death through mitochondrial damage. *Infect Immun.* 75: 4245-4254.

Braun, J., Sublett, J., Freyer, D., Mitchell, T., Cleveland, J., Tuomanen, E., Weber, J. (2002). Pneumococcal pneumolysin and H_2O_2 mediate brain cell apoptosis during meningitis. *J Clin Invest.* 109:19–27.

Brennan, S., Hering-Smith, K., Hamm, L. (1988). Effect of pH on citrate reabsorption in the proximal convoluted tubule. *Am J Physiol.* 255 (24): 301-306.

Brock, T., Smith, D., Madigan, M. (1984) *Biology of microorganisms* (4th Ed.). New Jersey: Prentice-Hall.

Callard, R., Gearing, A. J.H. (1994). *The cytokine FactsBook.* London: Academic Press.

Camacho, D., Fuente, A., Mendes, P. (2005). The origin of correlations in metabolomics data. *Metabolomics* 1(1): 53-63.

Cemek, M., Caksen, H., Bayiroglu, F., Cemek, F., Dede, S. (2006). Oxidative stress and enzymic–non-enzymic antioxidant responses in children with acute pneumonia. *Cell Biochem Funct.* 24: 269–273.

Chan, J., Nwokoro, N., Schachter, H. (1979). L-Fucose metabolism in mammals. *J Biol Chem.* 254 (15): 7060.

Chapman, A., Hampton, M., Senthilmohan, R., Winterbourn, C., Kettle, A. (2002). Chlorination of bacterial and neutrophil proteins during phagocytosis and killing of *Staphylococcus aureus. J Biol Chem. 277*(123), 9757-9761.

Chen, Y., Zuchlinsky, A. (1994). Apoptosis induced by bacterial pathogens. *Microb Pathogen.* 17: 203-212.

Chong, K.T. (1987). Prophylactic administration of interleukin-2 protects mice from lethal challenge with Gram-negative bacteria. *Infect Immun.* 55 (3): 668-673.

Clancy, C. (1989). *Staphylococcus.* In O'Leary (Ed.). *Practical handbook of microbiology.* Boca Raton: CRC Press.

Coen, M., Lenz, E., Nicholson, J., Wilson, I, Pognan, F., Lindon, J. (2003). An integrated metabonomic investigation of acetaminophen toxicity in the mouse using NMR spectroscopy. *Chem Res Toxicol. 16*, 295-303.

Colice, G., Morley, M., Asche, C., Birnbaum, H. (2004). Treatment costs of community-acquired pneumonia in an employed population. *Chest 125*(6): 2140-2145.

Coffee, C.J. (1998). *Metabolism.* Madison: Fence Creek Publishing. pp. 85-87,187-193, 367.

Corrin, B., Nicholson, A. (2006). *Pathology of the lungs.* (2nd Ed.). Philadelphia: Elsevier.

Craig, S. (2004). Betaine in human nutrition. *Am J Clin Nutr.* 80(3):539-549.

Cuisinier, C., de Welle J.M., Verbeeck, R., Poortmans, J., Ward, R., Sturbois, X., Francaux, M. (2002). Role of taurine in osmoregulation during endurance exercise. *Eur J Appl Physiol.* (2002) 87: 489–495.

Cunha, B., Ortega, A. (1997). Atypical pneumonias. In Conn, R., Borer, W., Snyder, J. (Eds.). *Current diagnosis*: 9th ed. Philadelphia: *W. B. Saunders Company*. pp. 311-313.

Dallaire, F. Ouellet, N., Bergeron, Y., Turmel. V., Gauthier, M., Simard, M., Bergeron, M. (2001). Microbiological and inflammatory factors associated with the development of pneumococcal pneumonia. *J Infect Dis.* 184:292-300.

Daniely, D., Portnoi, M., Shagan, M., Porgador, M., Givon-Lavi, Givon-Lavi, N., Ling, E., Dagan, R., Mizrachi, . (2006). Pneumococcal 6-phosphogluconate-dehydrogenase, a putative adhesin, induces protective immune response in mice. *Clin Exp Immunol* 144(2).

DeAzavero, J.C.S., Russell, R.J. (1988). A simple method for study of bacterial characteristics and growth in vivo. In P.Owen and T.J.Foster (ed.), *Immunochemical and molecular genetic analysis of bacterial pathogenesis.* (313-319). Oxford: Elsevier.

deVelasko, A., E., Verheul, A., Verhoef, J., Snippe, H. (1995). Streptococcus pneumoniae: virulence factors, pathogenesis, and vaccines. *Microbiol. Reviews,* 59(4): 591–603.

Decombaz, J., Reinhardt, P., Anantharaman, K., von Glutz, G., Poortmans, J. R. (1979) Biochemical changes in a 100 km run: free amino acids, urea, and creatinine. *Eur J Appl Physiol* 41:61–72.

Deresiewicz, R., Parsonnet, J. (1998). Staphylococcal infectoions. In Fauci, A., Braunwald, E., Isselbacher, K., Wilson, J., Martin, J., Kasper, D. *Harrison's principles of internal medicine.* (14th ed.). New-York: McGraw-Hill, Inc. pp. 875-885.

Deretic, V. (2006). Autophagy as an immune defence mechanism. *Current Opinion in Immunology.* 18 (4): 375-382.

Diaper, J., Tither, K., Edwards, C. (1992). Rapid assessment of bacterial viability by flow cytometry. *Applied Microbiology and Biotechnology.* 32(2): 268-272.

Dinarello, C.A., Abraham, E. (2001). The role of interleukin-1 in sepsis. In Holland, S. (Ed.), *Cytokine therapeutics in infectious diseases.* Philadelphia: Lippincott Williams and Wilkins.

Dinges, M., Orwin, P., Schlievert, P. (2000). Exotoxins of *Staphylococcus aureus. Clin Microb Rev.* 13(1): 16-34.

Dockrell, D., Lee, M., Lynch, M., Read, M. (2001). Immune-mediated phagocytosis and killing of *Streptococcus pneumoniae* are associated with direct and bystander macrophage apoptosis. *J Inf Dis.* 184:713–22.

Dorman, R., Wunder, C., Saba, H., Shoemaker, J., MacMillan-Crow, L., Brock R. (2005). NAD(P)H oxidase contributes to the progression of remote hepatic parenchymal injury and endothelial dysfunction, but not microvascular perfusion deficits. *Am J Physil Gastrointest Liver Physiol. 290*(5): 1025-32.

Drider, D., Bekal, S., Prévost, P. (2004). Genetic organization and expression of citrate permease in lactic acid bacteria. *Gen Molec Res. 3*(2): 273-281.

Dumas, M., Barton, R., Toye, A., Cloarec, O., Blancher, C., Rothwell, A., Fearnside, J., Tatoud, R., Blanc, V., Lindon, J., Mitchell, S., Holmes, E., McCarthy, M, Scott, J., Gauguier, D., Nicholson, J. (2006). Metabolic profiling reveals a contribution of gut microbiota to fatty liver phenotype in insulin-resistant mice. PNAS, *103*(33): 2511-12516.

Duncan, J., Cho, G. (1972). Production of staphylococcal alpha toxin. II. Glucose repression of toxin formation. *Infect Immun.* 6: 689-694.

Edwards, K. G., Blumenthal, H. J., Khan, M., Slodki, M. (1981). Intracellular mannitol, a product of glucose metabolism in staphylococci. *J Bacteriol.* 146: 1020-1029.

Egert, M., de Graaf, G., Smidt, H., de Vos, W., Venema, K. (2006). Beyond diversity: functional microbiomics of the human colon. *Trends Microb. 14*(2): 86-91.

Englert, R., Shacter, E. (2002). Distinct modes of cell death induced by different reactive oxygen species. Amino acyd chloramines mediate hypochlorous acid-induced apoptosis. *J Biol Chem. 277*(23): 20518-20526.

Essmann, F. Bantel, H., Totzke, H., Engels, I., Sinha, B., Schulze-Osthoff, K, Janicke, RU . (2003). *Staphylococcus aureus'* alpha-toxin-induced cell death: predominant necrosis despite apoptotic caspase activation. *Nature*. 10. 1260-1272.

Etienne, J. (2005). Panton-Valentine leukocidin: a marker of severity for *Staphylococcus aureus* infection? *Clin Inf Dis.* 41: 591-3.

Ezepchuk, Y.V., Leung, D., Middleton, M., Bina, P., Reiser, R., Norris, D. (1996). Staphylococcal toxins and protein A differentially induce cytotoxicity and release of tumor necrosis factor- α from human keratinocytes. *J Invest Derm. 107*(4): 603-609.

Farr, B., Mandell, J. (1994). Gram-positive pneumonia. In Pennington, J.E. (Ed.), *Respiratory infections. Diagnosis and management*. New York: Raven Press.

Ferreira, O., Murilo, B. (2003). Acute pneumonia - a theme we should all be studying. *J Ped. 79*(6): 478- 479.

Fischer, W. (2000). *Pneumococcal* lipoteichoic and teichoic acid. In Tomasz, A. (Ed.), *Streptococcus pneumoniae: Molecular biology and mechanisms of disease*. New York: Mary Ann Liebert Inc.

Fliss, H. (1988). Oxidation of proteins in rat heart and lungs by polymorphonuclear leukocyte oxidants. *Molec Cel Biochem*. 84: 177-188.

Forbes, B., Sahm, D., Weissfeld, A. (2002). *Bailey and Scott's diagnostic microbiology*. (11 eds.). Philadelphia: Mosby.

Fournier, B., Philpott, D. (2005). Recognition of Staphylococcus aureus by the Innate Immune System. *Clin Microb Rev. 18*(3): 521–540.

Frayn, K. (2003). *Metabolic regulation: a human perspective.* Blackwell Publishing Company, Padstow. p. 36.

Frederick, S.E., Gruber, P.J., Tolbert, N.E.(1973). The occurrence of glycolate dehydrogenase and glycolate oxidase in green plants. An evolutionary survey. *Plant Physiol. 52*(4): 318–323.

Freshney, I. (2000). *Culture of animal cells: a manual of basic technique* (4th Ed.). New York: J. Wiley.

Garcia, J., Sanchez-Beato, A., Medrano, F., Lopez, R. (2000). Versatility of choline binding domain. In Tomasz, A. (Ed.), *Streptococcus pneumoniae: Molecular biology and mechanisms of disease*. New York: Mary Ann Liebert Inc.

Geibel, J., Giebisch, G., Boron, W. (1990). Angiotensin II stimulates both Na^+-H^+ exchange and Na^+/HCO^- cotransport in the rabbit proximal tubule. *Proc Natl Acad Sci USA*. 87: 7917-7920.

Geng, W., Pang, S. (1999). Differences in excretion of hippurate, as a metabolite of benzoate and as an administered species, in the single-pass isolated perfused rat kidney explained. *J Pharmacol Exp Therap.* 288: 597–606.

German, J., Hammock, B., Watkins, S. (2005). Metabolomics: building on a century of biochemistry to guide human health. *Metabolomics, 1*(1), 3- 9.

Gernardin, G., Pradier, C., Tiger, F., Deloffre, P., Mattei, M. (1996). Blood pressure and arterial lactate level are early indicators of short-term survival in human septic shock. *Intens Car Med. 22*(1): 17-25.

Gillis, C.N., Greene, N.M. (1977). Possible clinical implications of metabolism of bloodhome substrates by the human lung. In: Bakhle, Y.S., Vane, J.R., ecis. Metabolic functions of the lung. New York: Marcel Dekker.

Gingles, N., Alexander, J., Kadioglu, A., Andrew, P., Kerr, A., Mitchell, T., Hopes, E., Denny, P., Brown, S., Jones, H., Little, S., Booth, G., McPheat, W. (2001). Role of genetic resistance in invasive pneumococcal infection: identification and study of susceptibility and resistance in inbred mouse strains. *Infect Immun*. 69: 426–434.

Graham, J., Wilkinson, B. (1992). *Staphylococcus aureus* osmoregulation: Roles for choline, glycine betaine, proline, and taurine. *J Bacteriol. 174*(8): 2711-2716.

Grodzinski, B. (1979). A study of formate production and oxidation in leaf peroxisomes during photorespiration. *Plant Physiol. 63*(2): 289-293.

Hampton, M., Kettle, A., Winterbourn, C. (1998). Inside the phagosome: oxidants, myeloperoxidase and bacterial killing. *Blood, 92*(9), 3007-3017.

Harford, C., Hara, M. (1950). Pulmonary edema in influenzal pneumonia of the mouse and the relation of fluid in the lung to the inception of pneumococcal pneumonia. *J Exp Med.* 91: 245-259.

Hartmann, A. (2002). Nitrogen metabolites and renal function. In McClatchey, K. (Ed.), *Clinical Laboratory Medicine* (2nd ed.). Philadelphia: Lippincott Williams and Wilkins.

Haslett, C. (1999). Granulocyte apoptosis and its role in the resolution and control of lung inflammation. *Am J Respir Crit Care Med. 160*(5): S5-S11.

Haslinger-Loffler, B., Wagner, B., Bruck, M., Strangfeld, K., Grundmeier, M., Fischer, U., Volker, W., Peters, G., Schulze-Osthoff, K., Sinha, B. (2006). *Staphylococcus aureus* induces caspase-independent cell death in human peritoneal mesothelial cells. *Kidney Int.* 70: 1089-1098.

Henderson, B., Wilson, M., McNab, R., Lax, A. (1999). *Bacteria-host interactions in health and disease*. Chichester: John Wiley and Sons.

Henger, A., Tutt, P., Riesen, W., Hulter, H., Krapf, R. (2000). Acid-base and endocrine effects of aldosterone and angiotensin II inhibition in metabolic acidosis in human patients. *J Lab Clin Med. 136*(5): 379-89.

Hinsbergh, V., Veerkamp, J., Glatz, J. (1979). 4-methyl-2-oxopentanoate oxidation by rat skeletal-muscle mitochondria. *J Biochem.* 182: 353-360.

Hoskins, J, Alborn, W., Arnold, J., Blaszczak, L., Burgett, S., DeHoff, B., at el. (2001). Genome of the bacterium *Streptococcus pneumoniae* strain R6. *J Bacteriol. 183*(19): 5709-17.

Hostetter, M. (2000). Opsonic and nonopsonic interactions of C3 with *Streptococcus pneumoniae.* In Tomasz, A. (Ed.), *Streptococcus pneumoniae: Molecular biology and mechanisms of disease*. New York: Mary Ann Liebert Inc.

Ieven, M., Loens, K., Goossens, H. (2004). Detection and characterisation of bacterial pathogens by nucleic acid amplification: state-of-the-art review. (Eds.). In Presing, D., Tenover, F., Versanovich, J., Tang, Y.-W., Unger, E., Relman, D. *Molecular Microbiology: Diagnostic principles and practice.* Washington: ASM Press.

Illingworth, J.A. (2007). *Muscle structure and function.* <http://www.bmb.leeds.ac.uk/illingworth/muscle/amino.gif>

Isselbacher, K., Braunwald, E., Wilson, J., Martin, J., Fauci, A., Kasper, D. (1994). *Harrison's principles of internal medicine.* (13th ed.). Companion handbook. New-York: McGraw-Hill, Inc. pp. 421-422.

Jenner, A., Ruiz, J., Dunster, C., Halliwell, B., Mann, G., Siow, R. (2002). Vitamin C protects against hypochlorous acid-induced glutathione depletion and DNA base and protein damage in human vascular smooth muscle cells. *Arterioscler Thromb Vasc Biol.* 22: 574-580.

Jorgensen, J., Swenson, J., Tenover, F., Ferraro, M., Hindler, J., Murray, P. (1994). Development of interpretive criteria and quality control limits for broth microdilution and disk diffusion antimicrobial susceptibility testing of *Streptococcus pneumoniae*. *J Clin Microbiol. 32*(10): 2448-2459.

Joseph, J., Badrinath, P., Basran, G. S., Sahn S. A. (2003). Do we need all three criteria for the diagnostic separation of pleural fluid into transudates and exudates? An appraisal of the traditional criteria. *Med Sci Monit.* 9(11): CR474-6.

Joshi, J., Handler, P. (1960). "Biosynthesis of Trigonelline". *J. Biol. Chem.* 235 (10) 2981-2983.

Kahl, B., Herrmann, M., Schulze-Everding, A., Koch, H., Becker, K., Harms, Proctor, R., Peters, G. (1998). Persistent infection with small colony variant strains of *Staphylococcus aureus* in patients with cystic fibrosis. *J Infec Disease.* 177: 1023–1029.

Kamerling, J. (2000). Pneumococcal polysaccharides: a chemical view. In Tomasz, A. (Ed.), *Streptococcus pneumoniae. Molecular Biology and Mechanisms of Disease.* New York: Mary Ann Liebert Inc.

Kell, D. (2004). Metabolomics and system biology: making sense of the soup. *Curr Op Microb.* 7: 296-306.

Kelley, J. (2000). Cytokines and the resolution of lung inflammation. In Nelson, S., Martin, T.R. (Eds), *Cytokines in pulmonary disease.* New York: Marcel Dekker.

Kerr, A. R., Irvine, J. J. Search, J.J., Gingles, N.A., Kadioglu, A., Andrew, P.W., McPheat, W.L., Booth, C.G., and Mitchell, T.G. (2002). Role of inflammatory mediators in resistance and susceptibility to pneumococcal infection. *Infect Immun.* 70: 1547-1557.

Kerr, J. F. R., Harmon, B. (1991). Definition and incidence of apoptosis: an historical perspective. In Tomei, D., Corei, F. (Eds.). *Apoptosis: The molecular basis of cell death.* New York: Cold Spring Harbor Laboratory Press.

Kettle, A., Winterborn, C. (1997). Myeloperoxidase: a key regulator of neutrophil oxidant production. *Redox Re.* 3: 3-15.

Kisaki, T., Tolbert, N.E. (1969). Glycolate and glyoxylate metabolism by isolated peroxisomes or chloroplasts. *Plant Physiol. 44*(2): 242-250.

Kloosterman, T., Hendriksen, W., Bijlsma, J., Bootsma, H., Hijum,S., Kok, J., Hermans, P., Kuipers, O. (2006). Regulation of glutamine and glutamate metabolism by GlnR and GlnA in *Streptococcus pneumoniae. J Biol Chem. 281*(35): 25097-25109.

Knepper, MA, Packer R, Good, D. (1989). Ammonium transport in the kidney. *Physiol Rev.* 69: 179-249.

Krut, O., Utermohlen, O., Schlossherr, X., Kronke, M. (2003). Strain-specific association of cytotoxic activity and virulence of clinical *Staphylococcus aureus* isolates. *Infect Immun. 71*(5): 2716-2723.

Kluytmans, J., van Belkum, A., Verbrughan, H. (1997). Nasal Carriage of *Staphylococcus aureus*: epidemiology, underlying mechanisms, and associated risks. *Clin Microbiol Rev. 10*(3): 505-520.

Kussmann, M., Raymond, F., Affolter, M. (2006). OMICS-driven biomarker discovery in nutrition and health. . *Biotech. 124*(4): 758-787.

Labandeira-Rey, M., Couzon, F., Boisset, S., Brown, E.L. Bes, M.,

Bes, M., Benito, Y., Barbu, E., Vazquez, V., Höök, V., Etienne, J., Vandenesch, F., Bowden, G. (2007). *Staphylococcus aureus* Panton-Valentine leukocidin causes necrotizing pneumonia. *Science. 315*(5815): 1130-1133.

LabDiet, Retrieved from < http://www.labdiet.com/indexlabdiethome.htm> 12 September 2007.

LaCasse, E., Holcik, M., Korneluk, R., MacKenzie, A. (2005). Apoptosis in health, disease, and therapy: overview and methodology. In Holcik, M., LaCasse, E., MacKenzie, Korneluk, R. (Eds.), *Apoptosis in health and disease*. Cambridge, Cambridge University Press.

Lang, C.H. (1995). Role of cytokines in glucose metabolism. In Aggrawal, B.B., Puri, R.K. (Eds), *Human cytokines: their role in disesase and therapy*. Cambridge, MA: Balckwell Science.

Lang, C.H., Dobrescu, C. & Bagby, G.J. (1992). Tumor necrosis factor impairs insulin action on peripheral glucose disposal and hepatic glucose output. *Endocrinology* 130, 43–52.

Langen, R.C., Schols, A.M., Kelders, M.C., van der Velden, J.L., Wouters, E.F., Janssen-Heininger, Y. (2006). Muscle wasting and impaired muscle regeneration in a murine model of chronic pulmonary inflammation *Am J Respir Cell Mol Biol. 35*(6): 689-96.

Lee, W. (2006). Characterizing phenotype with tracer based metabolomics. *Metabolomics*. 2 (1): 31-39.

LeMessurier, K., A., Ogunniyi, Paton, J. (2006). Differential expression of key pneumococcal virulence genes in vivo. *Microbiology* 152: 305-311.

LeVine, A., Whitsett, J., Gwozdz, J., Richardson, T., Fisher, J., Burhans, M., Korfhagen, T. (2000). Distinct Effects of Surfactant Protein A or D Deficiency During Bacterial Infection on the Lung. *J Immunol.* 165: 3934-3940.

Levison, M. (1998). Pneumonia, including necrotising pulmonary infections (Lung abscesses). In Fauci, A., Braunwald, E., Isselbacher, K., Wilson, J., Martin, J., Kasper, D. (Eds). *Harrison's principles of internal medicine.* (14th ed.). New-York: McGraw-Hill, Inc. pp. 1437-1445.

Lee-Levandrowski, E., Burnett, R., Levandrowski, K. (2002). Electrolytes and acid-base balance. In McClatchey, K. (Eds). *Clinical Laboratory Medicine*. Philadelphia. Lippincott-Williams and Wilkins. pp. 382-385.

Li, X., Donaldson, K., Brown, D., MacNee, W. (1995). The role of tumor necrosis factor in increased airspace epithelial permeability in acute lung inflammation. *Am J Respir Cell Mol Biol.* 13: 185-195.

Lincoln, R, Leigh, J., Jones, N. (1995). The amino acid requirements of *Staphylococcus aureus* isolated from cases of bovine mastitis. *Veterin Microb. 45*(2-3): 275-279.

Lowenstein, J. (Ed), (1969). *Citric acid cycle. Control and compartmentation.* New York: Marcel Dekker. pp. 147-152.

Lutz, N. (2005). From metabolic to metabolomic NMR spectroscopy of apoptotic cells. *Metabolomics. 1*(3): 251-268.

Lutz, N., Tome, M., Cozzone ,P. (2003). Early changes in glucose and phospholipid metabolism following apoptosis induction by IFN-gamma/TNF-alpha in HT-29 cells. *FEBS Lett.* 544: 123-128.

Ma, B., Simala-Grant, J., Taylor, D. (2006). Fucosylation in prokaryotes and eukaryotes. *Glycobiology. 16*(12): 158R–184R.

Macfarlane, S., Macfarlane, G. (2003). Regulation of shortchain fatty acid production. *Proc Nutr Soc.* 62, 67–72.

Macfarlane, J. (2000). Acute lower respiratory tract infections. In Ledingham, J., Warrell, D. (Eds) *Concise Oxford textbook of medicine.* New York: Oxford University Press, Inc. pp. 369-375.

Mandell, L., Wunderink, R., Anzueto, A., Bartlett, J., Douglas Campbell, G., Dean, N., Dowell, S., File, T., Musher, D., Niederman, N., Torres, A., Whitney, G. (2007). Infectious diseases society of America/American Society consensus guidelines on the management of community-acquired pneumonia in adults. *Clin Infect Diseas.* 44 (Suppl 2).

Mandell, L., Marrie, T., Grossman, R., Chow, A., Hyland, R., (2000). Canadian guidelines for the initial management of community-acquired pneumonia: an evidence-based update by the Canadian Infectious Diseases Society and the Canadian Thoracic Society. *Clin Infect Diseas.* 31: 383-421.

Mannaerts, G.P., Van Veldhoven. P.P., Casteels. M. (2000). Peroxisomal lipid degradation via β-and α-oxidation in mammals. *Cell Biochem Biophys. 32*(1-3): 73-87.

Marshall, W. (1995). *Clinical chemistry.* (3rd ed). London: *Mosby.* pp. 23-26, 43.

Marrie, T. (1997). Bacterial pneumonia. In Conn, R., Borer, W., Snyder, J. (Eds.). *Current diagnosis* (9 ed.). Philadelphia: W. B. Saunders Company. pp. 307-311.

McMurray, W. (1983). *Essentials of human metabolism.* Philadelphia: Harper & Row, Publishers. pp. 95-97, 206-214, 218-227, 230-236, 260-280.

Menzies, B., Kourteval, I. (1998). Internalisation of *Staphylococcus aureus* by endothelial cells induces apoptosis. *Infect Immun.* 5994-5998.

Mergner, W., Jones, R.; Trump, B. (Ed), (1990). *Cell Death. Mechanisms of Acute and Lethal Cell Injury*. New York: F/W. pp. 67-87, 201-218.

Michaelson, J. (1991). The significanse of cell death. In Tomei, D., Corei, F. (Eds). *Apoptosis: The molecular basis of cell death.* New York: Cold Spring Harbor Laboratory Press.

Miller, R Fung, D. (1973). Amino acid requirements for the production of enterotoxin B by *Staphylococcus aureus* S-6 in a chemically defined medium. *Appl Microbiol. 25*(5): 800–806.

Mitchell, T. (2000). Virulence factors and the pathogenesis of disease caused by *Streptococcus pneumoniae*. *Res Microbiol*. 151: 413–419.

Mitchell, T., Andrew, P. (2000). Biological properties of pneumolysin. In Tomasz, A. (Ed.), *Streptococcus pneumoniae: Molecular biology and mechanisms of disease*. New York: Mary Ann Liebert Inc.

Mohler, J., Azoulay-Dupuis E., Amory-Rivier , C., Mazoit, J.X., Bedos, J.P., Rieux, V., Moine, P. (2003). *Streptococcus pneumoniae* strain-dependent lung inflammatory responses in a murine model of pneumococcal pneumonia. *Inten Care Med.* 29: 808-816.

Murray, J., Barbara, J., Dunkley, S., Lopez, A., Van Ostade, X., Condliffe, A., Dransfield, I., Haslett, C., Chilvers, E. (1997). Regulation of neutrophil apoptosis by Tumor Necrosis Factor-alpha: Requirement for TNFR55 and TNFR75 for induction of apoptosis *in vitro*. *Blood*, 90(7): 2772-2783.

Murdoch, D., Laing, R., Mills, G., Karalus, N., Town, G., Mirrett, S., Reller, L. (2001). Evaluation of a rapid immunochromatographic test for detection of *Streptococcus* *pneumoniae* antigen in urine samples from adults with community-acquired pneumonia. *J Clin Microbiol. 39*(10):3495-3498.

Musher, D. (1998). Pneumococcal infections. In Fauci, A., Braunwald, E., Isselbacher, K., Wilson, J., Martin, J., Kasper, D. (Eds). *Harrison's principles of internal medicine.* (14th ed.). New-York: *McGraw-Hill, Inc.* pp. 870-874.

McNally, L., Jeena, P., Gajee, K., Sturm, W., Tomkins, A., Coovadia, H., Goldblatt, D. (2006). Lack of Association between the Nasopharyngeal Carriage of *Streptococcus pneumoniae* and *Staphylococcus aureus* in HIV-1–Infected South African Children. *J Inf Dis.* 194: 386 -390.

Nagami, G. (1995). Effect of luminal angiotensin II on ammonia production and secretion by mouse proximal tubules. *Am J Physiol Renal Fluid Electrolyte Physiol* 269: F86-F92.

Nagami, G. (2002). Enhanced ammonia secretion by proximal tubules from mice receiving NH_4Cl: role of angiotensin II. *Am J Physiol Renal Physiol. 282*(3): F472-7.

Navarro, D., García-Maset, L., Gimeno, C., Escribano, A., García-de-Lomas, J. (2004). Performance of the Binax NOW *Streptococcus pneumoniae* urinary antigen assay for diagnosis of pneumonia in children with underlying pulmonary diseases in the absence of acute pneumococcal infection. *J Clin Microbiol.* 42(10): 4853–4855.

Nicholls, A., Mortishire-Smith, R., Nicholson, J. (2003). NMR spectroscopic-based metabonomic studies of urinary metabolite variation in acclimatizing germ-free rats. *Chem Res Toxicol.* 16 (11): 1395 -1404.

Nicholson, J., Holmes, E., Wilson, I. (2005).Gut microorganisms, mammalian metabolism and personalized health care. *Nat Rev Microb. 3*(5): 431-8

Nicholson, J., Holmes, E., Lindon, J., Wilson, I. (2004). The challenges of modeling mammalian biocomplexity. *Nat Biotech. 22*(10): 1268-1274.

Nicholson, J., Holmes, E., Wilson, I. (1999). 'Metabonomics': understanding the metabolic responses of living systems to pathophysiological stimuli via multivariate statistical analysis of biological NMR spectroscopic data. *Xenobiotica*. 29: 11, 1181-1189.

Nicholson, J., Timbrell, J., Sadler, P. (1985). Proton NMR spectra of urine as indicators of renal damage. Mercury-induced nephrotoxicity in rats. *Mol Pharmacol.* 27: 644-651.

Oei, E., Kalb,T., Beuria, T., Allez, M., Nakazawa, A., Azuma, M., Timony, M., Stuart, Z., Chen, H., Sperber, K. (2004). Accessory cell function of airway epithelial cells. *Am J Physiol Lung Cell Mol Physiol.* 287: L318–L331.

Papa, S., Guerrieri, F., Tager, J.M. (Eds), (1999). *Frontiers of Cellular Bioenergetics. Molecular Biology, Biochemistry, Physiopothology*. New York: Kluwer Academic. pp. 777-795.

Parfentjev, I., Perlzweig, W. (1936). The composition of the urine of white mice. *J Biol Chem*. 551-555.

Pears, M., Rubtsov, D., Mitchison, H., Cooper, J., Pearce, D., Mortishire-Smith, R., Griffin, J. (2007). Strategies for data analyses in a high resolution ^{1}H NMR based metabolomics study of a mouse model of Batten disease. *Metabolomics*, 3(2): 121-136.

Peluso, G., Barbarisi, A., Savica, v., Reda, E., Nicolai, R., Benatti, P., Calvani, M. (2000). Carnitine: an osmolyte that plays a metabolic role. *J Cel Biochem.* 80(1): 1–10.

Pennington, J.E. (1994). Community-acquired pneumonia and acute bronchitis. In Pennington, J.E. (Ed.), *Respiratory infections. Diagnosis and management*. New York: Raven Press.

Pericone, C., Park, S., Imlay, J., Weiser, J. (2003). Factors contributing to hydrogen peroxide resistance in *Streptococcus pneumoniae* include pyruvate oxidase (SpxB) and avoidance of the toxic effects of the Fenton reaction. *J Bacteriol.* 185: 6815-6825.

Pericone, C., Overweg, K., Hermans, P., Weiser, J. (2000). Inhibitory and bactericidal effects of hydrogen peroxide production by *Streptococcus pneumoniae* on other inhabitants of the upper respiratory tract. *Infect Immun.* 68(7): 3990-3997.

Petit, M. C., Francois, M. H., Berriche, S., Burckel, A., Lucotte, G. Detection of *Chlamydia trachomatis* by PCR. (1991). In Rolfs, I., Schumacher, H. C., Marx, P. (Eds.). *PCR Topics: Usage of polymerase chain reaction in genetics and infectious diseases.* Berlin: Springer-Verlag.

Preston, J. A., Beagley, K. W., Gibson, P. G., Hansbro, P. M. (2004). Genetic background affects susceptibility in nonfatal pneumococcal bronchopneumonia. *Eur Respir J.* 23:224-231.

Prevost, G., Mourey, L., Collin, D., Menestrina, G. (2001). Staphylococcal pore-forming toxins. In van der Goot, G (Eds). *Pore-forming toxins.* Geneve: Springer.

Pullar, J., Winterbourn, C., Vissers, M. (1999). Loss of GSH and thiol enzymes in endothelial cells exposed to sublethal concentrations of hypochlorous acid. *Am J Physiol – Heart.* 277: 1505-1512.

Puren, A., Feldman C., Savage N., Becker, P., Smith, C. (1995). Patterns of cytokine expression in community-acquired pneumonia. *Chest.* 107: 1342–1349.

Rahman, I., MacNee, W. (2000). Oxidative stress and regulation of glutathione in lung inflammation. *Eur Respir J. 16*(3):534-54.

Ratner, A., Hippe, K., Aguilar, J., Bender, M., Nelson, A. (2006). Epithelial cells are sensitive detectors of bacterial pore-forming toxins. *J Biol Chem. 281*(18): 12994-12998.

Renz, M., Seeling, R., Czichos, J., Scholz, V., Stockinger, K., Seeling, H. P. (1991) Rapid diagnosis of tuberculosis infection by PCR. In Rolfs, I., Schumacher, H. C., Marx, P. (Eds.). *PCR Topics: Usage of polymerase chain reaction in genetics and infectious diseases.* Berlin: Springer-Verlag.

Reo, N. NMR-based metabolomics. (2002). *Drug and Chemical Toxicology, 25* (4), 375-382.

Reynolds, H. (1994). Normal and defective respiratory host defences. In Pennington, J. (Eds). *Respiratory infections: Diagnosis and Management.* (3rd ed). New-York: Raven Press. pp. 9-15.

Rice, K., Nelson, J., Patton, T., Yang, S., Bayles K. (2005). Acetic acid induces expression of the *Staphylococcus aureus* cidABC and lrgAB murein hydrolase regulator operons. *J Bacteriol.* 187: 813-821.

Rietschel, E., Schletter, J., Weidermann, B., Samalouti, V., Mattern, T., Zahlinger, U., Seydel, U., Brade, H., Flad, H., Kusumoto, S., Gupta, D., Dziarski, R., Ulmer, A. (2000). Lipopolysaccharide and peptidoglycan: CD14-dependent bacterial inducers of inflammation. In Tomasz, A. (Ed), *Streptococcus pneumoniae: Molecular biology and mechanisms of disease*. New York: Mary Ann Liebert Inc.

Rodgerson, D. (1991). Renal function. In Howanitz, J.H., Howanitz, P.J., (Eds.), *Test selection and interpretation*. New York: Churchill Livingstone.

Rosen, H., Crowley, J., Heinecke J. (2002). Human neutrophils use the myeloperoxidase-hydrogen peroxide-chloride system to chlorinate but not nitrate bacterial proteins during phagocytosis. *J Biol Chem.* 99(3), 424.

Roth, B., Poot, M., Yue, S., Millard, J. (1997). Bacterial viability and antibiotic susceptibility testing with SYTOX green nucleic acid stain. *Appl Environ Microbiol.* 63(6): 2421–2431.

Rochfort, S. (2005). Metabolomics reviewed: a new “omics” platform technology for systems biology and implications for natural products research. *J Nat Prod.* 68: 1813-1820.

Rubins, J., Duane, P., Charboneau, P., Janoff, E. (1992). Toxicity of pneumolysin to pulmonary endothelial cells in vitro. *Infect Immun.* 60: 1740-1746.

Rubins, J., Duane, P., Clawson, D., Charboneau, D., Young, J., Niewoenhner, D. (1993). Toxicity of Pneumolysin to Pulmonary Alveolar Epithelial Cells. *Infect Immun.* 61: 1352-1358.

Rubins, J., Mitchell, T., Andrew, P., Niewoehner, E. (1994). Pneumolysin activates phospholipase A in pulmonary artery endothelial cells. *Infect Immun. 62*(9): 3829–3836.

Rubins, J. B., Charboneau, D., Paton, J. C., T. J. Mitchell, P. W. Andrew, and E. N. Janoff. (1995). Dual function of pneumolysin in the early pathogenesis of murine pneumococcal pneumonia. *J Clin Invest.* 95:142-150.

Ruiz-Gonzalez, A., Falguera, M., Nogues, A., Rubio-Caballero, M. (1998). Is *Streptococcus pneumoniae* the leading cause of pneumonia of unknown etiology? A microbiologic study of lung aspirates in consecutive patients with community-acquired pneumonia. *Am J Med.* 106: 385-390.

Rydell-Törmänen, K., Uller, L., Erjefalt, J. (2006). Direct evidence of secondary necrosis of neutrophils during intense lung inflammation. *Eur Respir J.* 28:268–274.

Salway, J. (1994). *Metabolism at a glance.* Oxford: Blackwell Scientific Publications. pp. 36-46, 78-80.

Sawers, R. (2005). Formate and its role in hydrogen production in Escherichia coli. *Biochem Soc Trans*. *33*(1): 42-46.

Severin, A., Tomasz, A. (2000). The peptidoglycan of *Streptococcus pneumoniae.* In Tomasz, A. (Ed.), *Streptococcus pneumoniae. Molecular Biology and Mechanisms of Disease*. New York: Mary Ann Liebert Inc.

Schachter, D., Taggart, J. (1954). Glycine N-acylase: purification and properties. *J Biol Chem*. 208: 263-275.

Schmid, D., Schmid, D., Dengjel, J., Schoor, O., Stevanovic, S., Munz, C. (2006). Autophagy in innate and adaptive immunity against intracellular pathogenes. *J Mol Med.* 84: 194-202.

Schmitt, S. (2002). Pneumonias. In Stoller, J., Ahmad, M., Longworth, D. *Intensive review of internal medicine.* Philadelphia: Lippincott, Williams and Wilkins.

Schmitz, J., Kettunen, M., Hu, M., Brindle, K. (2005). ^{1}H MRS-visible lipids accumulate during apoptosis of lymphoma cells *in vitro* and *in vivo*. *Magn Res Med.* 54:43–50.

Schwab, A., Tao, L., Yoshimura, T., Simard, A. Barker, A., Pang K. (2001). Hepatic uptake and metabolism of benzoate: a multiple indicator dilution, perfused rat liver study. *Am J Physiol.* 280: G1124–G1136.

Shedd, S.F., Lutz, N.W., Hull, W.E. (1993). The influence of medium formulation on phosphomonoester and UDP-hexose levels in cultured human colon tumor cells as observed by ^{31}P NMR spectroscopy. *NMR Biomed.* 6: 254 -263.

Sicard, A. (1964). A new synthetic medium for *Diplococcus pneumoniae* and its use for the study of reciprocal transformations at the amiA locus. *Genetics* 50: 31-44.

Smith, H., Tang, C., Exley, R. (2007). Effect of host lactate on gonococci and meningococci: new concepts on the role of metabolites in pathogenicity. *Infect Immun. 75*(9): 4190–4198.

Somerville, G., Cockayne, A., Dürr, M., Peschel, A., Otto, M., Musser, J. (2003). Synthesis and deformylation of *Staphylococcus aureus* delta-toxin are linked to tricarboxylic acid cycle activity. *J Bacteriol.* 185: 6686-6694.

Somerville, G., Said-Salim, B., Wickman, J., Raffel, S., Kreiswirth, B., Musser, J. (2003). Correlation of acetate catabolism and growth yield in *Staphylococcus aureus*: Implications for host-pathogen interactions. *Infect Immun.* 71, 4724–4732.

Somerville, G., Chaussee, M., Morgan, C., Fitzgerald, J., Dorward, D., Reitzer, L., Musser, J. (2002). Staphylococcus aureus aconitase inactivation unexpectedly inhibits post-exponential-phase growth and enhances stationary-phase survival. *Infect Immun.* 70: 6373-6382.

Stryer (1995). *Biochemistry.*

<http://www.library.csi.cuny.edu/~davis/Biochem_3521/lect23/aminoAAcat.GIF>

<http://scholar.library.csi.cuny.edu/~davis/Biochem_3521/lect23/lect23.html>

Su, X., Looney, M., Robriquet, L., Fang, X., Matthay, M. (2004). Direct visual instillation as a method for efficient delivery of fluid into the distal airspaces of anesthetized mice. *Exp Lung Res.* 30: 479-493.

Taylor, E. (1985). *Difficult Diagnosis.* Philadelphia: Saunders. pp. 326, 328–330.

Taryle, D.A., Potts, D E., Sahn S. (1978). The incidence and clinical correlates of parapneumonic effusions in pneumococcal pneumonia. *Chest. 74*(2):170-173.

Thukkani, A., Martinson, B., Albert, C., Vogler, G., Ford, D. (2005). Neutrophil-mediated accumulation of 2-ClHDA during myocardial infarction: 2-ClHDA-mediated myocardial injury. *Am J Physiol Heart Circ Physiol.* 288: 2955–2964.

Tilley, S., Orlova, E., Gilbert, R., Andrew, P. Saibil, H. (2005). Structural basis of pore formation by the bacterial toxin pneumolysin. *Cell.* 121: 247–256.

Todar, K. (2006). Microbial Metabolism. < www.bact.wisc.edu/.../ metabolism.html >

Tolbert, N., Oeser, A., Yamazaki, R., Hageman, R., Kisaki, T. (1969). A survey of plants for leaf peroxisomes. *Plant Physiol. 44*(1):135-47.

Tolbert, N.E., Oeser, A., Kisaki, T., Hageman, R.H., Yamazaki, R.K. (1968). Peroxisomes from spinach leaves containing enzymes related to glycolate metabolism. *J Biol Chem.* 243(19): 5179-6184.

Tsikas, D., Thum, T., Becker, T., Pham, Y., Chobanyan, K., Mitschke, A., Beckmann, B., Gutzki, F., Bauersachs, J., Stichtenoth, D. (2007). Accurate quantification of dimethylamine (DMA) in human urine by gas chromatography–mass spectrometry as pentafluorobenzamide derivative: Evaluation of the relationship between DMA and its precursor asymmetric dimethylarginine (ADMA) in health and disease. *J Chromatography B.* (851) 229-239.

Tuomanen, E., Masure, R. (2000). Molecular and cellular biology of pneumococcal infection. In Tomasz, A. (Ed), *Streptococcus pneumoniae: Molecular biology and mechanisms of disease.* New York: Mary Ann Liebert Inc.

Tweten, R., Parker, M., Johnson, A. (2001). The cholesterol-dependent cytolysins. In van der Goot, G (Eds). *Pore-forming toxins.* Geneve: Springer.

Valonen, P., Griffin, J., Lehtima K., Liimatainen, T., Nicholson, J., Gro, O., Kauppinen, R. (2004). High-resolution magic-angle-spinning ^{1}H NMR spectroscopy reveals different responses in choline-containing metabolites upon gene therapy-induced programmed cell death in rat brain glioma. *NMR Biomed.* 18: 252–259.

van der Werf, M., Jellema, R., Hankemeier, T. (2005). Microbial metabolomics: replacing trial-and-error by the unbiased selection and ranking of targets. *J Ind Microbiol Biotechnol. 32*(6): 234-52.

Vaux, D., Strasser, A. (1996). The molecular biology of apoptosis. *Proc Natl Acad Sci USA*. 93: 2239-2244.

Viola, A., Lutz, N.W., Maroc, C., Chabannon, C., Julliard, M., Cozzone, P.J. (2000). Metabolic effects of photodynamically induced apoptosis in an erythroleukemic cell line. A ^{31}P NMR spectroscopic study of Victoria-Blue-BO-sensitized TF-1 cells. *Int J Cancer.* 85: 733-739.

Wajant, H., Scheurich, P., Henkler, F. (2005). Interleukin-1 receptor/Toll-like receptor signaling. In Rich, T. (Ed), *Toll and toll-like receptors: an immunologic perspective*. New York: Kluwer Academic/Plenum Publishers.

Wang, E., Ouellet, N., Simard, M., Fillion, I., Bergeron, Y., Beauchamp, D., Bergeron, M. (2001). Pulmonary and systemic host response to *Streptococcus pneumoniae* and *Klebsiella pneumoniae:* Bacteremia in normal and immunosuppressed mice. *Infect Immun. 69*(9): 5294-5304.

Wang, L., Scabilloni, J.F., Antonini, J.M., Rojanasakul, Y., Castranova, V. (2006). Induction of secondary apoptosis, inflammation, and lung fibrosis after intratracheal instillation of apoptotic cells in rats. *Am J Physiol Lung Cell Mol Physiol*. 290(4): L695-L702.

Wannemacher, R. (1977). Key role of various individual amino acids in host response to infection. *Am J Clin Nutrition.* 30: 1269-1280.

Waters, N., Waterfield, C., Farrant, C., Holmes, E., Nicholson, J. (2006). Integrated metabonomic analysis of bromobenzene-induced hepatotoxicity: novel induction of 5-Oxoprolinosis. *J Prot Res*. 5: 1448-1459.

Watson, A. D. (2006). Lipidomics: a global approach to lipid analysis in biological systems. *J Lipid Res*. 47: 2101–2111.

Watson, B., Gauci, C., Blache, L., O'Grady, F. (1969). A simple turbidity cell for continuously monitoring the growth of bacteria. *Phys Med Biol*., 14 (4), 565-558.

Weckwerth, W. (2003). Metabolomics in system biology. *An Rev Plant Biol.* 54: 669-89.

Weinstein, A.M. (2003). Mathematical models of renal fluid and electrolyte transport: acknowledging our uncertainty. *Am J Physiol Renal Physiol*. 284(5): F871-84.

Wishart, D. (2006). Metabolomics: The principles and potential applications to transplantation. *Am J Transpl. 5*(12):2814-2820.

White, D. (2007). *The physiology and biochemistry of prokaryotes.* (3rd ed). New York: Oxford University Press. pp. 210-234.

Williams, S. N., Anthony, M. L., Brindle, K. M. (1998). Induction of apoptosis in two mammalian cell lines results in increased levels of fructose-1,6-bisphosphate and CDP-choline as determined by ^{31}P MRS. *Magn Reson Med*. 40: 411-420.

Woods, D. (1994). Bacterial colonisation of the respiratory tract: Clinical significance. In Pennington, J. (Eds). *Respiratory infections: Diagnosis and Management.* (3rd ed). New-York: Raven Press. pp. 34-40.

Wyss, M, Kaddurah-Daouk, R. (2000). Creatine and Creatinine Metabolism. *Physiol Rev. 80*(3): 1107-1213.

Zhang, A., Mitchell, S. and Smith, R. (1999). Dietary Precursors of Trimethylamine in Man: A Pilot Study. *Food Chem Toxicol.* 37: 515-520.

Zhen, Y., Krausz, K., Chen, C., Idle, J., Gonzalez, F. (2007). Metabolomic and genetic analysis of biomarkers for peroxisome proliferator-activated receptor α expression and activation. *Mol Endocrin. 21*(9): 2136-2151.

Ziebandt, A. K., Becher, D., Ohlsen, K., Hacker, J., Hecker, M., Engelmann, S. (2004). The influence of agr and sigma(B) in growth phase dependent regulation of virulence factors in *Staphylococcus aureus*. *Proteomics*. 4: 3034-3047.

Zwarta, F., Slow, S., Paynea, R., Levera, M., Georgea, P., Gerrard, J., Chambers, S. (2003). Glycine betaine and glycine betaine analogues in common foods. *Food Chem. 83*(2): 197-204.

Zweigner, J., Jackowski, S., Smith, S. H., Van Der, M. M., Weber, J. R., and Tuomanen, E. I. (2004). Bacterial inhibition of phosphatidylcholine synthesis triggers apoptosis. *J Exp Med. 200*(1): 99-106

Zuppi, C., Messana, I., Forni, F., Rossi, C., Pennacchietti, L., Ferrari, F., Giardina, B. (1997). ^{1}H NMR spectra of normal urines: Reference ranges of the major metabolites. *Clin Chim Acta.*265: 85-97.